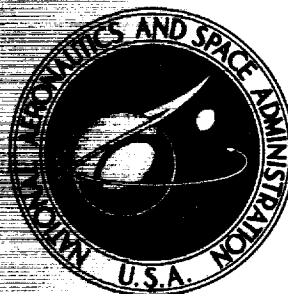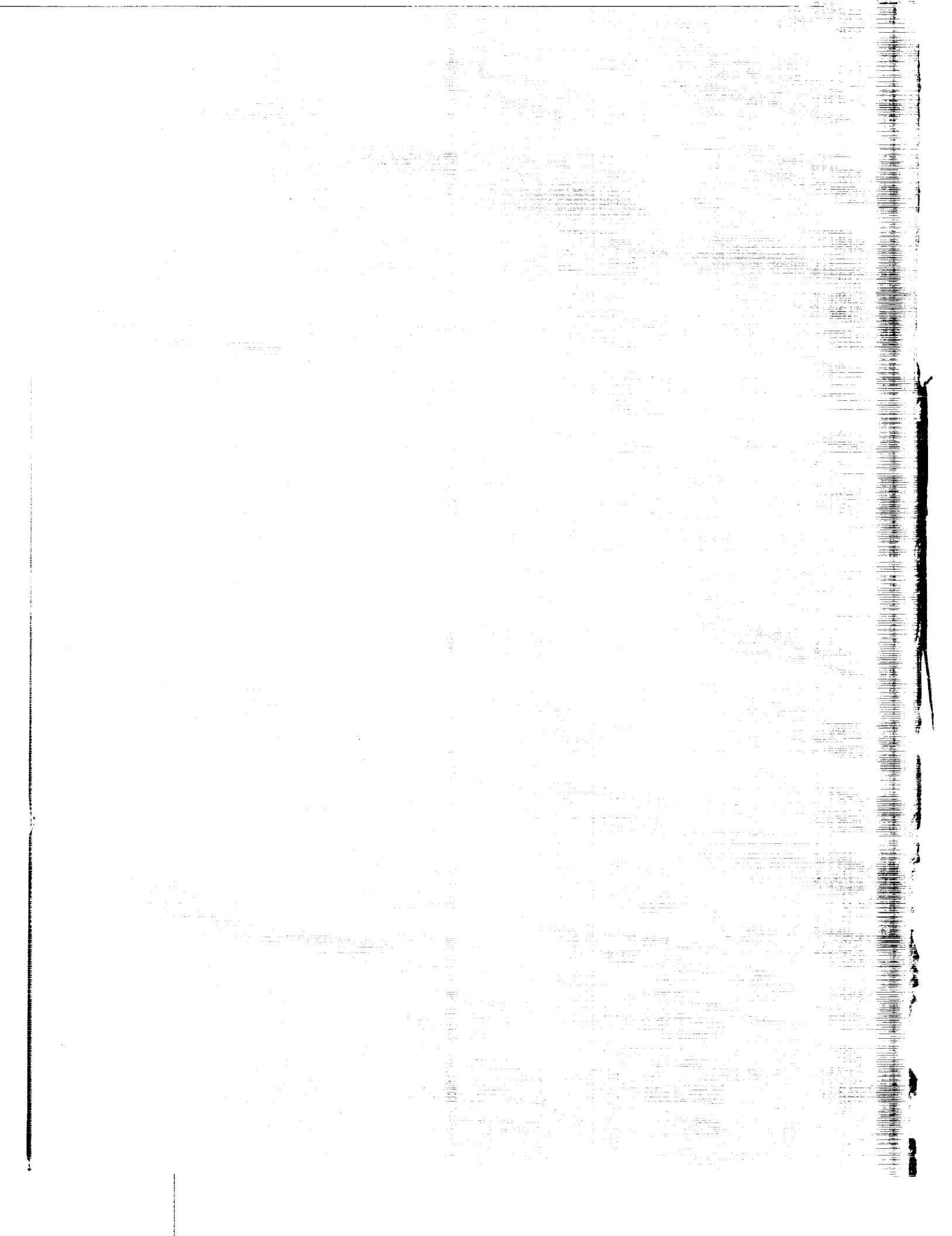# NASA CONTRACTOR REPORT

NASA CR-1388

NASA CR-1388

CASE FILE COPY

REMOVAL OF ACID GASES AND OXIDES OF NITROGEN FROM SPACECABIN ATMOSPHERES

*by A. J. Gully, R. M. Bethea, R. R. Graham,
and M. C. Meador*

NATIONAL AERONAUTICS AND SPACE ADMINISTRATION • WASHINGTON, D. C. • JULY 1969

REMOVAL OF ACID GASES AND OXIDES OF NITROGEN

FROM SPACECABIN ATMOSPHERES

By A. J. Gully, R. M. Bethea, R. R. Graham,
and M. C. Meador

TABLE OF CONTENTS

LIST OF TABLES

LIST OF FIGURES

REMOVAL OF ACID GASES AND OXIDES OF NITROGEN

FROM SPACECABIN ATMOSPHERES

By A. J. Gully, R. M. Bethea, R. R. Graham, and M. C. Meador

SUMMARY

Investigations were made on methods of removal of oxides of nitrogen and of the acid gases sulfur dioxide, hydrogen chloride, hydrogen fluoride and chlorine in low concentrations from air as part of the effort to develop an effective atmospheric purification subsystem for long-term manned space missions. Methods investigated were: (1) reaction with basic solid materials, (2) adsorption and (3) for oxides of nitrogen, catalytic reduction of nontoxic to less toxic gases.

Adsorption at ambient temperature of both chlorine and nitrogen dioxide on activated carbon was found to be rapid with sulfur dioxide being adsorbed to a lesser extent. In exploratory work, nickel oxide and copper oxide were found to exhibit appreciable activity in the catalytic decomposition of nitrogen dioxide. Maximum decomposition of nitrogen dioxide observed (nickel oxide catalyst at 482°C) was 53%. Nitric oxide was the major decomposition product.

Solid-gas reaction was found to be the most generally effective method of contaminant removal.

The solid reactants tested included sodium carbonate, sodium bicarbonate, barium carbonate, calcium carbonate, lithium carbonate, and manganese dioxide. Of these, lithium carbonate and manganese dioxide were the most effective by a large margin for acid gas removal. Manganese dioxide reacts faster with sulfur dioxide and chlorine, and lithium carbonate faster with the hydrogen halides at the temperature of interest (340-380°C). Reaction rates increase rapidly with temperature. The reaction between nitrogen dioxide and any solid tested was too slow for effective removal.

A mathematical model of the solid-gas reaction system, based on the shrinking core concept, was developed. This model served both as a basis for experimental data interpretation and as a design tool. The model, which requires only two experimentally determined constants for each gas-solid pair, adequately fits the breakthrough data on all solid-gas reaction systems investigated.

On the basis of information developed in this study, it is confidently estimated that by using a 11 cm reaction bed containing both manganese dioxide and lithium carbonate, over 88% of the sulfur dioxide and over 99% of the chlorine and hydrogen halides in the entering stream can be removed on a once-through basis for up to 750 hours of operation.

2.0 INTRODUCTION

In a closed system such as a spacecabin simulator or spacecabin, the volume of free atmosphere per inhabitant is extremely small, resulting in large increases in the concentration of contaminants, with addition of only relatively small amounts of the undesired gases. Even in short periods of time, the metabolic processes of man, the decomposition of materials and equipment, and the many interactions, may contribute sufficient quantities of toxic gases to the system atmosphere to exceed allowable limits of concentration.

There are many possible methods of removal of contaminants from closed system atmospheres, including cryogenic condensation, adsorption on high surface area materials, chemical conversion to inert or more easily removed gases, and adsorption with or without chemical conversion. Of these, adsorption on activated charcoal, and chemical conversion by catalytic burning, have proved effective in controlling contaminant concentrations in both submarine and spacecraft atmospheres. Charcoal has fairly high capacity for adsorption of many contaminants, particularly the less volatile ones. Catalytic oxidation is capable, from a potential standpoint, of converting carbon, hydrogen and oxygen containing compounds to carbon dioxide and water, the atmospheric concentrations of which must be controlled by other subsystems. The rates of carbon dioxide and water generation in trace contamination removal is negligible in comparison with rates of generation from metabolic and other system processes. The additional load on the water and carbon dioxide control subsystems resulting from catalytic oxidation of trace contaminants, therefore, is insignificant.

The problem of trace contaminant control is not completely solved, however, by catalytic burning, charcoal adsorption, or the combination of the two. Highly volatile materials may be adsorbed only weakly on activated carbon. Catalytic oxidation over metal oxide catalysts has proved to be effective in the vapor phase oxidation of many organic compounds. Certain gaseous products from the combustion process, however, are toxic in trace concentrations. Nitrogen compounds such as ammonia, hydrogen cyanide, indole, amines, etc., will be oxidized in the burner. The nitrogen containing combustion products will undoubtedly depend upon the nature of the catalyst and processing conditions in the catalytic chamber. Nitrogen can exist in several oxidation states, such as N_2, N_2O, NO, N_2O_3, NO_2, N_2O_4, N_2O_5, and NO_3. It has been reported (1)* that catalytic combustion of nitrogen compounds gives high yields of nitrous oxide (N_2O). Nitrogen dioxide (NO_2), and nitric oxide (NO), are other probable products. Each of these oxides of nitrogen is toxic, affecting skin and eyes, respiratory, digestive or nervous systems. Continuous exposure threshold limit values for concentrations of these contaminants are 0.4, 0.4 and 0.2 ppm for nitrous oxide, nitric oxide and nitrogen dioxide, respectively (2). Ideally, a catalyst which is specific to reactions which yield nontoxic N_2 as the reaction product would be employed.

---

*Numbers in parentheses refer to the list of references included at the end of the report.

2

Other products of the catalytic burner are sulfur dioxide, chlorine, hydrogen chloride, and hydrogen fluoride. The last three are probably derived largely from halogen containing refrigerants and plastics, and could be eliminated by prohibiting the use of such in the spacecraft system. Sulfur dioxide, however, is formed by combustion of sulfur containing compounds such as hydrogen sulfide, mercaptans and organic sulfides, which are products of metabolic processes. Sulfur dioxide is highly toxic, affecting the eyes, respiratory, and nervous system (1). As sulfur dioxide, hydrogen halides, and nitrogen dioxide are all acidic gases, the probability of removing them from the atmosphere by reaction with a basic material was considered high. The term adsorption as used in this report refers to the process of contacting a contaminant-laden gas with a solid material in such a way as to remove the contaminant from the gas.

2.1 Objectives

The objective of the research reported here was to develop a postcatalytic subsystem capable of removing sulfur dioxide, the oxides of nitrogen, and hydrogen halides from the atmospheres of spacecabin simulators. In order to accomplish this objective, the following research and development program was followed:

1. Screening of commercial and laboratory prepared processing agents for the removal of acidic contaminants (SO_2, NO_2, HCl, HF, Cl_2) from the atmospheric gases.

2. Experimental determination of rates of adsorption as functions of processing variables for the most promising agents developed in Phase 1.

3. Study of the reduction of the oxides of nitrogen effected by various catalysts and development of kinetic data on the most promising.

4. Development of quantitative design relationships from which subsystems may be confidently designed for the control of the concentration of acid gases and the oxides of nitrogen in closed atmospheric systems.

Following discussions with the Technical Monitor for this project, (before the subject contract was signed) step 5 in the original proposal (design, construction, and delivery of a prototype adsorber to the Government) was modified to substituting experimental scale-up work required to verify the validity of the design relationships developed for the actual construction and delivery of a prototype adsorber.

Consideration of the overall problem of contaminant removal and the nature of other components of the atmospheric control system of the Integrated Life Support System (ILSS) at the Langley Research Center led to major emphasis being placed on reactions between contaminant gases and solid basic materials. This was felt to be the most direct route for and to hold the greatest promise of the removal of most of the contaminants under consideration. Physical adsorption, although probably insignificant at catalytic burner exit

temperatures, could be profitably employed at other locations within the system where the temperatures are lower. As the activated charcoal beds in most systems now in use may remove some of the contaminants studied, a study of adsorption behavior was believed pertinent to any investigation concerned with contaminant removal. Such a study was performed as part of this research.

Catalytic reduction of the oxides of nitrogen, rather than adsorption, was believed to hold potentially greater promise for the removal of these contaminates. It was recognized from the outset that development of technology for effective contaminant removal in this manner would be relatively difficult to accomplish. Because catalyzed reductions such as these are not well understood and since the degree of success is highly dependent on the amount of experimental effort expended, the research in this portion of the project was intended to be exploratory in nature rather than exhaustive.

2.2 Research Outline

The removal of the oxides of nitrogen and acidic gases from spacecabin atmospheres presents two separate problems. In the original proposal it was assumed that nitrogen dioxide would react with basic materials in much the same manner as the other more acidic gases sulfur dioxide and hydrogen halides. Experimental evidence obtained during this project, however, shows that nitrogen dioxide is much less reactive toward basic materials than was assumed. Since none of the three oxides of nitrogen under consideration could be efficiently removed in the same system as the acidic gases, the next most promising method for removal of these oxides appeared to be catalytic reduction to molecular nitrogen.

2.2.1 Acidic Gas Adsorption. - It is highly probable that the acid gas components of the catalytic burner effluent will consist primarily of carbon dioxide, sulfur dioxide, nitrogen dioxide, chlorine, and hydrogen halides. These gases must be emoved in the contaminant control system. Hydrogen halides, if present, will react more rapidly and irreversibly with basic materials than any other gases present. For this reason, reaction rates and the rates of approach to equilibrium for removal of these gases by scrubbing will not be controlling factors in the adsorber design. This being the case, it was decided in conjunction with the Technical Monitor, that the post-burner development work should be primarily concerned with removal of nitrogen dioxide and sulfur dioxide. Carbon dioxide will undoubtedly be adsorbed by any fresh basic reagent. Since it is less acidic than the other gases, it will be displaced by them and returned to the atmospheric system.

Selection of an adsorbing medium was governed by the rates and equilibria of adsorption of the acid gas contaminants. The search for adsorption materials was restricted to solids since this eliminated the zero gravity separation problem involved in gas-liquid systems. While the development of spaceworthy liquid absorption media is believed possible, it did not appear sufficiently promising at the time this research was initiated to warrant inclusion in this project.

4

Screening studies of adsorbent materials, both commercial and laboratory prepared, were made. The two best contaminant removal agents were selected on the basis of preliminary screening tests and were then subjected to extensive investigations of rate and capacity characteristics for design purposes. Among the materials selected for screening were several low molecular weight carbonates and bicarbonates. These materials were tested in various physical forms: fine powders, granules, pellets, and sintered chunks. These materials were on occasion supported on large-pore alumina to increase the surface area available for mass transfer. In addition, several commercial acid gas removal agents were evaluated.

Since adsorbent capacity can be calculated stoichiometrically, the screening test procedure was designed to discriminate between adsorbents upon the basis of their adsorption rates. Selection of the most promising materials for further study was based on the residual NO_2 and SO_2 in the effluent stream from the adsorber when separate air-SO_2 and air-NO_2 mixtures of standard composition were passed over a standard mass of adsorber at a fixed temperature.

In order to develop information from which an acid gas adsorber could be designed the factors which affect effluent concentration were investigated for the two most effective adsorbents. The effects of the primary variables temperature, contaminant concentration, and space velocity were determined using a fixed bed adsorber through which the contaminant-laden air was passed. The inlet and exit concentrations were determined by analytical methods described in Appendix C. The raw data generated were in the form of exit concentration versus time curves from which gas-solid diffusion coefficients and reaction constants were calculated using techniques described in Chapter 4.0. Experiments were designed to develop information from which predictions of contaminant removal efficiency and adsorber life could be made for given contaminant generation rates and adsorber operation conditions.

2.2.2 Removal of Oxides of Nitrogen. - Of the several oxides of nitrogen which occur in simulated spacecabin atmospheres, the ones of greatest concern are nitrous oxide, nitric oxide, and nitrogen dioxide. Each of these compounds is metastable under either ambient or processing conditions. Thermodynamic consideration of the available physical and chemical data indicates that each oxide can be decomposed to elemental nitrogen and oxygen if an effective catalyst can be found.

Reports in the literature have shown that nitrous oxide can be catalytically reduced at temperatures as low as 300°C (3), and one patent (4) claims complete decomposition of pure nitrous oxide at temperatures of 490°C. The catalysts reported for nitrous oxide decomposition are very similar to those reported for nitrogen dioxide decomposition. Therefore, it appeared that the most promising route to a solution of the problem of removal of the oxides of nitrogen was to search for a decomposition catalyst for nitrogen dioxide. Chemical analysis problems make experimental decomposition data much more difficult to obtain for nitrous oxide than for nitrogen dioxide.

In the initial stages of the experimental work, screening tests for nitrogen dioxide reduction were carried out using the most promising commercial

catalysts. These were composed of copper and nickel oxides. The criterion used in the screening process was conversion of nitrogen dioxide under standard processing conditions.

2.3 Limitations and Restrictions

In order to achieve the objectives of the programs in the most efficient manner, certain limitations were placed on the experimental program. It was not feasible to duplicate the atmosphere of the ILSS with regard to pressure; all work was carried out at essentially atmospheric pressure. Commercial compressed air, free from any measurable amounts of reactive gases, was used in this work. Water and carbon dioxide were added in the test system as required for operation at 50% relative humidity at 295°K and 0.5% carbon dioxide content.

The inlet contaminant concentrations were held below 60 ppm and above 4 ppm in all cases. Working at these levels, while one order of magnitude greater than anticipated in the ILSS, was advantageous from the analysis standpoint. The contaminant levels were high enough so that all analyses could be made in the most accurate regions of the methods for the individual gases and small absolute changes in reactive gas concentration could be more readily observed at high levels than at low levels. It was believed that concentration effects could be confidently extrapolated into lower concentration regions.

For the sake of experimental convenience, the amount of adsorbent and/or catalyst used was from 0.4 to 4.0 g. The reaction bed dimensions were 1 to 5 cm long by 0.94 cm diameter.

Primary emphasis was placed on developing suitable post-burner removal techniques for nitrogen dioxide and sulfur dioxide. This was done because these two compounds are generally much less reactive than chlorine and the hydrogen halides. It seemed logical to assume that any material satisfactory for the removal of nitrogen dioxide and sulfur dioxide would be more than adequate for the removal of the other reactive gases. Once these methods were proved to be satisfactory, they were evaluated with respect to the other project gases.

6

b	=	stoichiometric coefficient of solid, mole solid reacted/mole gas reacted
B_x	=	constant for each contaminant gas, used in calculating calibration curve for converting percent transmittance in ppm
C_A	=	reactant A concentration, g mole/cc
C_{Ag}	=	reactant A concentration in the bulk air stream, mole/cc
C_x	=	contaminant concentration, moles absorbed/liter of colorimetric reagent
D_e	=	apparent diffusivity of gaseous component through the product layer, cm^2/hr
F	=	air flow rate through reactor, g mole/hr
G_M	=	molal velocity based on total reactor cross sectional area; $moles/(hr)(cm)^2$
j_d	=	dimensionless mass transfer number
K_1	=	thermodynamic equilibrium constant = $(P_{NO_2})/(P_{NO})(P_{O_2})^{1/2}$
k_1	=	forward rate constant for reaction 1, mole/hr g cat atm
k_f	=	external mass transfer coefficient, cm/hr
k_g	=	forward rate constant for the solid-gas reaction, cm/hr
M_B	=	equivalent weight of solid, g solid reacted/mole contaminant removed
N_A	=	moles of contaminant A
N_{RE}	=	Reynolds number
N_{SC}	=	Schmidt number
P	=	pressure, atm
P_{NO_2}	=	partial pressure of NO_2, atm
r'	=	local reaction rate, mole/hr/g cat
r	=	particle radius, cm
$\tilde{R}$	=	reaction rate, moles/particle/hr
R	=	outer radius of solid particle
$\%T$	=	percent transmittance
T	=	temperature, °C or °K
t	=	time, hr
v	=	superficial gas velocity through the reactor cm/hr
W	=	amount of catalyst in reactor, g
x	=	fraction of original solid which is unreacted, $(r_c/R)^3$
Z	=	reactor length, cm; also axial position
Δt	=	time increment, hr
ΔZ	=	length increment, cm
ε_B	=	void fraction of packed bed
ε_p	=	void fraction of the solid particle

η = number of solid particles per cm^3

ρ_{bed} = bulk density of the packed bed, g/cc

ρ_{solid} = density of the solid, g/cc

4.0 SIMULATION AND DESIGN OF GAS-SOLID REACTORS

A major overall objective of the present study was to develop the data and techniques necessary to design and predict the operating performance of an acid gas adsorber. In order to economize on the amount of experimental data necessary, it is desirable to develop mathematical expressions which show the quantitative relationship of the principal variables involved in the reactor design and operation. In the following section the mathematical relationships used to correlate the experimental data and simulate mathematically the full scale reactor are developed.

Of the various types of gas-solid contacting arrangements, the one considered in this study is a tubular cylinder packed with granular solid. This type of adsorber is inherently complex from a fundamental standpoint. Both the solid and gas compositions change with time and with position within the reactor; thus, even at constant inlet gas composition and adsorber temperature, the system will reach steady state only after the adsorption capacity is completely exhausted. A mathematical description of the system requires as a minimum the following equations:

1. A material balance accounting for contaminant added to and removed from the gaseous space within the reactor.

2. A material balance accounting for contaminant added to and removed from the solid occupied space within the reactor.

3. An expression describing the reaction rate as a function of the independent variables contaminant concentration, time, temperature, and physical properties of the gas and solid.

Each of these relationships is developed in the following sections. Since heat effects are likely to be insignificant, energy balance, heat generation rate, and heat transfer rate equations are not required.

4.1 Material Balance on the Gas Phase for a Tubular Reactor

As a starting point in the development of a mathematical description of the contaminant removal system, a simple material balance is made on a differential element of the reactor.
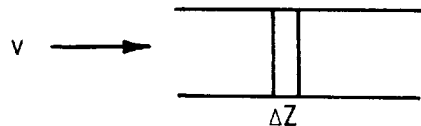
Using a Taylor series approximation of the differential contaminant material balance with truncation of the higher ordered terms and assuming no axial mixing

or gradients in the radial direction, the following expression is obtained:

$$
\begin{bmatrix} \text{contaminant} \\ \text{movement} \\ \text{into} \\ \text{element} \end{bmatrix} - \begin{bmatrix} \text{contaminant} \\ \text{movement} \\ \text{out of} \\ \text{element} \end{bmatrix} = \begin{bmatrix} \text{accumulation} \\ \text{in} \\ \text{gas} \\ \text{phase} \end{bmatrix} + \begin{bmatrix} \text{reaction} \\ \text{with} \\ \text{solid} \\ \text{phase} \end{bmatrix}
$$

$$
- v \frac{\partial C_{Ag}}{\partial Z} = \varepsilon_B \frac{\partial C_{Ag}}{\partial t} + \eta \tilde{R} \tag{4.1}
$$

where

v = superficial gas velocity, cm/hr
C_{Ag} = reactant A concentration in the bulk air stream, mole/cc
Z = reactor length, cm
ε_B = void fraction of bed
t = time, hr
η = number of solid particles per cc
$\tilde{R}$ = reaction rate, moles/particle/hr

In almost all applications the term for depletion of the contaminant in the gas phase is very small compared to the other two terms, thus the material balance may be simply expressed as

$$
v \frac{\partial C_{Ag}}{\partial Z} + \eta \tilde{R} = 0 \tag{4.2}
$$

4.2 Material Balance on the Solid Phase for Fixed Bed Reactor

Using the same approximations as for the gas phase, an unsteady state material balance may be made on the solid reactant. For a differential element of the bed the following expression is obtained:

$$
\begin{bmatrix} \text{depletion} \\ \text{of solid} \\ \text{reagent} \end{bmatrix} = \begin{bmatrix} \text{g of solid} \\ \text{consumed} \\ \text{per mole of} \\ \text{contaminant} \\ \text{removed} \end{bmatrix} \times \begin{bmatrix} \text{movement} \\ \text{of} \\ \text{contaminant} \\ \text{into} \\ \text{element} \end{bmatrix} - \begin{bmatrix} \text{movement} \\ \text{out of} \\ \text{element} \end{bmatrix}
$$

$$
\rho_{bed} \left(\frac{\partial X}{\partial t} \right) = b M_B \qquad v \frac{\partial C_{Ag}}{\partial Z} \tag{4.3}
$$

10

where

x = fraction of original solid unreacted

b = stoichiometric coefficient of solid, moles solid reacted/mole gas reacted

M_B = molecular weight of reactant B, g/mole

ρ_{bed} = density of bed g/cc

4.3 Development of Expression for the Rate of Reaction

Although a complete understanding of the reaction mechanism is not necessary for design purposes, an understanding of the relative resistances of physical diffusion (both external and internal) and of chemical reaction to the overall reaction is important. The rates of gas-solid reactions in which one reactant and one product are solids are particularly susceptible to diffusional resistances. Since diffusional resistances are almost always important, the relatively simple unreacted shrinking core model for solid-gas reactions often gives very good results. This model was developed by Yagi and Kunii (5) and has been successfully applied to several gas-solid reactions (6,7). Further discussion of this and similar techniques may be found in References 8 through 10.

Let the reaction be represented by the equation

$$A(gas) + bB(solid) \rightarrow Products$$
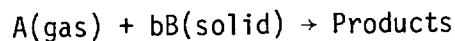
where at least one product is a solid. In the model a spherical particle is assumed with the reaction zone consisting of a thin shell surrounding the unreacted solid. (See Figure 4.1) This shell is initially the outer surface of the solid particle. Later, as the reaction progresses the reaction zone moves into the solid, and a product layer is formed. Since the quantity of the gaseous reactant is extremely small in this study, complications arising from the pellet being non-isothermal need not be considered. The apparent diffusivity of the gaseous reactant (D_e) is considered constant through the product layer. A mass balance for gaseous reactant A gives

$$D_e \left[\frac{\partial^2 C_A}{\partial r^2} + \frac{2}{r} \frac{\partial C_A}{\partial r} \right] = \varepsilon_p \frac{\partial C_A}{\partial t} \tag{4.4}$$

where

D_e = apparent diffusivity of component A through solid B, cm^2/hr

C_A = concentration of component A, mole/cm^3

r = radius axis, cm

ε_p = void fraction of the solid
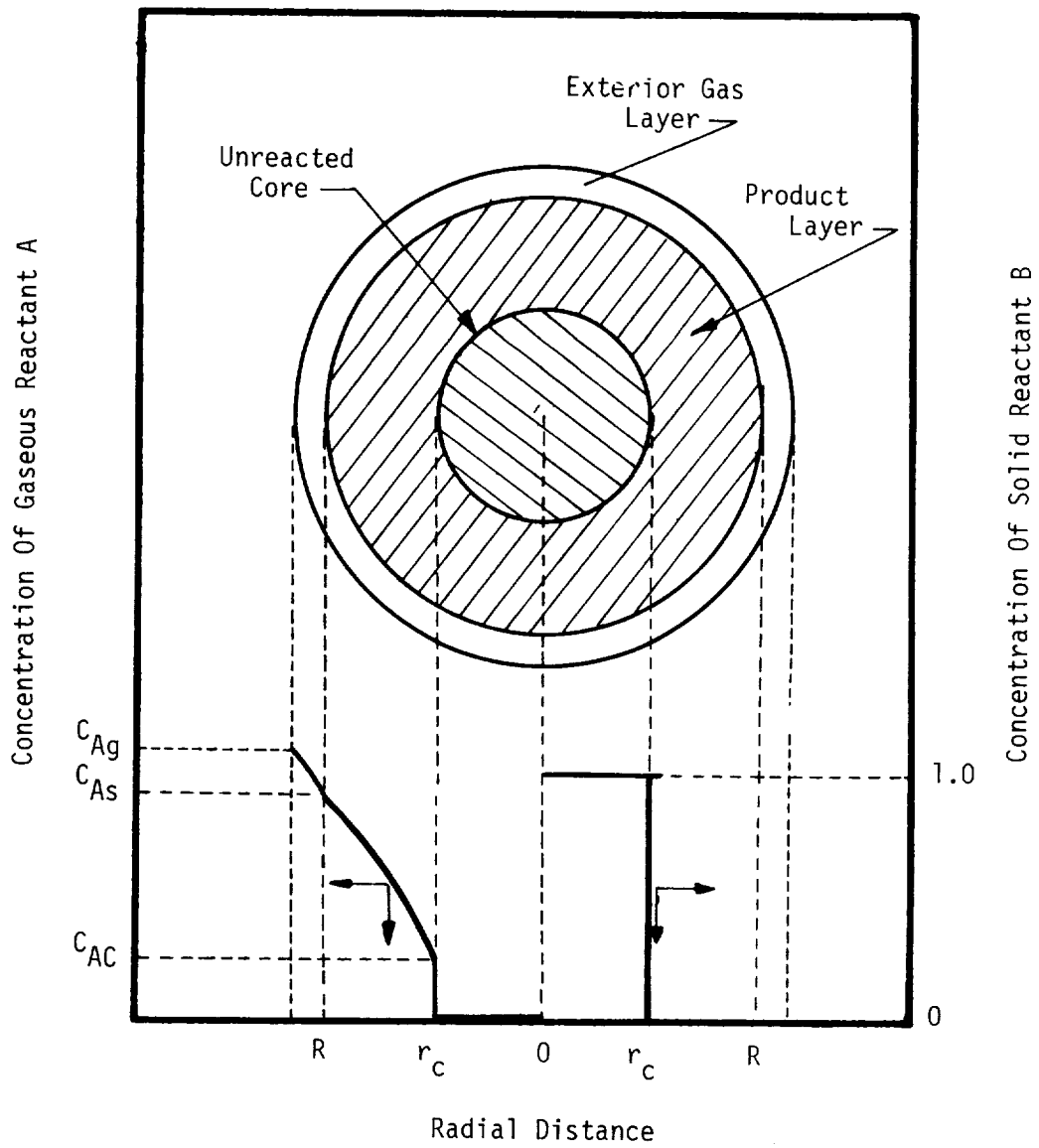
Figure 4.1 - Concentration Profile For Shrinking
Core Model

Since the solid reactant is very slowly exhausted, then a pseudo steady state may be assumed, i.e., the term $\varepsilon_p \, \partial C_A/\partial t$ may be neglected. With this approximation, Equation (4.4) becomes the Cauchy differential equation which may be solved by assuming a solution of the form $C_A = r^m$. The boundary conditions are

$$C_A = C_{AC} \quad \text{at } r = r_c$$

$$C_A = C_{AS} \quad \text{at } r = R$$

where

r_c = radius of unreacted core
R = outer radius of solid particle

and the concentration profile for component A within the solid particle is found by the solution of Equation (4.4) to be

$$\frac{C_A - C_{AC}}{C_{AS} - C_{AC}} = \left[\frac{1 - \dfrac{r_c}{r}}{1 - \dfrac{r_c}{R}} \right] \tag{4.5}$$

For any single pellet the rate of movement of gas A through the external boundary layer is equal to the rate of diffusion through the product layer which in turn is equal to the rate of reaction at the product-reactant interface. If the gas-solid reaction rate can be described by a first order equation, the following three differential equations result

$$\frac{dN_A}{dt} = - 4\pi R^2 k_f (C_{Ag} - C_{AS}) \tag{4.6}$$

$$\frac{dN_A}{dt} = - 4\pi r_c^2 D_e \left[\frac{dC_A}{dr} \right]_{r=r_c} \tag{4.7}$$

$$\frac{dN_A}{dt} = - 4\pi r_c^2 k_g C_{AC} \tag{4.8}$$

where

N_A = moles of component A
k_f = external mass transfer coefficient, cm/hr
k_g = forward rate constant for the reaction, cm/hr

13

By manipulation of Equations (4.4), (4.6), (4.7), and (4.8) the concentration of component A at the core radius may be expressed as a function of the bulk concentration (C_{Ag}) as follows

$$C_{AC} = \frac{C_{Ag}}{k_g \left[(\frac{r_c}{R})^2 \frac{1}{k_f} + \frac{r_c}{D_e} (1 - \frac{r_c}{R}) + \frac{1}{k_g} \right]}$$ (4.9)

Equation (4.9) conveniently shows the manner in which the three series resistances are connected. If the external mass transfer coefficient is large then the first term will vanish, likewise if the diffusivity through the product layer is large then the second term is insignificant.

Assuming a homogeneous solid then the rate of reaction is related to the rate at which the core radius changes by the expression

$$b \frac{dN_A}{dt} = \frac{dN_B}{dt} = \frac{\rho_{solid}}{M_B} 4\pi r_c^2 \frac{dr_c}{dt}$$

where

$$\rho_{solid} = \text{solid density, g/cm}^3$$

The reaction rate per particle, $\tilde{R}$, is obtained as a function of the series resistances and the bulk concentration by substitution of Equation (4.9) into (4.8)

$$- \tilde{R} = \frac{dN_A}{dt} = \frac{4\pi r_c^2 C_{Ag}}{(\frac{r_c}{R})^2 \frac{1}{k_f} + \frac{r_c}{D_e} (1 - \frac{r_c}{R}) + \frac{1}{k_g}}$$ (4.10)

The unreacted core radius can be expressed in terms of the fraction of the unreacted solid, x

$$x = (\frac{r_c}{R})^3$$

$$\tilde{R} = \frac{4\pi R x^{2/3} C_{Ag}}{\frac{x^{2/3}}{k_f} + \frac{Rx^{1/3}}{D_e} (1 - x^{1/3}) + \frac{1}{k_g}}$$ (4.11)

14

4.4 Numerical Solution Technique for Design Equations

By combining Equations (4.2) and (4.11) an equation results which can be used to correlate experimental data and to design a contaminant removal subsystem. As developed in the previous sections the equations are in the form of partial differential equations which must be integrated in order to provide design information.

The method of solution chosen for the project was to convert the differential equations into difference equations containing increments for both the time axis and the reactor length axis. The equation for marching down the length of the reactor at a constant value of time is given by (4.12)

$$C_{Ag}(t, Z+1) = C_{Ag}(t,Z) \, \text{Exp} \left[\frac{-4\pi R^2 n \Delta Z x^{2/3}}{v \left[\frac{x^{2/3}}{k_f} + \frac{Rx^{1/3}}{D_e}(1 - x^{1/3}) + \frac{1}{k_g} \right]} \right] \qquad (4.12)$$

In the above equation the value for the fraction of unreacted solid is taken from the previous iteration, i.e., $x(t,Z)$. The equation for calculation of x for the next time increment is given by (4.13).

$$x(t+1, Z) = x(t,Z) + \frac{M_B v \Delta t}{\rho_{bed} \Delta Z} [C_{Ag}(Z+1, t) - C_{Ag}(Z,t)] \qquad (4.13)$$

The application of Equations (4.12) and (4.13) to either experimental data or to reactor design is straightforward. The physical properties of the packed bed (R, n, ρ_{bed}, M_B) are measured directly. The value for the mass transfer coefficient (k_f) may be calculated as discussed in Section 4.5, thus only two constants $(D_e$ and $k_g)$ remain to be determined from experimental data.

The constants were set at values which resulted in the best fit for one experimental run and then using the same constants the other runs were simulated. The value of the constants for the first data was determined by a trial and error calculational technique. The magnitude of k_g determines the initial reaction rate for a particular system while the value of D_e is related to how well the reaction progresses as more of the solid is depleted. The higher the value of each of these, the faster the reaction progresses. These constants would be expected to be functions of temperature and to a lesser degree pressure, and if the model is applicable they should be independent of such variables as flow rate, contaminant concentration, and reactor geometry.

4.5 External Mass Transfer Coefficient Calculation

Before reaction can occur on the surface of a solid particle the gaseous reactant must move from the bulk air stream through the air "film" surrounding the particle. The concentration gradient established across this gas "film" can

constitute an important resistance to the overall rate of chemical reaction especially for relatively fast reactions such as might be expected with the highly acidic gases and strong bases.

The method of estimating the value of the mass transfer coefficient (k_f) is based on the Chilton and Colburn (11) equation

$$k_f = \frac{j_d G_M}{P} N_{SC}$$ (4.14)

and the correlation for the j_d factor is given (12) by the equation

$$j_d = 1.82 \, N_{RE}^{-.51}$$ (4.15)

where

j_d = dimensionless mass transfer number

G_M = molal velocity, moles/hr cm^2

N_{SC} = Schmidt number

N_{RE} = Reynolds number

P = pressure, atm

These general correlations have been sufficiently well established that they may be used with confidence without experimental verification on the specific system under study.

4.6 Summary of Design Equations

In the previous paragraphs the equations which were used for design of the contaminant removal subsystem have been developed. These equations were incorporated in a computer program for making the exit concentration calculations for the experimental data and for calculating the full scale reactor performance. The actual calculations were made using an IBM 360-40 digital computer. A printout of the program is included in Appendix A. A flow diagram of the program is shown in Figure 4.2 along with the major equations used to make these calculations.

```
┌─────────────────────────────────────────────┐
│   READ INPUT DATA FOR EACH GAS AND BED       │
└─────────────────────────────────────────────┘

┌─────────────────────────────────────────────┐
│    READ INPUT DATA FOR PARTICULAR RUN        │
│       PRINT SELECTED INPUT DATA              │
│                                              │
│    CALCULATE NUMBER OF PARTICLES IN          │
│    EACH BED USING AN ASSUMPTION OF           │
│    SPHERICAL PARTICLE AND FCC PACKING        │
│                                              │
│              CALCULATE                       │
│    AIR VISCOSITY AND MOLAR FLOW RATE         │
│            REYNOLDS NUMBER                    │
│         MASS TRANSFER COEFFICIENTS           │
│                                              │
│           INITIALIZE X AND C                 │
└─────────────────────────────────────────────┘

┌─────────────────────────────────────────────┐
│          I = 1 (I IS TIME COUNTER)           │
└─────────────────────────────────────────────┘

┌─────────────────────────────────────────────┐
│              PRINT TIME                      │
│    PRINT SOLID CONCENTRATION PROFILE         │
└─────────────────────────────────────────────┘

┌─────────────────────────────────────────────┐
│        L = 1 (L IS LENGTH COUNTER)           │
└─────────────────────────────────────────────┘

┌─────────────────────────────────────────────┐
│          M = 1 (M IS GAS COUNTER)            │
└─────────────────────────────────────────────┘

┌─────────────────────────────────────────────┐
│       CALCULATE C(M,I,L+1) FROM              │
│         C(M,I,L) USING EQ 4.12               │
└─────────────────────────────────────────────┘

          M=M+1
┌─────────────────────────────────────────────┐
│    SUBTRACT FROM X THE CONSUMPTION           │
│    RESULTING FROM GAS M USING EQ 4.13        │
└─────────────────────────────────────────────┘

┌─────────────────────────────────────────────┐
│       IF M = NUMBER OF CONTAMINANTS          │
└─────────────────────────────────────────────┘
          NO

  L=L+1
          NO
┌─────────────────────────────────────────────┐
│   IF L = NUMBER OF INCREMENTS IN REACTOR     │
└─────────────────────────────────────────────┘

┌─────────────────────────────────────────────┐
│           TIME = TIME + DEL T                │
│                                              │
  I=I+1         IF TIME = TOTAL TIME           │
       NO                                      │
└─────────────────────────────────────────────┘
                        YES
```

Figure 4.2 - Computer Program Flow Diagram

17

5.0 EXPERIMENTAL SYSTEM

The experimental system consisted of two distinct subsystems. The first subsystem was an atmosphere preparation train capable of providing a reliable supply of synthetically prepared, polluted air of specified composition, humidity, and pressure. The second subsystem consisted of several test sections which could be operated independently of each other. These test sections were designed to provide kinetic and capacity data for both the adsorption studies and the nitrogen dioxide reduction studies.

5.1 Atmosphere Preparation Train

The flow diagram of the atmosphere preparation train is presented in Figure 5.1. The breathable grade air was supplied in commercial compressed air cylinders (Position 1 in Figure 5.1) and was completely oil free. The air contained no measurable amounts of any of the reactive gases used in this study. The air passed through a standard pressure regulator, through a microfilter (Position 2), and then through a flow regulating needle valve (Position 4). Pressure taps were located on each side of the flow control valve (Positions 3 and 5). A Hastings mass flowmeter (Position 6) was used to measure the air flow. After flow measurement, the dry air was then split (Position 7) into two streams. One of these streams was then routed through a flow control valve (Position 8) to a water filled, ceramic packed humidification column (Position 9). A specified humidity was achieved in the final atmosphere through suitable pressure and temperature control within this column.

The original humidifier was a 65 cm long section of 7.6 cm I.D. steel pipe packed with 5 mm glass Raschig rings. Air leaving the humidifier was routed immediately to a 25 cm long x 7.6 cm I.D. steel knock-out drum for removal of any entrained water. With the small humidifier water entrainment in the humidified air was significant; therefore, the original humidifier was replaced with a 150 cm long section of 15.3 cm I.D. steel pipe packed with 1.2 cm ceramic Berl saddles. The increase in cross sectional area in the humidifier lowered the linear air velocity sufficiently so that water entrainment ceased to be a problem.

The humid air (100% relative humidity) was then combined (Position 10) with CO_2 (Position 11) and mixed (Position 12) with contaminated air (Position 13). The CO_2 concentration was adjusted to the desired level by metering in CO_2 through a Brooks rotameter (Position 14) and into the air stream after the humidifier.

The other air stream was passed over a sealed Teflon tube (Position 15) which contained the pure liquid contaminant. The contaminant diffused through the walls of the tube into the flowing air stream. Detailed discussion of the permeation tube contamination method is given in Section 5.2. The stream of contaminated air (Position 16) was mixed with the humid air containing CO_2 (Position 17). The combined air stream (Number 18) then passed through a manifold (Position 19) and was split into constant composition streams for

18
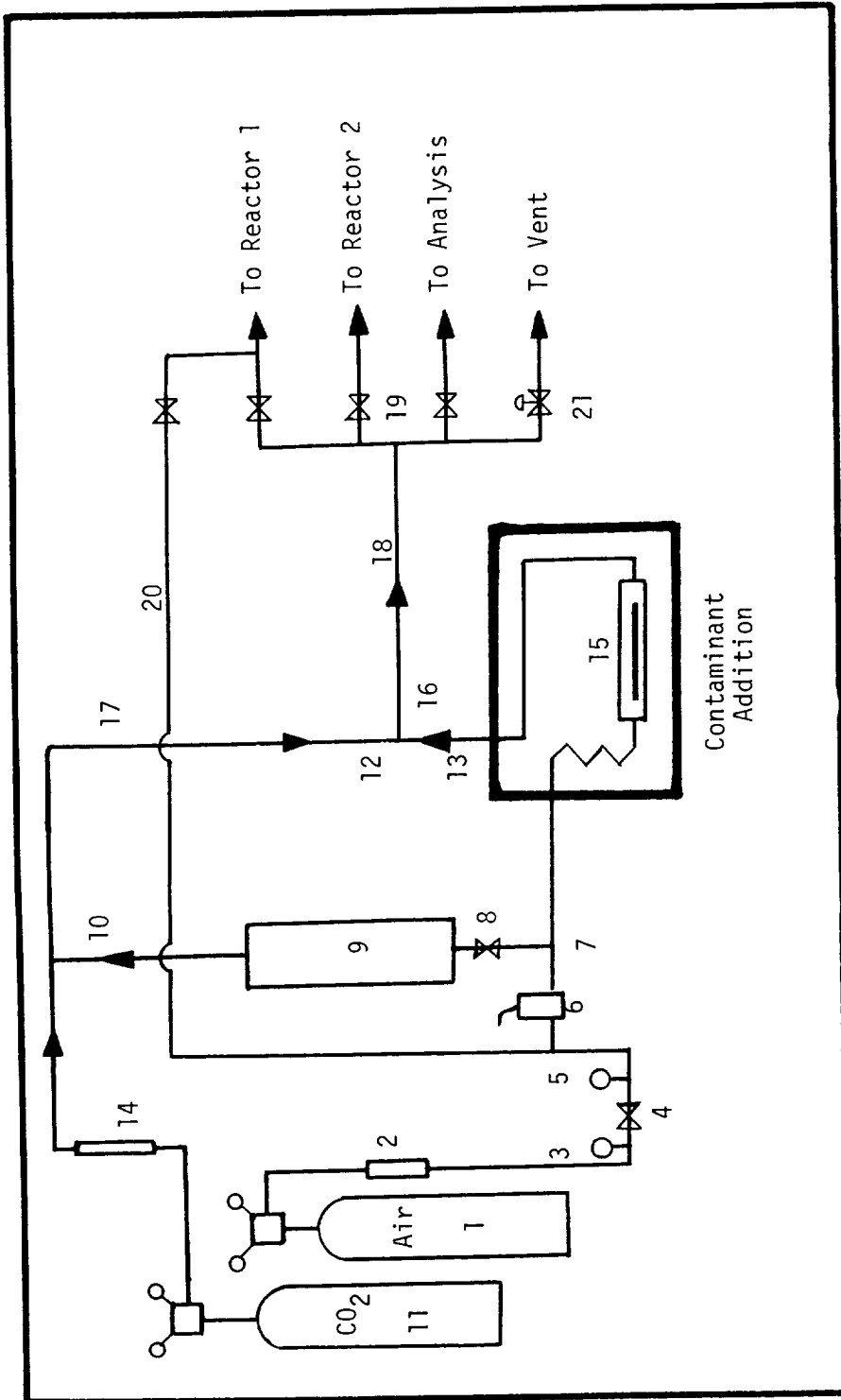
Figure 5.1 - Atmosphere Preparation Train

absorption and kinetic studies. Provision was also made for the installation of a system for forward flush (Position 20) with uncontaminated air. The pressure control valve (Position 21) maintained a constant pressure in the system downstream of the flow control valve (Position 4) and vented any excess contaminated air.

The flow system described above was the result of many minor modifications to the originally proposed system. One of the more serious problems encountered was in the order of addition of H_2O and the contaminant.

In the initial work on the addition of NO_2 by the permeation tube method, humid air was passed through the contaminant addition chamber. Upon investigation of erratic NO_2 addition rates, it was noted that a liquid film had formed on the outside of the permeation tube. It was apparent that this film was inhibiting permeation of the NO_2 and/or was absorbing NO_2 as it passed through. Efforts to correct the situation through mist eliminators ahead of the permeation tube were unsuccessful. It was postulated that the film had its origin in the reaction of water and NO_2 to form nitric acid on the surface of the tube. This nitric acid then adsorbed water from the gas stream and continued to grow thus causing decreases in NO_2 contamination rates. The appearance of the film and variations in contamination rates were eliminated by passing dry air through the permeation tube chamber. The contaminated dry air was then mixed with humid air containing CO_2 in suitable rate ratios to yield the desired air composition. This air had 50% relative humidity at 22°C and contained 0.5% CO_2 and the desired contaminant level.

The humidifier temperature was manually controlled and the temperature of the bath surrounding the permeation tubes was automatically controlled. These temperatures along with other system temperatures were measured and recorded using a Honeywell multipoint recorder.

5.2 Permeation Tubes

The permeation tubes were used in three ways: to provide constant contaminant concentrations for the gas, to serve as direct calibration standards for the various colorimetric analytical determinations, and to prepare low concentration samples for the gas chromatographic column evaluations. Because of the importance of the permeation tubes to the overall project and the skills required in their effective use, they are treated in considerable detail in this section.

5.2.1 Previous Work. - In 1966 O'Keeffe and Ortman (13) proposed Teflon permeation tubes as primary standards for the preparation of standard sources of low concentrations of certain liquefiable gases. These tubes consist of short lengths of Teflon tubing sealed at each end. The liquefied gas is sealed into the tube by forcing steel balls approximately 1.5 times the diameter of the tubing into each end of the tube. The gas diffuses through the walls of the tubing at a very slow rate which is essentially independent of wall thickness. After initial conditioning, the permeation rate remains quite constant, directly dependent on temperature but independent of external pressure changes.

20

The rate is easily measured gravimetrically and depends on the area available for permeation which is a function of length and diameter of the tubing.

Scaringelli, Frey, and Saltzman (14) demonstrated exact equivalence between weight loss and SO_2 diffusion from such permeation tubes by colorimetric techniques. Successful tests were also reported by Thomas and Amtower (15).

5.2.2 Permeation Tube Preparation. - The permeation tube technique for contaminant addition was thought to be very promising. Teflon tubing 0.8 cm O.D., 0.6 cm I.D. was used. Steel ball bearings approximately 0.8 cm diameter were used to make the seals.

The first work was with NO_2, which boils at 22°C, using the method of filling the tubes proposed by O'Keeffe and Ortman (13). A steel ball was placed in each end of a 15 cm segment of tubing. The tube was then squeezed at the ball with pliers in order to create a small filling passage past the ball. Difficulty in venting air from the tube to allow entry of liquid NO_2 was encountered with this method. A much easier method was finally adopted utilizing reduced temperatures to decrease the vapor pressure of the gas. An ice bath produces a temperature well below that of the boiling point of NO_2. A ball was placed in only one end of the Teflon tube and the other end was placed onto the tapered connector on the lecture bottle valve. The lecture bottle was inverted and the Teflon tube placed in an ice bath. Opening the lecture bottle valve allowed liquid NO_2 to run into the cold Teflon tube. Maintaining a loose connection between the tube and the lecture bottle allowed the liquid NO_2 to force the air out of the tube. When the immersed portion of the tube was full, the tube was removed from the ice bath and the top sealing ball was inserted.

The first step in preparing the length of tubing for filling is to stretch the end in which the final ball will be inserted. This enables the final seal to be made more easily when the tubing is cold. The ball is inserted down to its final position (an inch from the end was found adequate) and removed several times.

A ball is then placed permanently two to three centimeters from the other end of the tube. The stretched end is then connected to the lecture bottle and the tube filled as described. The final ball was inserted by removing the tube from the ice bath and using a tapered gas outlet to position the ball quickly without significant warming of the tube. All work was performed under a fume hood. With a minimum of practice, the method was found to be simple and fast.

Only minor modifications were found to be necessary for filling tubes with other gases. A dry ice-acetone bath was necessary when filling SO_2 tubes because of its greater vapor pressure. The end of the tube for the second ball must be very thoroughly stretched before filling the tube, otherwise the increased rigidity of the Teflon tube at -78°C will make the insertion of the ball very difficult. With this one precaution, the method was found equally as simple as working with NO_2.

A dry ice-acetone bath was also used for filling tubes with Cl_2. As Cl_2 has a higher vapor pressure than SO_2, cooling the lecture bottle to -15°C before

filling the tube greatly facilitated transferring the liquid Cl_2 to the tube. Hydrogen fluoride tubes were filled using the same technique as for NO_2.

Single balls were used exclusively to seal the tubes. No problems with leaks or movement of the balls was encountered even with the high pressures produced by Cl_2. Stretching the tube did not noticeably effect the permanence of the seal. Once the tube had been filled and the seal established, however, the ball could not be moved without causing leaks.

5.2.3 Determination of Permeation Rates. - Permeation tubes require at least 24 hours to reach equilibrium after being filled. The permeation rate is not constant during this period because of the time required for complete saturation of the tube walls.

Permeation rates at constant temperatures for the tubes were determined gravimetrically. The filled tubes were weighed on an analytical balance and then placed in a section of 2.54 cm O.D. type 304 stainless steel thin wall tubing. This permeation tube housing was fitted with air inlet and exit ports. This test section was placed in a temperature controlled ($\pm$ 0.17°C) water bath. Air was blown through the housing and over the tubes. The tubes were removed from the housing and weighed periodically. A glass Podbielniak double pass drying tube with a ground glass stopper held in place by removable springs was used as a temporary holder for the permeation tubes. This allowed easy access to the permeation tube for weighing and provides a good flow pattern over the tube.

The weight versus time data for all permeation tubes was linear. Typical examples for NO_2, SO_2, and Cl_2 appear in Figure 5.2. The weight loss was entirely due to permeation of the gas through the tube. Consequently, the tubes were used as standards for preparing known concentrations of the gases for subsequent analytical work with NO_2, SO_2, Cl_2, and HF.

5.3 Adsorption Bed or Catalytic Reactor

Shown in Figure 5.3 is a schematic diagram of a typical adsorption bed or catalytic reactor and auxiliary equipment. Both types of materials were tested in the same equipment. The prepared gas from the atmosphere preparation train was passed through a heating coil to bring the gas to the specified temperature. It then entered the reactor at the bottom and passed upward through the test section. The entering gas pressure was measured using a manometer. The inlet contaminant concentration was periodically determined from gas samples taken by syringe. After leaving the reactor, the gas was cooled and periodically sampled using a syringe. The air then passed through a water filled bubbler which served to saturate the air, prevent reverse flow through the wet test meter and to reduce corrosion on the wet test meter. Volumetric measurement of the exhaust gas was made using the wet test meter. The reactor was heated by a suitable constant temperature bath for all material evaluation tests. For operation in the temperature range of 620°F to 1000°F a molten lead bath was used. Early in the project a molten salt bath was used for operation in the range of 250°F to 600°F. The steel container for these baths was wrapped with two 800 watt beaded electrical resistance heaters and the outside thermally insulated. Each heater

22
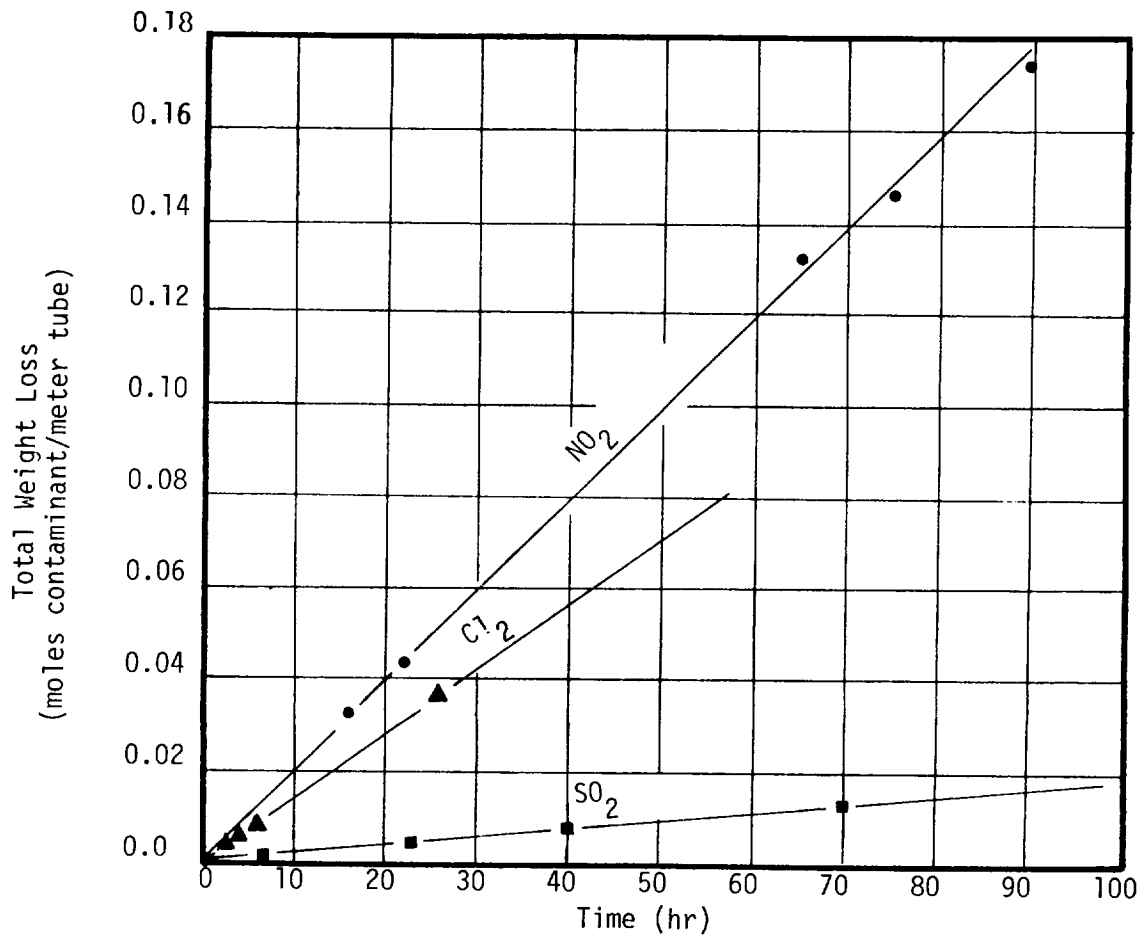
Figure 5.2 – Typical Weight Loss Curves For
Teflon Permeation Tubes
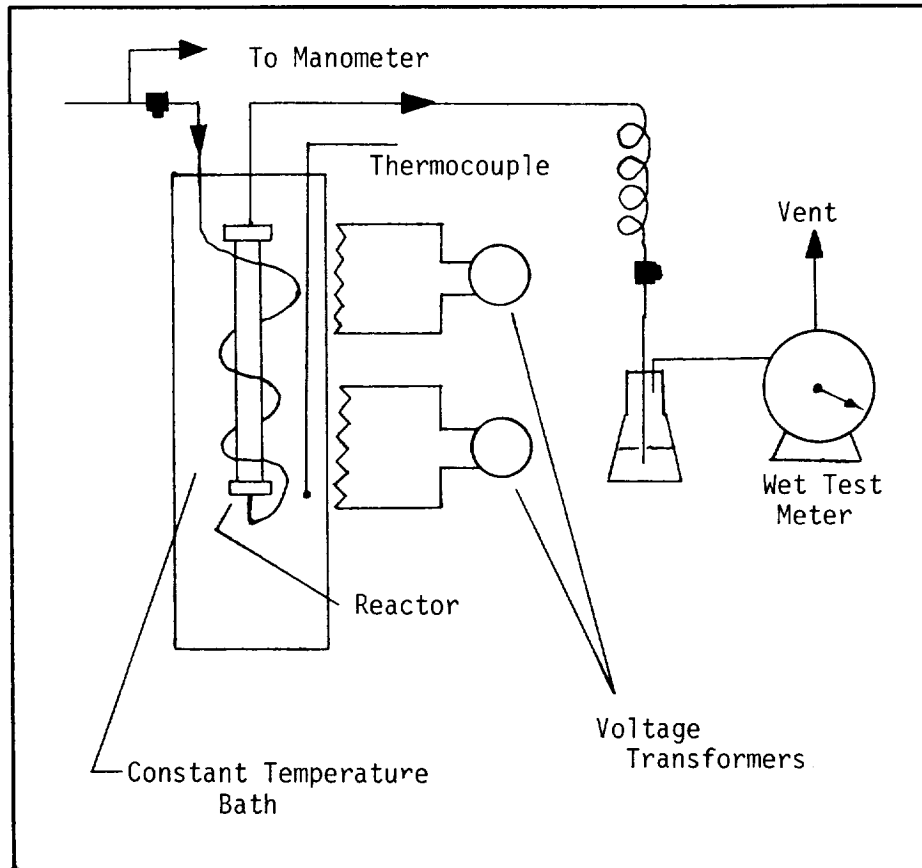
Figure 5.3 - Typical Reactor Assembly

was equipped with a variable voltage transformer which was used to control the heat input to the bath. The bath temperature was monitored using two stainless steel enclosed thermocouples and a multipoint temperature recorder.

The gas entering the reactor was heated using a 10 ft coiled section of 1/4 in. O.D. type 316 thin wall stainless steel tubing submerged in the constant temperature bath. The reactor was a 30 in. section of 1/2 in. O.D. type 316 stainless steel tubing with a wall thickness of 0.065 in. The test section was placed in the bottom of the reactor and consisted of a 1 cm thickness of glass wool, the test material, and a second 1 cm thickness of glass wool.

6.0 ANALYTICAL METHODS DEVELOPMENT

Study of the contaminant removal technique required analytical capability for each reactive gas in the range of 1 to 50 ppm. Each method had to be accurate, precise, simple, rapid, harmless, and inexpensive. Because of the changing value of the effluent concentration, a method was preferred which gave essentially point values, rather than an average value over a time interval. This section contains a brief account of the development of methods that fulfilled those requirements for each of the five gases.

The analytical methods which appeared most promising were colorimetric analysis and gas chromatography. Experimental work was performed in both areas concurrently. Detailed summaries of the previous work are given in Appendix B.

6.1 Colorimetric Analysis

In colorimetric analysis, air containing the contaminant is contacted with liquid reagent to produce a color change in the reagent proportional to the concentration of the contaminant in the gas. This change can be in the form of color development or color bleaching. The color change is measured electronically by a spectrophotometer or colorimeter and the output of the spectrophotometer is converted to concentration of the contaminant by a suitable calibration curve.

The emphasis placed on SO_2 and NO_2 by the United States Public Service as atmospheric pollutants has led to the development and continuous improvement of colorimetric methods for analysis of these contaminants in air. These methods appeared suitable for the initial contaminant absorption studies conducted with NO_2 and SO_2.

The other three gases, Cl_2, HCl, and HF, have not been considered serious problems in air pollution. Therefore, development of colorimetric methods of analysis for these gases in air has been slow. However, colorimetric methods are available for the analysis of chloride and fluoride ions and for free chlorine in water. Because all three gases are readily absorbed in water, it was believed that they could be absorbed from air by an essentially aqueous absorbing and/or color developing reagent.

The calibration data for NO_2, SO_2, and Cl_2 followed Beer's law. One form of that law is:

$$C_x = \frac{4.605 - \ln \%T}{B_x}$$

26

where

C_x = contaminant concentration moles absorbed/liter of reagent

%T = percent transmittance

B_x = constant for each gas

Plotting the log of percent transmittance versus concentration of the gas absorbed in the reagent on semilog paper yields a straight line. Thus, for these three gases, a standard least square fit could be used to determine the constants in the equation. Tables of concentration as a function of percent transmittance were then calculated for each gas from its corresponding equations and were used to minimize errors inherent in reading graphs. In all cases, the calibration equations were forced to go through zero ppm at 100 %T for color developing reactio

6.2 Gas-Reagent Contacting Methods

In colorimetric analysis, the gas can be contacted with the reagent in two general ways: batchwise or continuously. Batchwise analysis with bubblers was developed first. Continuous analysis was investigated concurrently in order to overcome the disadvantages of the bubbler technique. Eventually, sampling and analysis using syringes supplanted both of these methods.

6.2.1 Analysis Using Bubblers. - Bubblers, which disperse the contaminated air through a measured amount of reagent, have been widely used for atmospheric contaminant analysis. The main advantage of the bubbler type contactor is that a very large amount of air may be contacted with a small amount of reagent. The sensitivity can be increased by increasing the amount of air that is sampled. The bubblers were chosen for initial analysis because of their sensitivity and widespread use.

Bubblers are of two types: midget impingers and fritted glass bubblers. Midget impingers produce a fine stream of small bubbles when the gas is forced through a very small nozzle. Fritted glass bubblers concurrently disperse a multitude of small bubbles into the liquid. Saltzman (16) found the midget fritted bubbler highly efficient for NO_2 at concentrations below 1 ppm when using 10 ml of reagent. Meadows and Stalker (17) evaluated the collection efficiency and variability of single and multiple bubblers in series, equipped in each case with either fritted-tip or restricted-opening air dispersers. Although fritted-tip bubblers were found to be more efficient than restricted-opening bubblers, restricted-opening bubblers were preferable because their variability was about half that of the fritted-tip bubblers.

In the experimental work, bubblers were found to have several disadvantages. In order to maintain high absorption efficiency, the flow rate through the bubbler had to be kept below 1.5 cu ft per hour. At concentrations below 1 ppm, the time required to develop a color in a mid-range of the calibration might be as long as one hour. A shorter time was desired in order to obtain more data. At concentrations around 50 ppm, a large volume of reagent was required. If the amount of color developing reagent was too small, the total volume of gas required to produce a color change was so small that the errors in the measurement of the gas volume became significant. These disadvantages could be

partially offset by the use of various size bubblers. Three sizes were used: 10 ml, 125 ml, and 250 ml. The 125 ml and 250 ml Pyrex bubblers used in this study were type 125C and 250C (part No. 31760, Corning Glass Works), respectively. The 10 ml midget Pyrex bubblers were type 5534-10 (Ace Glass, Inc.). By interchanging the bubblers, suitably large gas volumes and short analysis times could be achieved. The bubblers had to be manually interchanged since the valving system available was not extensive enough to permit switching to the appropriate size bubbler if they had been permanently mounted. This manual interchange was inconvenient and required excessive handling of the glassware. Because the bubblers had to be connected into the gas flow system, the choice of location for taking a sample was limited if major rearrangement of the system was to be avoided. The pressure drop through the 250 ml fritted bubbler was approximately 2 psi. This caused undesirable variations in the total system pressure. These problems encountered in use of the bubblers led to attempts to develop a more flexible method of analysis.

6.2.2 Continuous Colorimetric Analysis. - Concurrent with the development of the bubbler technique, attempts were made to develop a continuous analysis system. Continuous analysis has several advantages over batch analysis in obtaining accurate information about a non-steady state system. The contaminant removal systems never reached steady state and it was necessary to determine effluent concentration as a function of time for each material under test. Using the bubbler method it was necessary to take spot samples for analysis at finite intervals of time. Since the exact nature of the breakthrough curves was determined only by the experimental work, bubbler analysis left undesirable gaps in the time-concentration data. With continuous analysis, it was hoped that the concentration of contaminant in the effluent system could be continuously monitored and the results recorded. This would enable changes in concentration to be detected rapidly and easily. The precision of measurement would also probably improve.

Critical analysis of the continuous analyzer components and their functions indicated that the two most critical components are the color measurement device and the gas liquid contactor; consequently, development was concentrated on these items.

A Bausch and Lomb Model 505 visible-ultraviolet spectrophotometer was equipped with a time rate accessory for the purpose of continuous color measurement. Static liquid cells were used for batch analysis and flow-through liquid cells were used for continuous analysis. The difference in color between exposed and unexposed reagent was determined electronically by a differential amplifier in the spectrophotometer. The amplifier output was continuously recorded. The grating optical system permitted a selection of various wavelengths for the light projected through the sample. The instrument could thus be used for the analysis of different acidic gases.

A major criterion for successful continuous colorimetric analysis is minimum lag. That is, the indicated concentration should not be more than, in this case, three minutes behind the true concentration in the reactor or absorber effluent. To achieve this, it is necessary that the gas-liquid contactor used have high absorption efficiency and minimum reagent holdup.

28

Glass contacting columns for scrubbing contaminants have been widely used. Packed columns (18,19,20), concentric glass tubes producing an annular contacting cavity (19,21), and other designs have been used. Atomization into a 1 liter balloon flask with subsequent condensation of the dispersed liquid was used by Schulze (22). Lyshkow (23) proposed a contactor using disks on a rotating horizontal shaft. The lower half of these disks dipped into the reagent while the upper half contacted the gas passing through the scrubber. High absorption efficiency was reported.

For the continuous contact of liquid reagent with contaminated air the contacting column first tried was of the Vigreaux design. The liquid flowed down the column as the dispersed phase while the gas flowed up the column. However, this column proved unsatisfactory because of insufficient contact between gas and liquid which limited the absorption efficiency. The absorption efficiency of the columns was evaluated by placing a fritted bubbler downstream from the column to measure the amount of NO_2 which was passed on through the column.

Several other designs for continuous columns were also investigated. A 3/4 in. column filled with 3 mm glass beads was prepared. Channeling which significantly reduced the contacting efficiency occurred in this column. Two columns packed with 6 mm Raschig rings were prepared: one of these had an inside diameter of 1-3/8 in.; the other one had an inside diameter of 3/4 in. These columns showed high absorption efficiency, but the liquid holdup was too high for the columns to be used. Evaluation was continued on other types of small absorption columns in an effort to find or develop one with high absorption efficiency and low holdup. None was found after expenditure of ι reasonable effort, and the attempt to develop an automatic continuous colorimetric analyzer was thus terminated.

6.2.3 Analysis Using Syringes. - Syringes had been suggested for analysis of higher concentrations (above 1 ppm) of atmospheric pollutants (16,24,25,26). Sampling with 50 ml syringes proved to be very convenient when the analysis involved direct color development with only one step. A small amount of color developing reagent (3 or 5 ml depending on its sensitivity) was drawn into the syringe. Then 47 to 45 ml of sample gas was drawn into the syringe. The syringe was shaken thoroughly to promote absorption of the gas. A period for color development followed the absorption. This period varied from 1 minute for Cl_2 to 3 minutes for SO_2. After color development, the liquid was expelled into a cuvette for colorimetric determination. Because of the small volume of gas used the detection limits for the syringe method were higher than those when using the bubblers. The method, however, was sufficiently sensitive for this research.

The syringe technique has several important advantages. The principal one being that analysis can be made rapidly. Even with the 3 minute color development period for SO_2, samples could be taken every 5 minutes with the same syringe. Three syringes could be easily handled at the same time. This allowed a large number of analyses to be made over a very short period of time.

The concentration range for which the syringes were applicable could be easily adjusted by changing the relative amounts of liquid and gas drawn into

the syringe. Three ml was the minimum amount of liquid which could be used in the B & L "Spectronic 20" colorimeter that was used in this project. This amount was used for Cl_2, SO_2, HCl, and HF in order to have maximum sensitivity. Five ml of reagent was adequate for NO_2 because of that method's greater sensitivity.

Arrangement for sampling at a particular point could be made with a minimum of effort. The gas flow system was built from 1/4 in. O.D. thin wall type 304 stainless steel tubing. Temporary connections from stainless steel to glass were made with short lengths of latex tubing. Samples could easily be taken through the tubing at the connections with a syringe. More permanent sampling locations were easily installed using Swagelok stainless steel tees installed so that the gas flowed straight through the tee. A silicone rubber gas chromatography septum was placed in the side-arm of the tee and sealed (finger tight) between the base of the front ferrule and the nut. Samples were taken through the septum with a syringe. Flows and pressures were such that sampling with a syringe caused no upset in the system.

The detection limit of the syringe was lowered when multiple gas volumes were used with a single reagent charge. While this procedure lowered the detection limit by almost half, the results were not sufficiently reproducible. This technique was discarded and was never used for the routine analysis of gas samples.

Disposable, 50 ml polypropylene syringes were used throughout the project. Each syringe was used for the analysis of only one gas. A new syringe required preconditioning prior to use. The oil used by the manufacturer for lubricating the plunger was removed by rinsing once with acetone. This left enough oil on the plunger so that it was relatively easy to operate. A very high concentration (several thousand ppm) of the gas for which a syringe would be used was then left in the syringe overnight. Reproducible results could then be obtained.

A noticeable effect occurs when the syringes are unused for periods greater than 1 hour. The initial results obtained after such a period indicated a lower concentration than was actually present. If the period between samples was less than an hour, usually only the first sample gave low results. After an overnight period, the first three samples would sometimes be in error. This indicates a very definite surface absorption phenomenon. After these initial samples the results were reproducible.

The plastic syringes gave much more reproducible results than glass syringes made by the same manufacturer. These consistently gave an indicated concentration lower than the actual concentration. They were tried for the analysis of NO_2, SO_2, and Cl_2. The same phenomenon occurred regardless of the amount of pretreatment or how many samples had been taken with the glass syringes. Because of these variations, the polypropylene syringes were selected instead of the glass syringes for routine gas analysis by colorimetric techniques.

30

6.3 Colorimetric Analysis of Nitrogen Dioxide

6.3.1 __Previous Work.__ - Saltzman's modification (16) of the original Griess-Illosvay colorimetric technique (27) for the analysis of NO_2 was the first such method to receive wide acceptance. Since the original development of this method, Saltzman and other workers have made many improvements by a series of modifications. One of the most important of these modifications was the addition of the R-salt by Lyshkow (18) to Saltzman's reagent. This change and others made by Lyshkow to optimize solvent identity, reagent concentrations and pH has resulted in increased color stability and absorption efficiency and the lowering of the color development time from 20 minutes to 1 minute. The lower detection limit for this modified procedure is 0.01 ppm NO_2 when using 1 liter gas samples.

6.3.2 __Experimental Evaluation.__ - The first contaminant removal studies were performed with NO_2. The colorimetric analytical methods for NO_2 were evaluated during the preliminary stages of these studies. The Saltzman method as modified by Lyshkow was selected for the analysis of NO_2. The analyses were performed in bubblers.

An analytical system using two fritted bubblers in series for absorption of NO_2 was used. Systems using one, two, and three bubblers were evaluated. Color was consistently produced in the second bubbler indicating NO_2 absorption but no absorption could be detected in a third bubbler when placed in series with the first two bubblers.

As mentioned earlier, bubblers with three different liquid capacities were used: 250 ml, 125 ml, and 10 ml. The selection of the particular bubbler size required a compromise between length of sampling time and accuracy of analysis. The following approximate guidelines were used: 10 ml bubblers were used for NO_2 concentrations between 0 and 10 ppm; 125 ml bubblers were used for NO_2 concentrations from 10 to 25 ppm; and 250 ml bubblers were used for NO_2 concentrations in excess of 25 ppm. The formula for the color developing reagent was altered slightly from that proposed by Lyshkow (18). He recommended 0.25 ml Kodak Photoflow 200 per liter as a wetting agent. This was to compensate for the reduced foaming resulting from the substitution of tartaric acid for acetic acid. It was found using one-fourth the prescribed amount of Photoflow provided sufficient foaming for good gas-liquid contact but avoided excess foaming which caused liquid carry-over.

The first calibration curves for NO_2 were prepared by volumetrically diluting standard sodium nitrite solutions and then treating these with the color developing reagent. Saltzman (16) found empirically that 0.72 mole of sodium nitrite produced the same color as 1 mole of NO_2 absorbed in water, hence 2.03 µg of sodium nitrite was equivalent to 1 µl of NO_2. Table 6.1 compares NO_2 concentrations as determined by two different methods: bubbler analysis with a calibration curve prepared with the sodium nitrite solutions and concentrations determined from permeation tube weight loss data and gas flow rates in the sample preparation system. The results seem to bear out the findings of Meadows and Stalker (17) as to the variability of the fritted glass bubblers.

Two sets of analyses, as shown in Table 6.1, were made in order to estimate experimental error. For both sets, pressures and flow rates in the sample

31

TABLE 6.1

NO$_2$ CONCENTRATIONS DETERMINED BY BUBBLER

ANALYSIS AND PERMEATION TUBE

Date	NO$_2$ Concentration, ppm; by Tube Weight Loss ($\pm$ 3%)	NO$_2$ Concentration by Chemical Analysis	Reagent Quantity, ml
11-18-67	11.55	14.30	300
11-18-67	11.55	12.78	300
11-18-67	11.55	13.09	300
11-18-67	11.55	12.72	300
11-18-67	11.55	13.41	300
11-21-67	39.20	40.20	300
11-21-67	39.20	37.60	300
11-30-67	38.90	40.90	125
11-30-67	38.90	41.10	60
11-30-67	38.90	39.40	60

preparation system were held constant. The NO_2 concentration in the system was assumed constant. Both sets were made with the 250 ml bubblers. The first set was made at a NO_2 concentration of 11.55 ppm determined from permeation tube weight loss. Five replicate analyses were made during the initial testing of the bubbler assembly. The relative error for the five was:

$$R. \ E. \ = \frac{standard \ deviation}{mean} \times 100 = 5.33\%$$

The second set of analyses, also consisting of five determinations, was made at 39.02 (average) ppm NO_2 after refinements in the analytical technique had been introduced. The relative error was:

$$R. \ E. \ = 3.23\%$$

The rate of color development was investigated for the NO_2 reagent. Immediately upon mixing the sodium nitrite and the color reagent, the solution was placed in the colorimeter. The time was recorded from the point of mixing until the reading on the colorimeter was constant. This was repeated for various concentrations. The mean time for development was 58 seconds. The longest time was 72 seconds and the shortest time was 46 seconds. In the bubbler system that was used, this time was insignificant since the minimum time required for disassembly of the system and transfer of the reagent to the colorimeter was 2 minutes.

Syringes were adopted for analysis of NO_2 during subsequent studies. The advantages of syringes over bubblers for analysis under unsteady state conditions have already been discussed. A color development period of 1 minute was adopted as a result of color development rate studies. The relative error for analysis of NO_2 by syringe was 1.09% at 29.2 ppm. The lower detection limit for NO_2 by the syringe technique was 0.07 ppm. Beer's law is followed to 60 ppm NO_2 in air.

6.3.3 Analysis of Nitric Oxide. - No satisfactory method has been developed for the direct chemical analysis of NO. The determination of NO is usually carried out by oxidation of the NO to NO_2 followed by analysis of the NO_2 with one of the standard methods.

In this research, the NO concentration was determined by difference. The amount of NO_2 in the air stream was first determined by Lyshkow's method. The air was then bubbled through a H_2SO_4-$KMnO_4$ (16,28) solution for oxidation of NO to NO_2. After this step, the air stream was again analyzed for NO_2. The difference between these two values was the amount of NO actually present.

6.3.4 Effect of Interfering Gases on the Analysis of Nitrogen Dioxide. - A five-fold ratio of ozone to nitrogen dioxide causes a small interference, the maximal effect occurring in 3 hours. A ten-fold ratio of sulfur dioxide produces no effect. A thirty-fold ratio slowly bleaches the color to a slight extent. The addition of 1% acetone to the reagent before use retards the fading (16) by forming a temporary addition product with sulfur dioxide. This permits reading

within 4 or 5 hours (instead of the 45 minutes required without acetone) without appreciable differences. The interference of sulfur dioxide can also be removed by chromium trioxide-sulfuric acid impregnated glass fiber paper (29). This method was the most practical of several recently investigated as it is insensitive to atmospheric humidity. It is preferred when using the R-salt modified Saltzman reagent. Once again, the paper is packed into a "U" tube.

The interferences from other nitrogen oxides and other gases which might be found in polluted air is negligible.

6.4 Colorimetric Analysis of Sulfur Dioxide

6.4.1 Previous Work. - West and Gaeke (30) developed a two-step spectro-photometric procedure for the determination of trace quantities of sulfur dioxide in air. The sulfur dioxide was absorbed in a sodium tetrachloromercurate solution and para-rosaniline was used for the color development reagent. The results obtained with the original method were erratic. Several researchers have made improvements in this method not only to increase sensitivity and repeatability of results but also to eliminate interferences from other atmospheric contaminants. As a result of these improvements, this method has become one of the most accurate and reproducible methods for SO_2 currently available. However, the use of the highly poisonous tetrachloromercurate absorbing solution is still required. Lyshkow (23) showed that water could be used as a direct absorbing reagent for SO_2. To accomplish this, Lyshkow used a rotary disc absorber for the continuous absorption of SO_2 in water. He then added the para-rosaniline color developing reagent and colorimetrically determined the amount of SO_2 present in the air sample. The use of the tetrachloromercurate salt was thus completely eliminated. The lower detection limit for Lyshkow's procedure was 0.01 ppm SO_2 with an estimated air sampling rate of 10 liters/min.

6.4.2 Experimental Evaluation. - The syringe technique was adopted for use with the SO_2 analysis because it had so greatly simplified the NO_2 analysis.

As the first part of the experimental work required the analysis for only one gas at a time, the reported interferences of NO_2 and Cl_2 on the SO_2 analysis presented no difficulties. Work was begun with the West and Gaeke method because of its wide acceptance. The modifications of Scaringelli et al. (31) were incorporated into the procedure. The method involved absorbing SO_2 into sodium tetrachloromercurate (II) reagent solution, transferring the exposed reagent to a 25 ml volumetric flask, adding the color developing reagent and diluting to volume. The tetrachloromercurate (II) solution is highly poisonous and is rapidly absorbed through the skin. The dilution to volume step inherently decreases the sensitivity of the method by correspondingly decreasing the color intensity. At this stage in the experimental work, Lyshkow (23) reported the development of a colorimetric method for SO_2 analysis which did not involve mercury salts. For this reason, Lyshkow's modification of the West and Gaeke method was selected for the determination of sulfur dioxide. The method is applicable in the concentration range from about 0.17 to 50 ppm and is not

34

subject to interference from other acidic or basic gases. The reagent and air flow rates were not given.

Ozone and nitrogen dioxide interfere if their concentrations are equal to or greater than that of the SO_2. The interference of nitrogen dioxide can be eliminated by the addition of sulfamic acid to the primary absorbing reagent (32). Sulfur dioxide can be quantitatively determined by this revised method within 48 hours after collection with no SO_2 loss from the sample. Sulfuric acid or sulfates do not interfere. There is no experimental evidence to indicate that SO_3 interferes.

At this point, it seemed that if the SO_2 could be satisfactorily absorbed in water, it probably could be absorbed directly into the para-rosaniline solution, thereby giving a one step procedure with direct color formation in the syringe. A calibration curve was prepared using a permeation tube and careful control of the flow rates. The data were linear on a semilogrithmic plot. The relative error was 2.5%. Because of these results, the method was accepted and used for all subsequent SO_2 analyses.

Using 3 ml of reagent and 47 ml of gas, the method provided a lower detection limit of 0.17 ppm. The method was better in the range of 1 to 33 ppm.

A concentrated para-rosaniline solution was prepared which was stable for 6 months. The working solution was prepared by dilution of the concentrated reagent. It was found to have a shelf life limited to about 1 week. This reagent was replaced whenever the relative analysis error showed significant deviation from that obtained during the initial calibration and standardization procedure.

6.5 Colorimetric Analysis of Free Chlorine

6.5.1 Previous Work. - One of the earliest colorimetric methods developed for the analysis of free chlorine in water used ortho-tolidine as the color developing reagent. This method and many of the methods developed since that time were compared and evaluated by Nicolson (33) on the basis of stability of the colored products, reproducibility, specificity for free chlorine, sensitivity, lower limit of detection, conformity to Beer's law, accuracy, effect of temperature, reagent stability, simplicity, and convenience. He concluded that there is no single method available for the analysis of free chlorine in water which is better than the ortho-tolidine method in the absence of major interferences. Andrew and Nichols (34) used the ortho-tolidine method for the continuous analysis of free chlorine in air. The reported lower detection limit for chlorine was 0.01 ppm when sampling at a rate of 10 liters of air per minute.

6.5.2 Experimental Evaluation. - The ortho-tolidine method was selected for primary evaluation. It offered direct, rapid color development which made it readily adaptable for use in the syringes.

When the reagent concentration recommended by Andrew and Nichols, 0.1 g ortho-tolidine plus 100 ml concentrated HCl per liter, was exposed to 50 ppm Cl_2

in air, a color was formed which faded very rapidly and disappeared completely in less than 5 minutes. Following the recommendations of Chamberlin and Glass (35), the amount of concentrated HCl was increased to 150 ml/liter. This did not alleviate the fading problem.

When a higher concentration of ortho-tolidine agent, 1.0 g/liter, was tried, no detectable color was formed on exposure to 50 ppm Cl_2 in air. As increasing the reagent concentration proved ineffective, the ortho-tolidine concentration was decreased in several increments. The colors produced when using ortho-tolidine concentrations less than 0.1 g/liter were all stable. The optimum concentration of ortho-tolidine was found to be 0.005 g/liter. Reagents prepared using this concentration gave reproducible colors and were stable.

To achieve maximum sensitivity, the minimum amount of liquid, 3 ml, was used in the syringes to absorb free chlorine from a 47 ml gas sample (23°C, 685 mm Hg abs). Under these conditions, the calibration curve showed the lower detection limit to be 0.12 ppm Cl_2 in air. The sensitivity can be increased by increasing the gas volume to reagent volume ratio. This would necessitate using bubblers or continuous analysis as discussed previously.

The manner of drawing the gas sample into the syringe affected the reproducibility of the method. The consistency was improved when the syringe was held above and nearly perpendicular to the gas sample line. In this way the Cl_2 bubbled through the ortho-tolidine reagent in the syringe and was immediately absorbed. Contact of the free chlorine with the syringe walls was thus minimized. This was necessary as free Cl_2 is apparently preferentially absorbed on the walls of the plastic syringe. Reproducibility was also enhanced by thoroughly rinsing the syringes with fresh reagent between each sample. The relative error using the above technique was 11.1% in the range of 0.5 to 50 ppm. Glass syringes did not improve the reproducibility. In fact, the results were significantly poorer.

6.6 Colorimetric Analysis of Hydrogen Chloride

6.6.1 Previous Work. - Iwasaki, Utsumi, and Ozawa (36) used slightly dissociated mercuric thiocyanate in the presence of ferric ions for the colorimetric determination of chlorides. Changing solvents for the color developing reagent and optimizing other parameters led to the development of an improved chloride ion analysis technique by Iwasaki, Utsumi, Hagino, and Ozawa (37). Andrew and Nichols (34) used a different ferric ion source in their revised technique for the colorimetric analysis of HCl in air. The lower detection limit of HCl in air was estimated to be 0.15 ppm when sampling at a rate of 10 liters air per minute.

6.6.2 Experimental Evaluation. - For the evaluation of the various colorimetric methods for HCl analysis, standard samples were prepared gravimetrically from reagent grade NaCl and a constant-boiling HCl-water solution. These samples were prepared to correspond to the amount of HCl which would be absorbed in 3 ml of reagent from a 47 ml gas sample at concentrations of 0.5 to 50 ppm by volume HCl in air.

36

The method reported by Andrew and Nichols (34) was evaluated first since it was the only method which had previously been used for the analysis of HCl in air. The method was found to be completely unsatisfactory when evaluated with the standard samples because of lack of sensitivity. This was due to the small ratio of gas to liquid reagent volume attainable with the syringe technique compared to that of the continuous analyzer used by Andrew and Nichols.

The revised method of Iwasaki et al. (37) was next evaluated and found to be marginally acceptable with respect to sensitivity. The unexposed reagent had a yellow color which deepened to a reddish-brown on exposure to HCl. The absorption maximum occurred at 460 mμ. The use of commercial distilled water containing less than 0.7 ppm total solids significantly reduced the color of the unexposed reagent. The increased solubility of $Hg(SCN)_2$ in the mixed solvent (2 volumes 1,4-dioxane plus 1 volume ethanol) used in this method greatly increased the sensitivity to HCl over that of the Andrew and Nichols method. Sensitivity was also increased by using spectrograde rather than technical grade 1,4-dioxane. Increasing the Fe^{+3} concentration by one-third of the recommended amount resulted in a further sensitivity increase of 25%.

After these improvements had been incorporated into the procedure, a calibration curve was prepared. This curve was prepared using 2 ml mixed reagent plus 1 ml standard solution in each cuvette. The resulting calibration curve is shown in Figure 6.1.

For the analysis of an air stream containing HCl, 2 ml of reagent plus 1 ml of water were used to correspond to the volume of liquid used in the calibration. Because of the flat slope of the calibration curve in the region of 5 to 50 ppm HCl, the relative errors for analysis of samples in this concentration region were quite high. At 35 ppm HCl in air, the relative error was 66% for five determinations. In the low ppm range, 0 to 5 ppm HCl by volume, corresponding to the absorber and reactor effluent concentrations, the relative error was only 8%. This was determined using ten determinations at the 2 ppm HCl in air level. It was thus felt that this method is acceptable for use with low concentrations of HCl in air even though the precision of the method leaves much to be desired at the higher HCl levels. The lower detection limit of this method was found to be 0.5 ppm HCl in air.

6.7 Colorimetric Analysis of Hydrogen Fluoride

6.7.1 Previous Work. - Colorimetric methods for fluoride analysis are of two types: those in which the reagent color is bleached by the fluoride ions and those in which the color is developed by the fluoride ions. The bleaching methods were the first to be developed and included the bleaching action of fluorides on various lakes, salts, and rare earth chelates. Lacroix and Labalade (38) proposed the bleaching action of fluoride ions on ferric sulfosalicylate for the colorimetric analysis. Andrew and Nichols (34) used this reagent for the continuous analysis of HF in air. Their lower detection was estimated to be 0.05 ppm when sampling at a rate of 10 liters of air per minute. One of the most promising color developing methods for the analysis of fluoride ions is that of Bertolacini and Barney (39) who used strontium
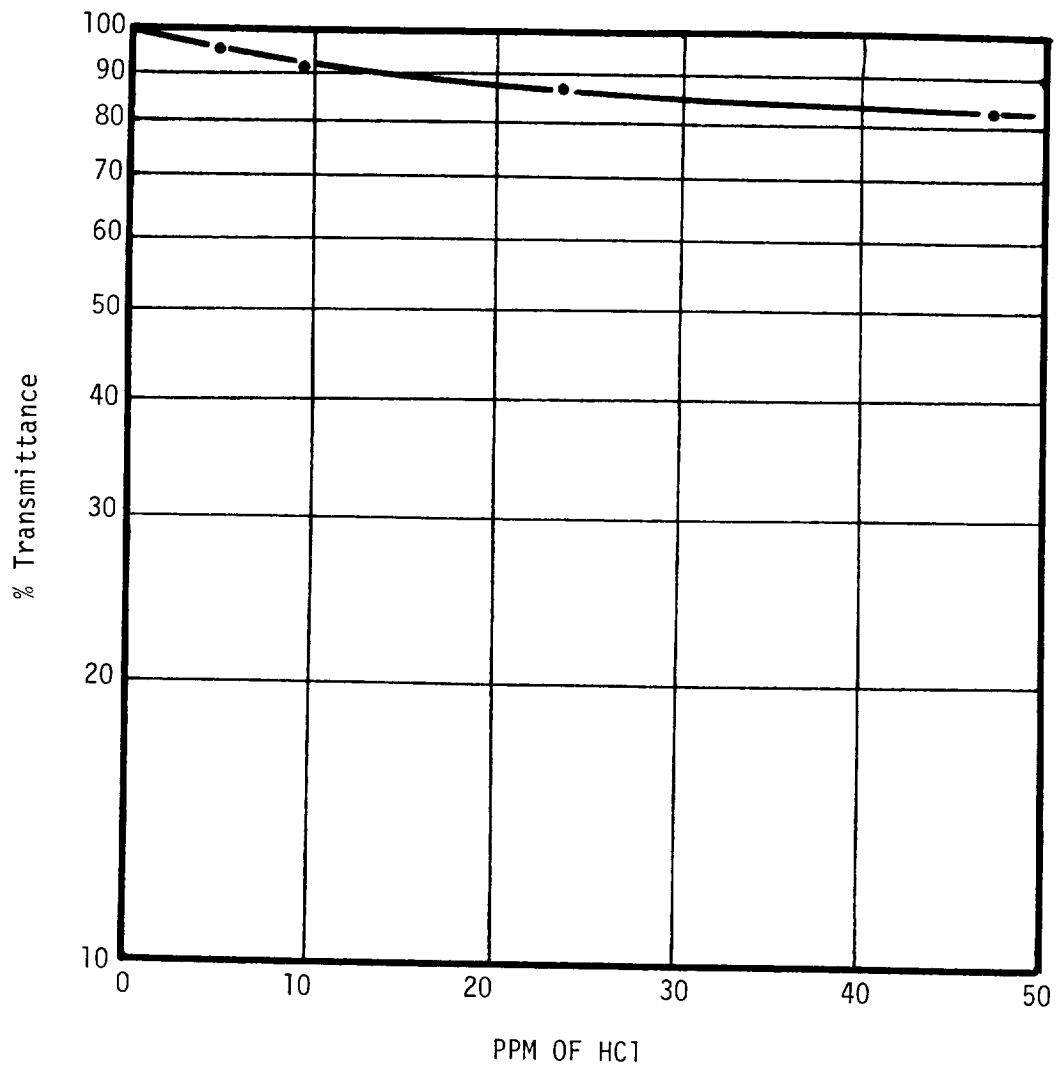
Figure 6.1 - HCl Calibration Curve

chloranilate for the analysis of fluoride ions in water. Even though color developing methods are preferable to bleaching reactions, this relatively unproven technique was not selected for evaluation because the lower detection limit for fluoride was only 5 ppm in water.

6.7.2 Utilization. - The method of Andrew and Nichols (34) was selected for use for the analysis of HF in air for several reasons: it had been previously used for the analysis of HF in air; it had an estimated lower detection limit of 0.05 ppm HF in air; and it involved simple inorganic chemistry. This method was found only marginally usable in the range of 5 to 50 ppm HF in air when using 47 ml gas samples. The bleaching was evaluated spectrophotometrically at 520 mμ. The precision of this method was $\pm$ 1.5 %T which corresponded to a relative analysis error of 16 to 19% depending on the concentration.

Analyses were performed using 2 ml of the fluoride reagent described in Appendix C plus 1 ml distilled water. Calibration standards were prepared using 2 ml of reagent plus 1 ml of standard NaF solution. These calibration solutions were prepared by appropriate dilutions of a standard NaF solution. Even when the unexposed reagent used as a blank was set at 80 %T for 0 ppm HF, the usable colorimetric range was only 14.1 %T. Thus, 47 ppm HF in air corresponded to 94.1 %T.

It was necessary to prepare all reagents with commercial fluoride-free distilled water containing less than 0.7 ppm total solids. The residual fluoride content in laboratory distilled water rendered this colorimetric method unusable because the blank exhibited 92 %T at the absorption maximum of 520 mμ. It was also necessary to rinse all pipets, syringes, and cuvettes five times with fluoride-free distilled water prior to preparing any calibration standard or taking any gas sample of HF analysis.

An attempt was made to verify the HF calibration curve by the permeation tube technique. The effluent HF concentration from the permeation tube housing was calculated from the air flow rate and tube weight loss data. Verification was impossible using pure HF as most of the HF had been removed by the piping before the exit air stream reached the sampling point.

6.8 Gas Chromatographic Analysis

Gas chromatography (GC) is the separation and quantitative analytical measurement of components of complex samples accomplished by passing the mixtures in the gas phase through a separation column. The components of the sample are separated into discrete moving bands by the carrier gas flowing through the column. As the separated components of the sample emerge from the column, they pass into a suitable detector. The analog response produced by the detector is in the form of an elution curve. The heights of the peaks of the elution curve are proportional to the amount of each component present. The elapsed time between the sample injection and the first appearance of the maximum peak height is the retention time and is used for qualitative analysis.

Chromatographic separations are based on purely physical absorption phenomena. Colorimetric methods, however, involve physical absorption of the contaminant followed by chemical reaction to produce the color change. The advantage of gas chromatographic separation and analysis over colorimetric procedures is thus significant. Each compound has an unique retention time under a specific set of operating conditions. Suitable selection of the column packing material provides distinct, reproducible, well spaced peaks for each component of a mixture. No interferences between mixture components is possible as no chemical reactions are involved in the analysis procedure. Thus gas chromatographic techniques are particularly important in the analysis of gas mixtures.

The gas chromatographic development work consisted initially of screening various column packings suggested in the literature for the project gases. The gases of primary interest were NO_2 and SO_2 since these were the limiting compounds in the contaminant removal study. The criterion for column evaluation was their ability to separate SO_2 and NO_2 from other atmospheric constituents such as N_2, O_2, and CO_2, and water and from each other.

After reviewing the current literature on the gas chromatographic separation of the oxides of nitrogen, sulfur dioxide, hydrogen chloride, and chlorine, several chromatographic systems were selected for further evaluation. As this work progressed discussions with other workers in this general area indicated that porous polymeric and silaceous material should also be evaluated for the chromatographic separations of these reactive gases. Table 6.2 lists the columns which were evaluated in this research program. In this screening work on the chromatographic systems all columns were 1/4 in. O.D. 22 gage type 304 or 316 stainless steel tubing except Columns 12, 13, and 18 through 20 which were 1/8 in. O.D. 22 gage wall thickness type 304 or 316 stainless steel tubing. For purposes of this screening study all columns were evaluated using constant samples of sizes of 1 ml of gas. A Varian-Aerograph Model 1520-1B gas chromatograph was used throughout the screening program. The detector used in all these evaluations was of the hot wire thermal conductivity type.

The results of the screening studies for these chromatographic columns are shown in Table 6.3. These entries represent only the best separations which were obtained when each chromatographic system was evaluated qualitatively with respect to the project gases at several different temperatures and flow rates.

Table 6.4 presents the separations obtained with these chromatographic systems and their corresponding operating conditions. Plus signs in the separation columns of the table indicate that those compounds were not separated from each other, i.e., they appeared as a single peak. Commas in this portion of the table indicate that those compounds were successfully separated. As an example, consider the entry for Column 10. Air, CO_2, and N_2O appeared as a single peak which was separated from individual peaks of NO, SO_2, and NO_2. From the data in Table 6.4 it is seen that three systems, Columns 11, 13, and 18 were satisfactory for the qualitative analysis of several of the project gases. Column 18 was the best single column for all the project gases. Columns 7 and 8 were the only ones which gave reproducible retention times and peak shapes for NO_2. Column 7 was slightly better than Column 8 with regard to peak shapes. The lower detection limits for these columns when using thermal conductivity detectors and 1 ml gas samples was 300 ppm.

40

TABLE 6.2

SPECIFICATIONS OF GAS CHROMATOGRAPHIC COLUMNS

Column Number	Partitioning Agent	Solid Support	Mesh U.S. Std.	% Liquid Loading	Length Ft.	Reference Number
1	Silicone Oil SF-96	Chromosorb T	40/60	10%	10	40
2	Triacetin	Chromosorb T	40/60	10%	10	41
3	Di-n-decyl Phthalate	Chromosorb T	40/60	10%	10	42
4	Arochlor 1232	Chromosorb T	40/60	10%	10	43
5	QF-1-(FS 1265)Flouro	Chromosorb T	40/60	10%	10	
6	Silicone XE-60 (Nitrile)	Chromosorb T	40/60	10%	10	
7	Flourolube HF 1200 Grease	Chromosorb W, AW, DMCS	40/60	10%	10	
8	Kel F 90 Grease	Chromosorb W, AW, DMCS	60/80	10%	10	44
9	Halocarbon 11-14	Chromosorb W, AW, DMCS	60/80	10%	10	
10	Silicone DC 200 Oil	Chromosorb W, AW, DMCS	60/80	10%	10	45
11	H_3PO_4	Porapak Q	80/100	3%	6	46
12	None	Polypak 1	80/120	N/A	6	47
13	None	Polypak 1	80/120	N/A	3	47
14	Di-n-ethyl-hexyl Adipate	Chromosorb W, AW	30/100	10%	10	48
15	None	Porapak Q	80/100	N/A	6	49
16	None	Porapak QS	80/100	N/A	6	50
17	None	Porasil B	80/100	N/A	6	50
18	Arochlor 1232	Porapak Q	50/80	5%	8	51
19	Arochlor 1232	Porapak R	50/80	5%	8	51
20	No. 18 in Series with No. 19	Porapak Q + R	50/80	5%	16	52
21	None	Porapak Q	50/80	N/A	8	49

TABLE 6.3

SUMMARY OF GAS CHROMATOGRAPHIC RETENTION DATA

Retention Times for Separated Compounds, Minutes

Col. No.	Temp. °C	Flow Rate ml/He min.	Carrier Gas Inlet Pressure psig.	Air	CO_2	N_2O	NO	NO_2	SO_2	Cl_2	HCl
1	32	20	20	2.85		3.52		4.56	4.65		
2	30	10	20	4.83	6.60	6.36		6.42	6.45		
3	35	20	20	2.55	3.09	3.12		2.07	3.00		
4	35	20	20	3.00				8.60	7.60		
5	100	16	20	2.89	3.07	3.08	3.25	3.00			
6	35	20	20	2.64				4.35			
7	32	10	32	3.04	3.04	3.04	3.04	3.42	3.18	3.31	3.04
8	32	10	20	1.10	1.12	1.12	1.12	1.43	1.25	1.25	1.16
9	33	4	80	1.92	2.17	2.21	1.92	4.61	2.97		
10	35	19	40	2.70	2.79	2.85	3.13	4.22	3.36		
11	30	27	20	2.00	6.80	8.85	2.22	>20			
12	30	20	100	1.11			1.98	2.42	2.02		
13	30	10	65	1.40		1.92	6.30	12.60	4.81		
14	30	20	70	3.00		3.84		3.51	3.60		
15	30	40	50	1.20	3.66	4.80		3.75	3.60		
16	30	40	50	1.05				3.30	3.30		
17	100	50	40	0.90				0.90	0.90		
18	100	10	30	0.81	1.07	1.07	0.81	7.20	4.95	5.13	2.55
19	100	50	20	0.40	0.40	0.40	0.40	1.45	1.15		
20	35	20	70	1.60		4.57	1.95	8.05			

TABLE 6.4

SUCCESSFUL QUALITATIVE GAS CHROMATOGRAPHIC SEPARATIONS

Column No.	Separations
1	air, CO_2, NO_2 + SO_2
2	air, N_2O + NO_2 + SO_2, CO_2
3	air, NO_2, CO_2 + N_2O + SO_2
4	air, NO, NO_2, SO_2
5	air, CO_2 + N_2O + NO_2
6	air, NO_2
7	air + CO_2 + N_2O + NO + HCl, NO_2, Cl_2, SO_2
8	air + CO_2 + N_2O + NO + HCl, SO_2 + Cl_2, NO_2
9	air + NO, CO_2 + N_2O, NO_2, SO_2
10	air + CO_2 + N_2O, NO, SO_2, NO_2
11	air, NO, CO_2, N_2O, NO_2
12	air, NO + SO_2, NO_2
13	air, N_2O, NO, SO_2, NO_2
14	air, SO_2 + NO_2, N_2O
15	CO_2 + NO_2 + SO_2, N_2O
16	air, NO_2 + SO_2
17	air + NO_2 + SO_2
18	air, CO_2, NO, SO_2, Cl_2, NO_2
19	air + CO_2 + N_2O + NO, SO_2, NO_2
20	air + NO, NO_2, CO_2 + N_2O, HCl, SO_2, Cl_2

43

As the lower detection limit using thermal conductivity detectors for most of these reactive gases is in the vicinity of 300 to 500 ppm when using a 1 ml gas sample, it was necessary to have a much more sensitive detector before quantitatively evaluating these chromatographic systems. An electron capture detector was procured for this purpose. When the electron capture detector was used in conjunction with Column 18 for the low level analysis of SO_2 and chlorine in air, the lower detection limit for SO_2 in air when using a 1 ml gas sample was 2.2 ppm; that for chlorine was 3.3 ppm. This was significantly different from the random instrument noise level. However, these detection limits were well above those of the colorimetric methods for SO_2 and Cl_2. Further evaluation of this system with respect to NO_2 was disappointing. Under the optimum separation conditions, the lower detection limit for NO_2 was 200 ppm in air. Not only was the electron capture detector not sufficiently sensitive, but it was also unstable. It was very sensitive to minor variations in flow rate and temperature which severely affected the reproducibility.

Because of these detector problems further development work on chromatographic methods was terminated. If sufficiently low detection limits could have been obtained, then optimum utilization of the gas chromatographic technique could have been achieved by standard industrial process chromatography methods. The gas sample would be sent through Column 7 for initial separations. The first peak contains air, CO_2, N_2O, NO, and HCl. This composite peak is followed by individual peaks for SO_2, Cl_2, and NO_2 in that order. The first two of the last three compounds are not completely separated on this column. The composite peak and the SO_2 and Cl_2 peaks would then be routed to Column 18 for complete separation. Quantitative analysis would be obtained for CO_2, N_2O, NO, HCl, SO_2, and Cl_2 on Column 18 and for NO_2 on Column 7. It is recommended that this chromatographic effort be pursued further since it offers high promise of success in the quantitative analysis of multi-contaminant samples containing air.

44

7.0 EXPERIMENTAL DATA FOR THE REACTION OF ACID GASES WITH SOLID MATERIALS

During this study experimental reaction rate data were obtained for the reaction between various bases and the gases nitrogen dioxide, sulfur dioxide, chlorine, hydrogen chloride, and hydrogen fluoride. These data consist of exit contaminant concentration versus time curves for a single contaminant gas with constant temperature and flow rate. Most of the data were collected at a temperature of 342°C (650°F) which would closely approach the minimum expected catalytic reactor effluent temperature. All of the reactions observed proceeded at a higher rate as the temperature was increased.

Because of the problems associated with zero gravity gas-liquid separation, aqueous solutions of basic materials were not tested even though there are several solutions which are known to be very effective for the removal of acidic gases from air.

7.1 Characteristics of Solid Materials

The initial screening tests were performed using powdered reagent grade solids except in the case of the manganese dioxide. By using the readily available powdered form of the bases it was thought that the maximum performance of any particular material would be measured with minimum interference due to the differences in particle size and porosity.

Lithium carbonate was shown to be one of the most reactive bases tested and because of its low molecular weight would appear to be a logical choice for inclusion in any acid gas removal system. The only physical form of Li_2CO_3 generally available is a very fine powder which is obviously not suitable for use in a closed system. Pressed pellets have also been found to be unsuitable. A satisfactory granule was made by sintering a mixture of 90% Li_2CO_3 and 10% $CaCO_3$ powder at 1150-1200°F for 4 to 5 hours. The sintered mass was crushed and screened to obtain the desired particle size. The bulk density of 12-14 mesh particles made in this manner was measured at 0.78 g/cc.

The manganese dioxide used in this study was exclusively Mallinckrodt "Multisorb" manganese dioxide gas absorbent. This material is granular with an average particle size of approximately 0.16 cm and bulk density between 0.45 g/cc and 0.53 g/cc. A comparison with other grades of MnO_2 was not made; however, laboratory samples of a technical grade MnO_2 appeared to have a much higher bulk density.

In the project proposal it was stated that several basic materials would be supported on high surface area materials such as alumina and shredded asbestos. Attempts to make these supported reactants showed that even using highly soluble bases the maximum base content obtainable was about 15-20%. Since experimental evidence showed that unsupported basic materials such as manganese dioxide and lithium carbonate have sufficient porosity to permit an acceptable reaction rate, it was concluded that the supported bases are non-competitive due to the large percent of unreactive supporting material required.

45

7.2 Removal of Nitrogen Dioxide Through Reaction With Solid Basic Materials

Nitrogen dioxide (NO_2) is a relatively high boiling (21.1°C) oxidizing gas which reacts with water to form nitric acid and nitric oxide (NO) according to the stiochiometric equation:

$$3 \ NO_2 + H_2O \rightarrow 2 \ HNO_3 + NO$$
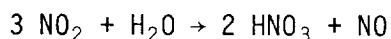
One of the primary assumptions made early in this study was that the acidic nature of NO_2 would permit its chemical removal through reaction with a solid basic material such as lithium carbonate.

$$2 \ NO_2 + Li_2CO_3 \rightarrow LiNO_3 + LiNO_2 + CO_2$$
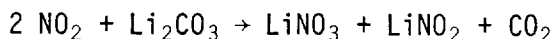
Screening tests were made to find a base which would undergo rapid reaction with NO_2 to form a solid nitrate and/or nitrite salt. Shown in Table 7.1 are the materials screened and the conditions for the tests. Of these materials, although several showed some initial reactivity, none removed NO_2 at an appreciable rate for a period longer than approximately 1 hour. All of the tests were made with air containing approximately 0.013 mole of water per mole of dry air. It is thought that the reactions proceed at a faster rate in humid air than in dry air.

The conclusion drawn from these tests is that gaseous NO_2 is not sufficiently acidic to be removed efficiently through reaction with solid bases. Experience in this work indicated that NO_2 does react with many organic materials particularly in a humid atmosphere. Large losses of NO_2 were noted when air containing NO_2 was passed through latex tubing or Tygon tubing. Silicone and hydrocarbon greases also cause removal of NO_2. This removal is presumed to be due to the well known oxidizing power of NO_2 in which the gas is reduced to NO.

Any NO_2 produced in a spacecabin will certainly tend to react with the hydrocarbon materials within the cabin and these will tend to reduce the ambient concentration of this contaminant; however, a control system will probably still be necessary. The most promising NO_2 removal methods appear to be absorption on activated carbon which is discussed in Chapter 8.0 and catalytic reduction to nitrogen and oxygen which is discussed in Chapter 9.0.

7.3 Removal of Sulfur Dioxide Through Reaction With Solid Basic Materials

Sulfur dioxide (SO_2) contaminated air is a serious problem to be considered any time a closed life support system is to be operated since sulfur dioxide is easily produced through the combustion of sulfur containing compounds. Typical SO_2 precursers produced within the life support system are hydrogen sulfide and mercaptans. This contamiant has been detected in the atmospheres of submarines and in life support test beds (53,54,55). Sulfur dioxide is known to react with several solid basic materials among which are calcium carbonate, manganese dioxide, magnesium oxide and calcium oxide. The alkali or alkaline earth oxides

46

TABLE 7.1

CONDITIONS FOR THE EXPERIMENTAL RUNS MADE TO MEASURE NITROGEN DIOXIDE REACTIVITY

| Run Number	2-27-1	2-20-1	2-24-1	2-27-1	2-27-2	2-28-1	2-29-1	8-2-1	8-12-1
Material	$K_2CO_3 \cdot 1\,1/2\,H_2O$ 6-12 Mesh	Bottom Layer from MSA GMB-SS Canister	Na_2CO_3 6-12 Mesh	Li_2CO_3 200 Mesh	Li_2CO_3 on 1/8" Alumina	MnO_2	Li_2CO_3 200 Mesh	Fused Li_2CO_3 12-14 Mesh	MnO_2
Amount of Packing, g	3.0641	2.9008	2.8117	2.7963	3.2712	2.8677	2.7959	0.401	1.0
Bed Temperature, °C	188	192-342	342-388	27	199-207	185-194	244-430	342	342
Air Flow Rate, mole/hr	1.2	1.2	3.7	4.66	3.7	2.0	2.0	5.49	8.3
Air Pressure, atm	0.9	0.9	0.9	1.25	0.9	0.9	1.0	0.9	0.9
Inlet Concentration, ppm of NO_2	37	37	40	37	37	37	38	26	39
Test Duration, hr	49	22	24	18	17	6	5	2	2
Minimum Outlet Concentration, ppm of NO_2	14	11	36	36	33	35	27	18	32

Bed Diameter = 0.94 cm ---- CO_2 Concentration = 0.5 mole %
Humidity = 0.013 ± .001 mole H_2O/mole dry air

were not tested for reactivity since in the presence of carbon dioxide and high humidity they undergo reaction to form the carbonate or bicarbonate.

Screening tests were made on the following materials in order to determine their relative effectiveness as SO_2 removing agents: manganese dioxide, lithium carbonate, sodium carbonate, sodium bicarbonate, calcium carbonate, and barium carbonate. Of these compounds, although each one reacted to some extent, manganese dioxide and lithium carbonate were by far the most promising at the conditions of the test. Shown in Table 7.2 are data on those materials which were tested and deemed unsuitable and the conditions of the screening test. The superiority of manganese dioxide and lithium carbonate may be seen in Figure 7.1 where the fraction of SO_2 passing through the bed is plotted versus the fraction of the solid which has been reacted for each solid. The conditions are uniform for all of the runs on the plot except for the one run at 415°C (780°F) with lithium carbonate. As may be noted, this higher temperature is required before lithium carbonate becomes competitive with manganese dioxide from a reaction rate standpoint. All of the materials used in the screening tests except MnO_2 were in the form of very finely ground powder. Also of interest is the very poor performance of $CaCO_3$ under the conditions of this test.

After manganese dioxide and lithium carbonate were singled out as being the most promising materials more data was collected on each. These materials are discussed separately in Section 7.3.1 and 7.3.2.

7.3.1 Sulfur Dioxide Reaction With Manganese Dioxide.

7.3.1 Sulfur Dioxide Reaction With Manganese Dioxide. - Manganese dioxide reacts readily with trace amounts of SO_2 in air at a temperature of 342°C (650°F). The reaction (which is an oxidation-reduction reaction) is given by the stoichiometric equation:

$$SO_2 + MnO_2 \rightarrow MnSO_4$$
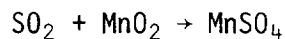
which results in the theoretical capacity of 0.736 g SO_2/g MnO_2. The equilibrium partial pressure of SO_2 in the presence of MnO_2 at 342°C is equivalent to less than 0.002 ppm; thus at this temperature there is no practical thermodynamic limitation on the removal of SO_2 with MnO_2. The reaction is exothermic and the equilibrium concentration of SO_2 increases with increased temperature.

Shown in Table 7.3 are the conditions for eight experimental runs made using MnO_2 to remove SO_2. As may be noted from the table, the principal varibles were extended over a rather wide range. One run (4-25-2) was made to test the low temperature (27°C) adsorptive capacity of MnO_2. This capacity was found to be rather high and thus could be of potential value. No further work was undertaken however since the high temperature reaction was thought to hold greater promise. The other seven runs were made to provide information on the high temperature reactivity of MnO_2 with SO_2.

The shrinking core mathematical model developed in Chapter 4.0 was applied to the reaction data and the best values for the two required constants were determined. At the base temperature of 342°C (650°F) the best values for the two constants were determined from Run 7-15-1 and the values were

48

TABLE 7.2

CONDITIONS FOR EXPERIMENTAL DETERMINATION OF SULFUR

DIOXIDE REMOVAL EFFICIENCY OF VARIOUS BASES

Run Number	5-10-1	5-14-1	5-15-1	5-18-1
Packing Material	$NaCO_3$ Granular	$NaHCO_3$ Powder	$CaCO_3$ Powder	$BaCO_3$ Powder
Amount of Packing	0.4000	0.4000	0.4000	0.4000
Bed Diameter, cm	0.94	0.94	0.94	0.94
Bed Temperature, °C	342	342	342	342
Air Flow Rate, mole/hr	6.0	6.0	6.0	6.0
Air Pressure, atm	0.9	0.9	0.9	0.9
Contaminant	SO_2	SO_2	SO_2	SO_2
Inlet Concentration, ppm	15	14	13-14	10
Humidity, mole/mole	0.0144	0.0144	0.0144	0.0
CO_2, mole %	0.5	0.5	0.5	0.0
Test Duration, hr	3.6	7.8	2.0	2.8
Minimum Exit Concentration, ppm	1.3	1.7	8.1	5.2
Theoretical Capacity g SO_2/g packing	0.602	0.762	0.64	0.325
Average Bed Loading g SO_2/g packing	0.0168 after 3.6 hr	0.0387 after 7.8 hr	0.0033 after 2.0 hr	0.0055 after 2.8 hr
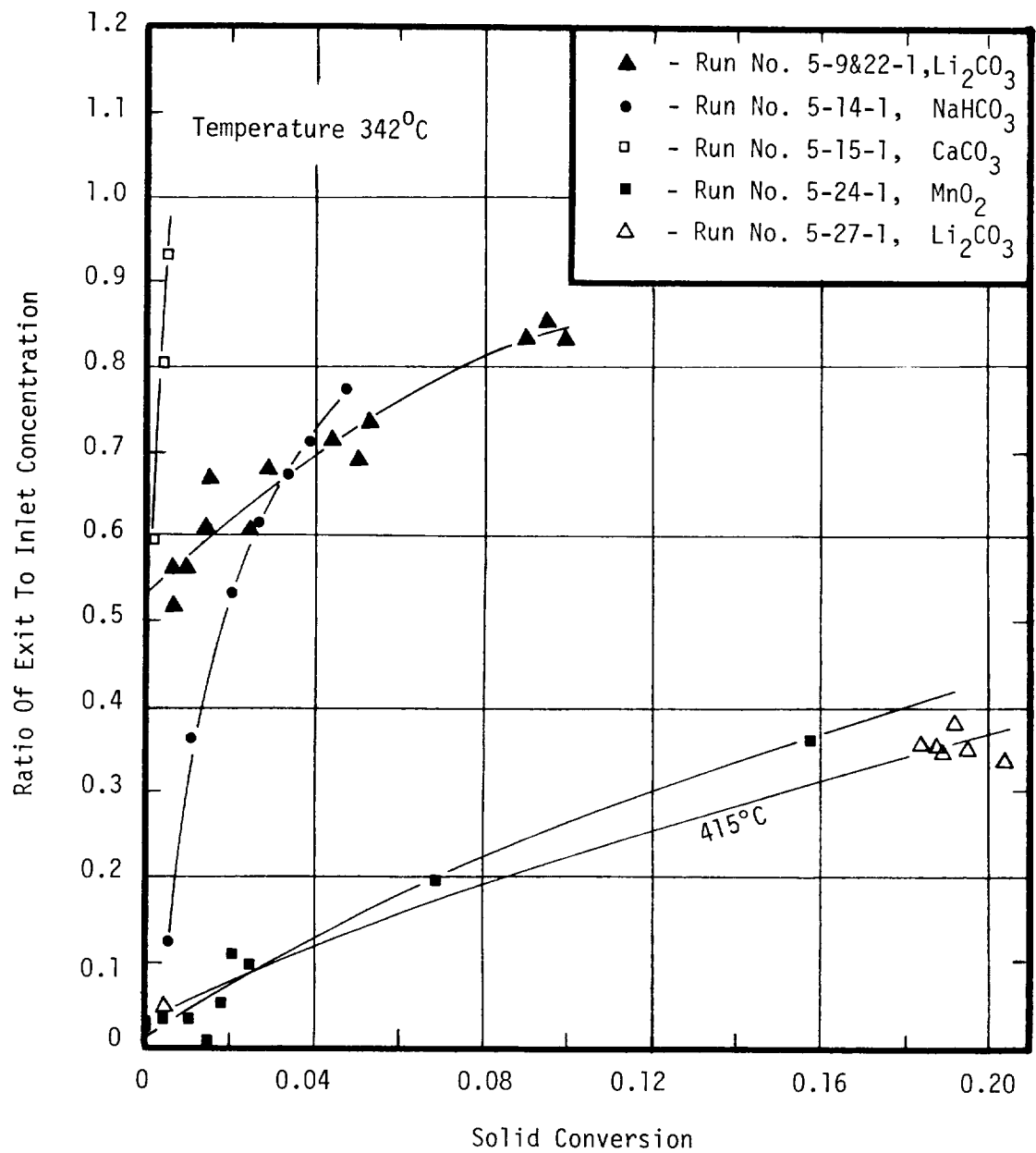
Figure 7.1 - Comparison Of Sulfur Dioxide Removal
Efficiency Of Various Bases

TABLE 7.3

SULFUR DIOXIDE REMOVAL USING MANGANESE DIOXIDE

Packing Material	Mallinckrodt "multisorb" MnO$_2$ 12-14 mesh							
Run Number	4-25-2	5-13-1	5-24-1	5-29-1	7-11-2	7-15-1	8-5-1	8-12-2
Amount Packing, g	2.6898	0.4000	0.4000	0.4000	0.601	0.604	0.603	1.002
Bed Temp., °C	27	342	342	416	342	342	342	342
Air Flow Rate, mole/hr	4.82	6.0	6.0	12.6	6.25	6.46	2.88	5.02
Inlet Concentration, ppm	13-14	13-14	10	4 ± .2	15	16	23.6	12.5
Humidity, mole/mole	0.0	0.0144	0.0146	0.0146	0.0	0.013	0.013	0.013
Carbon Dioxide, mole %	0.0	0.5	0.5	0.5	0.0	0.5	0.5	0.5
Test Duration, hr	100	7.5	25.5	13.5	70	114	100	87
Bed Loading, g SO$_2$/g packing	0.235 at equil.	0.0867 after 7.5 hr	0.18 after 25.5 hr	0.03 after 13.5 hr	0.41 after 70 hr	0.55 after 110 hr	0.34 after 50 hr	0.35 after 87 hr
Bed Diameter, cm	0.94	0.94	0.94	0.94	0.94	0.94	0.94	0.94
Air Pressure, atm	0.95	0.90	0.9	0.9	0.9	0.9	0.9	0.9
Contaminant	SO$_2$	SO$_2$	SO$_2$	SO$_2$	SO$_2$	SO$_2$	SO$_2$	SO$_2$
Theoretical Cap. g SO$_2$/g packing	0.737	0.737	0.737	0.737	0.737	0.737	0.737	0.737

$$D_e = 140 \text{ cm}^2/\text{hr}$$

$$k_g = 36000 \text{ cm/hr}$$

Using these values the model was able to account very well for changes in inlet concentration, air flow rate, and bed length. Shown in Figure 7.2 is the fitted and experimental outlet concentration history for Run 7-15-1 which was the data from which the constants D_e and k_g were determined for sulfur dioxide. The mass velocity for this run was 8.66 mole air/hr cm^2 which is about 57% of the value of 15.66 mole air/hr cm^2 (4.95 lb/hr through a 1 in. tube) reported used in the Langley ILSS test bed. After the constants were determined from Run 7-15-1, the model was used to predict the outlet concentration history for the other four runs.

Shown in Figure 7.3 is the experimental and calculated exit concentration curves for Run 8-5-1. The operating conditions were the same for both Run 8-5-1 and 7-15-1 except that for 8-5-1 the flow rate was only 4.15 mole air/hr cm^2 or less than half of that for 7-15-1, and the inlet concentration was 70% higher for 8-5-1. After 47 hours of operation the experimental and calculated removal efficiencies were almost identical at 75% removal of the entering SO_2.

Shown in Figure 7.4 are the calculated and experimental curves for Run 5-24-1. The conditions on this run are similar to those for 7-15-1 except for the lower inlet concentration and smaller bed. In order to test the capacity of the design equations to accurately reflect the outlet contaminant concentration for a scaled up bed length, Run 8-12-2 was made in which the bed length was approximately 3.2 cm or about 65% greater than the base run (7-15-1). The calculated and experimental outlet concentration curves for this run are shown in Figure 7.5. After 85 hours of operation the model predicted that the bed would be removing 69.5% of the inlet SO_2. This compares to a measured 72% removal after 85 hours, thus the calculated value is conservative.

One run (7-11-2) was made to test the effect of humidity variation on the reaction rate. At zero humidity the values of the constants necessary to fit the data were the same as for the runs at 0.013 mole H_2O/mole air (equivalent to about 50% RH at 72°F). Shown in Figure 7.6 are both the calculated and experimental exit curves. The calculated curve was obtained by using the same constants as for humid air. Since the data fit was excellent, the conclusion was drawn that the humidity level has little or no effect on the removal efficiency of MnO_2 for SO_2.

One run (5-29-1) was made in which both the temperature and the flow rate were changed from those of the standard run (7-15-1). The mass flux was set at 18.2 mole air/cm^2 and the temperature was increased to 416°C (780°F). Since both k_g and D_e are functions of temperature they were refitted to the data for this run and were found to be

52
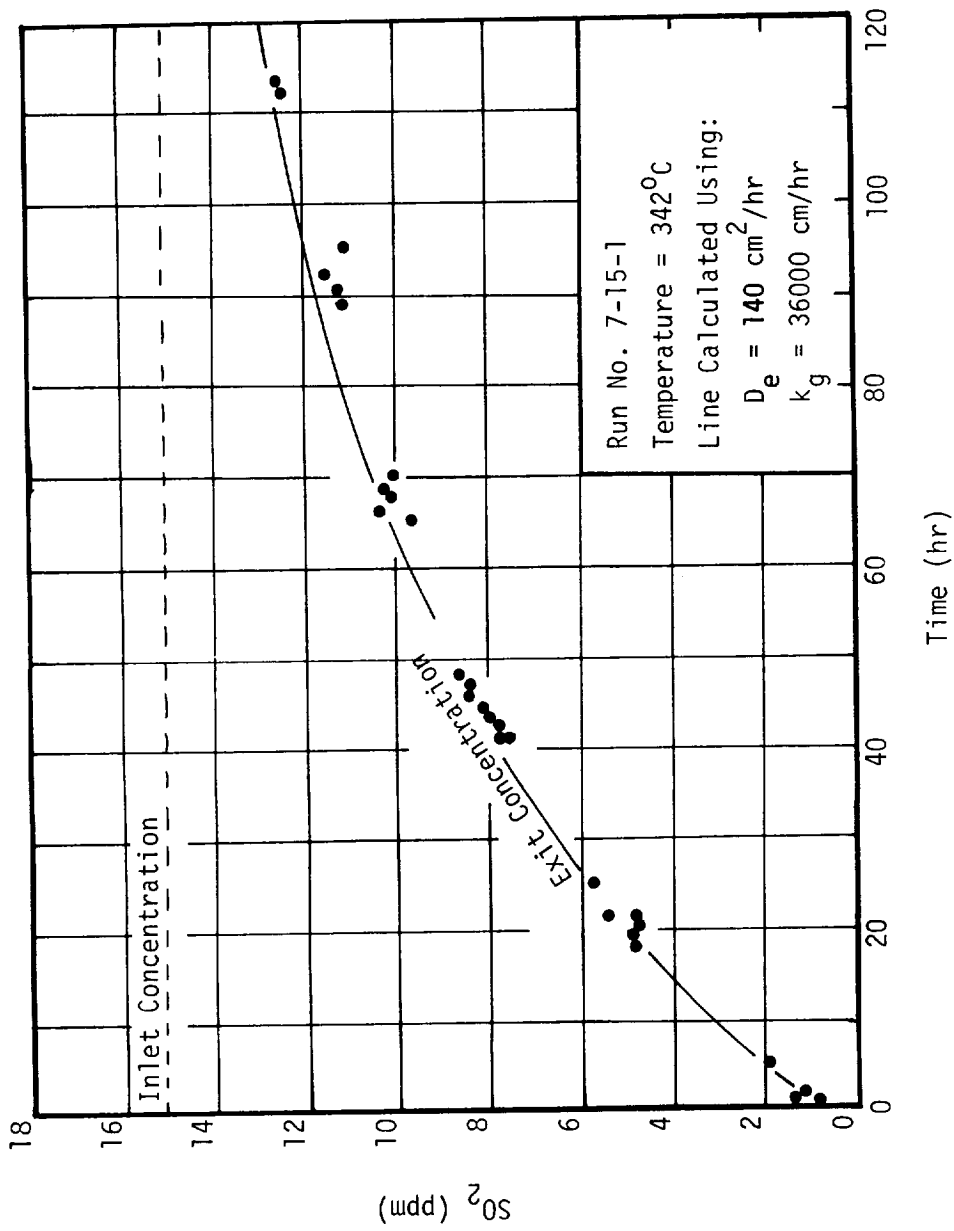
Figure 7.2 – Experimental Points And Fitted Curve For
Sulfur Dioxide Reaction With Manganese Dioxide
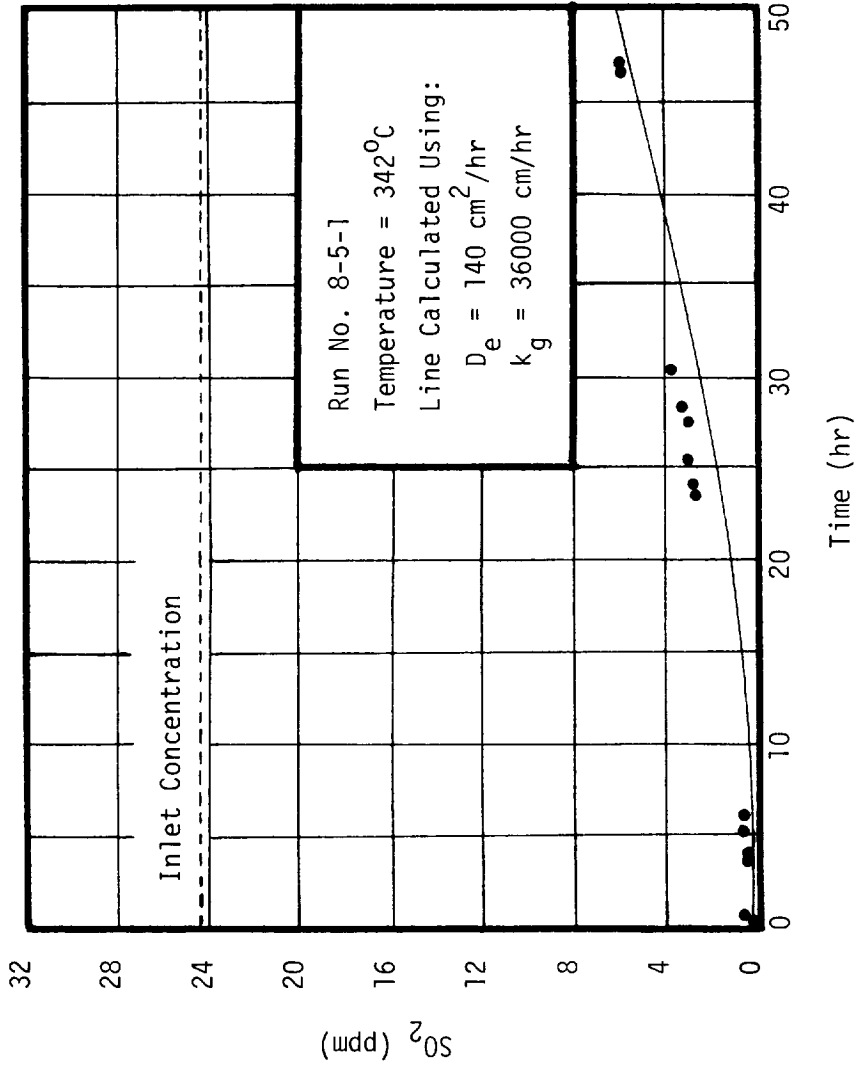
Figure 7.3 - Experimental And Calculated Exit Concentration
Curve For SO_2 Reaction With MnO_2 For An Air
Flow Rate Of 2.9 Mole/Hr

Run No. 8-5-1
Temperature = 342^oC
Line Calculated Using:
D_e = 140 cm^2/hr
k_g = 36000 cm/hr

Inlet Concentration

SO_2 (ppm)

Time (hr)

Figure 7.4 – Experimental Points And Calculated Exit Concentration Curve For SO_2 Reaction With MnO_2 Under Conditions Similar To Those For Run No. 7-15-1

55
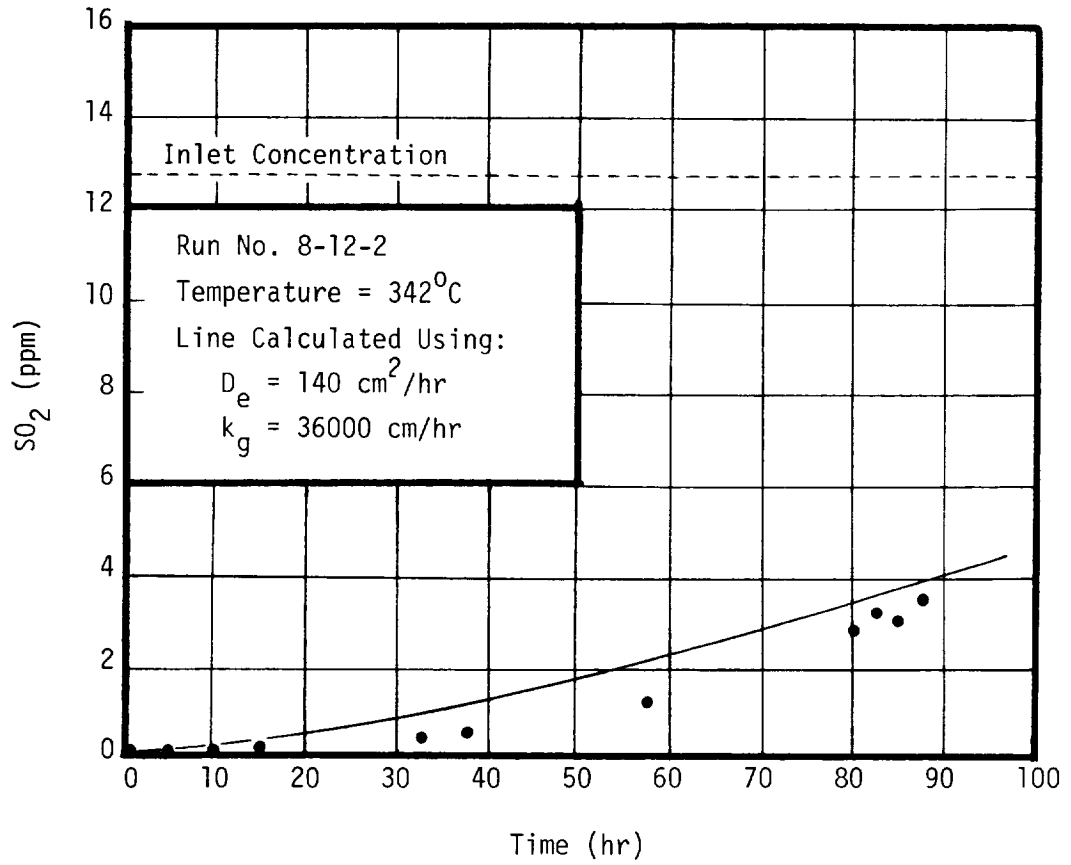
Figure 7.5 - Exit Concentration Curve For SO_2 Reaction
With MnO_2 For A Bed Which Is 65% Longer
Than That In Figure 7.2

56
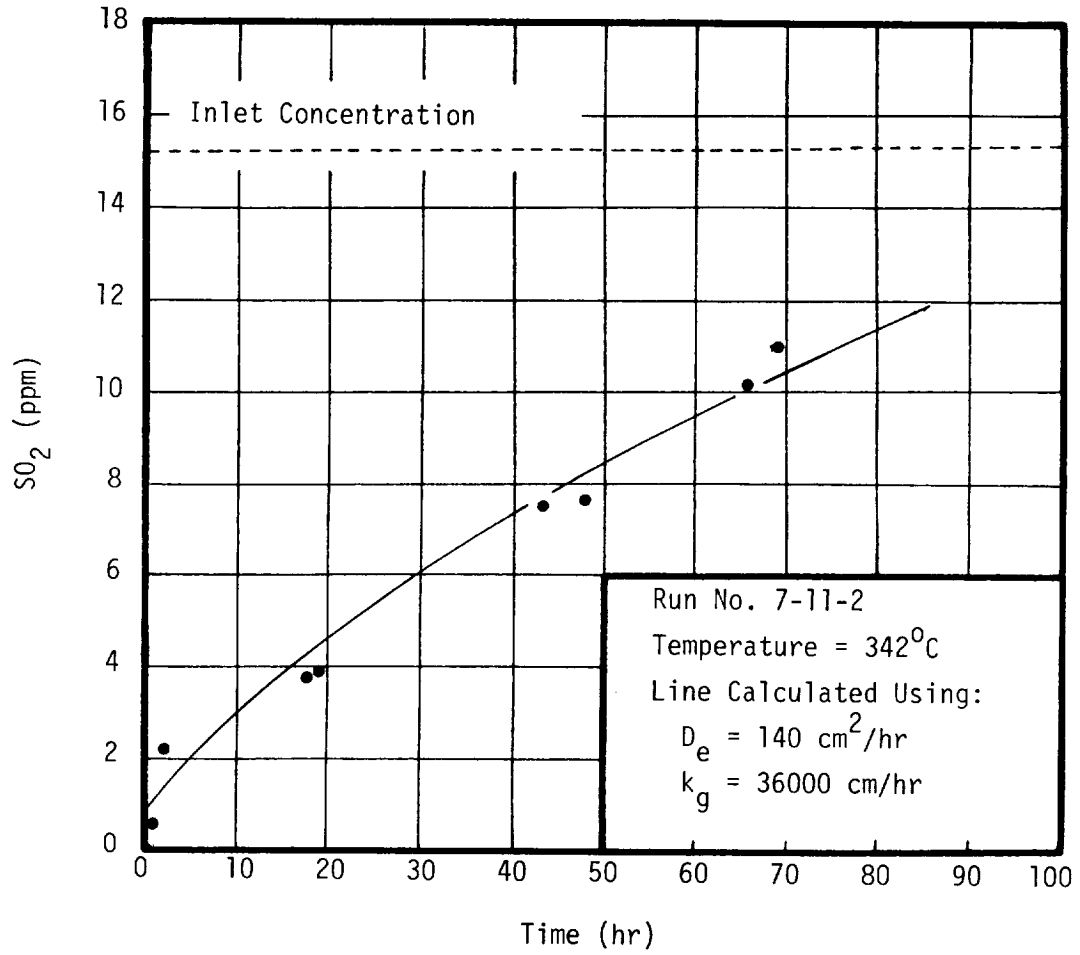
Figure 7.6 - Test Of The Model For Prediction Of
Exit SO_2 Concentration With A Zero
Humidity Inlet Air Stream

$$D_e = 150 \text{ cm}^2/\text{hr}$$

$$k_g = 53000 \text{ cm/hr}$$

Although with only two temperature levels the temperature dependency of these two constants cannot be determined with a high degree of confidence, rough estimates of this dependency can be made. The diffusivity increase appears to be proportional to the square root of the absolute temperature, corresponding to the theoretical temperature dependence of Knudsen diffusion.

$$D_e = 140\sqrt{\frac{T_2}{616}} \qquad (7.1)$$

The increase in the forward rate constant corresponds to an activation energy of about 4700 cal/mole. The Arrhenius equation describing the temperature dependence of the forward rate constant is:

$$k_g = 36000 \ e^{-(4700/1.98)(1/T_2 - 1/616)} \qquad (7.2)$$

Shown in Figure 7.7 are the experimental exit concentration data along with the curve calculated using $D_e = 150$ and $k_g = 53000$. The activation energy (4700/ cal/mole) of Equation (7.2) was calculated from this value of k_g and that for k_g determined from the 342°C data discussed previously.

The goodness of fit of the shrinking core model, Equations (4.13) and (4.14), to experimental results on the reaction between sulfur dioxide and manganese dioxide constitutes convincing evidence of the validity of the model. Effects of changes in flow rate, time, bed length, and contaminant concentration were accurately predicted by the model. The values of the constants D_e and k_g determined from experimental data at 342°C can be used with confidence in the design of manganese dioxide absorption beds to operate at that temperature. Equations (7.1) and (7.2) should be used with caution in predicting temperature dependence, particularly outside the 340-400°C temperature range.

7.3.2 Sulfur Dioxide Reaction With Lithium Carbonate. - Lithium carbonate reacts readily with SO_2 at elevated temperatures although the reaction is considerably slower than that of SO_2 with MnO_2. The reaction is given by the stoichiometric equation

$$Li_2CO_3 + SO_2 + 1/2 \ O_2 \rightarrow Li_2SO_4 + CO_2$$
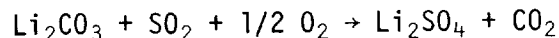
which results in the theoretical capacity of 0.864 g SO_2/g Li_2CO_3. As in the case for removal using MnO_2 the thermodynamic equilibrium concentration of SO_2
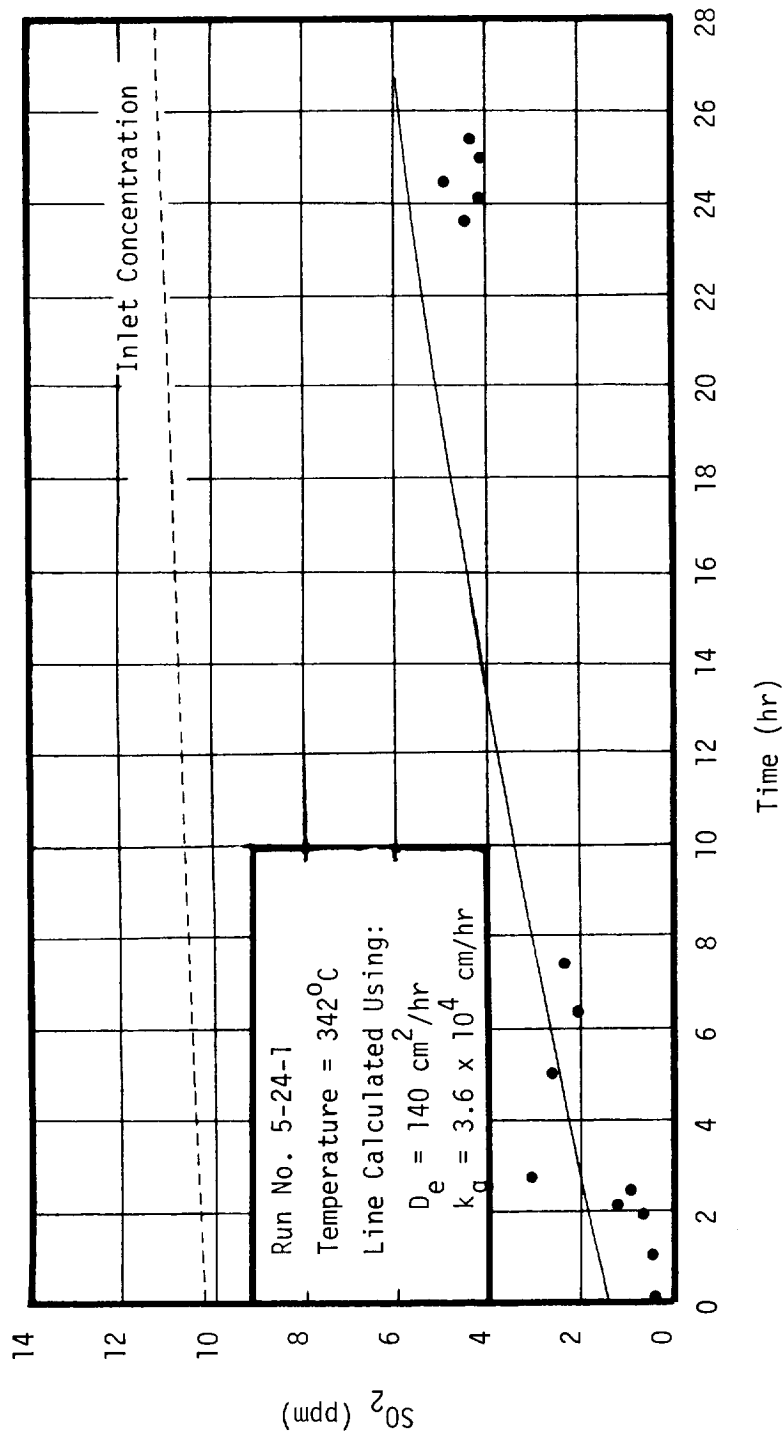
58

Figure 7.7 – Experimental Points And Calculated Exit Concentration Curve For Run Made At 416°C With A 12.6 Mole/Hr Air Flow Rate

59

in the presence of CO_2 and lithium carbonate is very low being of the order of 10^{-10} ppm at 342°C. The reaction is endothermic thus the equilibrium concentration increases with increased temperature.
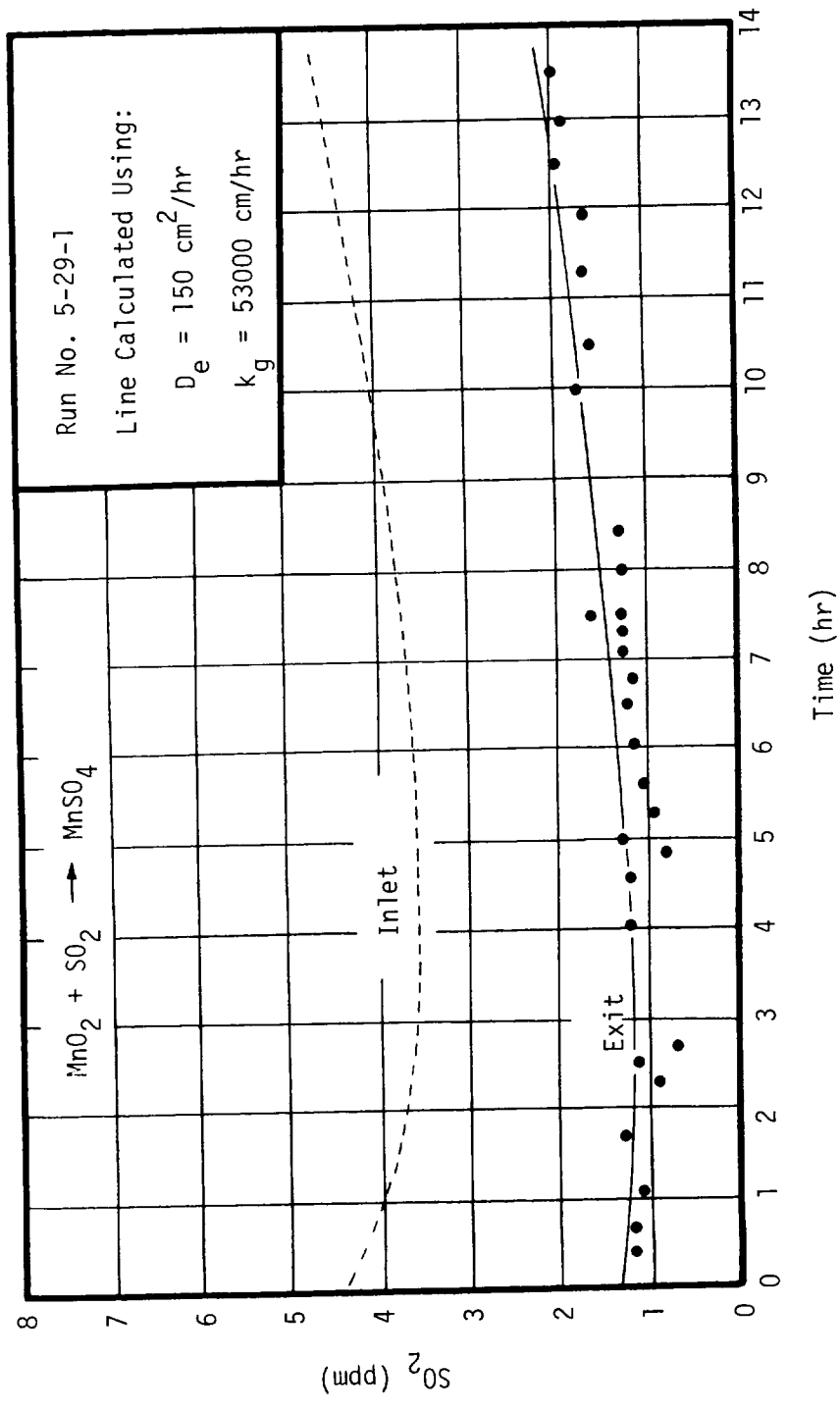
Reaction rate data were obtained using the three different lithium carbonate particle sizes of fine powder, 120 mesh sintered granules, and 12-14 mesh sintered granules. The observed reaction rates for these very different particles sizes were approximately the same although no doubt the importance of the various reaction resistances were quite different for each particle size. The shrinking core model developed in Chapter 4.0 was capable of fitting the data within any one particle size; however, the required constants for each particle size. Shown in Table 7.4 are the constants for each particle size.

TABLE 7.4

EFFECT OF PARTICLE SIZE ON EFFECTIVE DIFFUSIVITY AND

FORWARD RATE CONSTANT FOR Li_2CO_3- SO_2 REACTION

	Particle Size		
	320 mesh	120 mesh	12-14 mesh
D_e	0.0045	0.07	10
k_g	200.	1700.	25000.

Because of practical problems of excessive pressure drop and dusting with the smaller particles, the 12-14 mesh granules are considered to be superior for use in trace contamiant control. As may be seen the apparent diffusivity of SO_2 through the product Li_2SO_4 layer is relatively low compared to that for diffusion through the $MnSO_4$ layer discussed in 7.2.2.

Shown in Table 7.5 are the experimental conditions for the six runs made using Li_2CO_3 and SO_2. The conditions for each of these runs were similar except for particle size and temperature. The very small particle size was used on early runs in order to ascertain the reaction rate in a situation where internal diffusional resistances would be minimized.

The exit concentration history for Run 5-9-1 is shown in Figure 7.8. From these data the relatively slow reaction is seen as well as the relative importance of internal diffusion for this reaction. The SO_2 removal efficiency for this small sample decreased from an initial value of about 48% to about 13.5% after only 12% of the solid had reacted.

Shown in Figure 7.9 is the exit concentration for Run 5-27-1 in which the temperature was increased to 416°C (780°F). The much faster reaction rate as

60

TABLE 7.5

SULFUR DIOXIDE REMOVAL USING LITHIUM CARBONATE

Run Number	4-30-1	5-9-1	5-22-1	5-27-1	6-6-1	6-7-1
Packing Material	325 Mesh Li_2CO_3	325 Mesh Li_2CO_3	325 Mesh Li_2CO_3	325 Mesh Li_2CO_3	12-14 Mesh Li_2CO_3	120 Mesh Li_2CO_3
Amount of Packing, g	3.0000	0.4000	0.4000	0.4000	0.4000	0.4000
Bed Diameter, cm	0.94	0.94	0.94	0.94	0.94	0.94
Bed Temperature, °C	358	342	342	416	342	342
Air Flow Rate, mole/hr	2.42	6.0	6.0	6.0	6.0	6.0
Air Pressure, atm	0.9	0.9	0.9	0.9	0.9	0.9
Contaminant	SO_2	SO_2	SO_2	SO_2	SO_2	SO_2
Inlet Concentration, ppm	14-15	14-15	10	11-12	8.7	8.7
Humidity, mole H_2O/mole air	0.0	0.0144	0	0.0144	0.013	0.013
Carbon Dioxide, mole %	0.0	0.5	0	0.5	0.5	0.5
Test Duration, hr	156	23.25	19.8	42.1	18	18
Theoretical Cap. g SO_2/g packing	0.866	0.866	0.866	0.866	0.866	0.866
Average Bed Loading g SO_2/g packing		0.059 after 23.25 hr	0.0437 after 19.8 hr	0.312 after 42.1 hr		
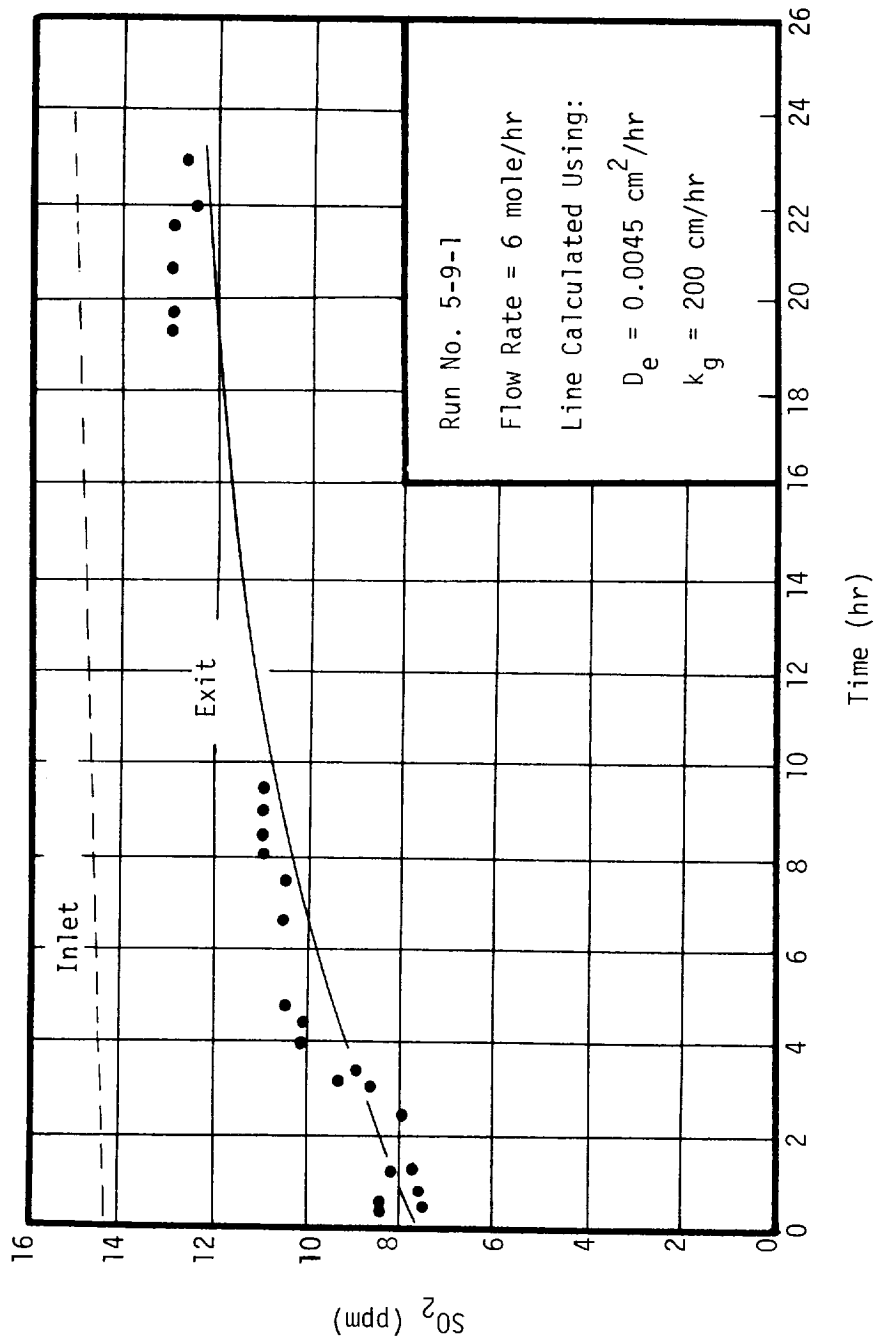
Figure 7.8 - Exit Concentration Curve For SO_2 Reaction With Li_2CO_3 Powder At 342^oC

Run No. 5-9-1

Flow Rate = 6 mole/hr

Line Calculated Using:

$D_e = 0.0045$ cm^2/hr

$k_g = 200$ cm/hr

Figure 7.9 - Exit Concentration Curve For SO_2 Reaction With Li_2CO_3 Powder At 416^oC

compared to Run 5-9-1 is seen. The initial removal efficiency is 95% which is reduced to 48% after the sample was approximately 32% reacted.

Shown in Figure 7.10 is the exit concentration curve for Run 6-6-1 and 6-7-1. These runs were made using fused granules of Li_2CO_3. The overall reaction rate for each of the two different particle sizes is essentially the same as for the very fine powder.

7.4 Removal of Chlorine Using Solid Reactants

Chlorine is a strongly oxidizing gas which reacts readily with most metals and hydrocarbons at higher temperatures (56 p. 37). Free chlorine can be released into the atmosphere of a spacecabin through several routes of which two of the more probable are (a) the direct result of combustion of chlorinated hydrocarbon compounds and (b) the oxidation of hydrogen chloride according to the reaction

$$4 \ HCl + O_2 \rightarrow 2 \ Cl_2 + 2 \ H_2O$$

Experimental work completed during this project showed that at 300-400°C the reaction of chlorine with type 304 stainless steel is slow and that reaction is very rapid with MnO_2 and is somewhat slower with Li_2CO_3.

In the presence of water chlorine reacts to form hydrochloric acid and hypochlorous acid.

$$Cl_2 + H_2O \rightarrow HCl + HClO$$
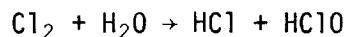
Thus it is highly probable that the humidity level is important for the reaction of chlorine with basic materials since the reacting species could be the very reactive compounds HCl and HClO.

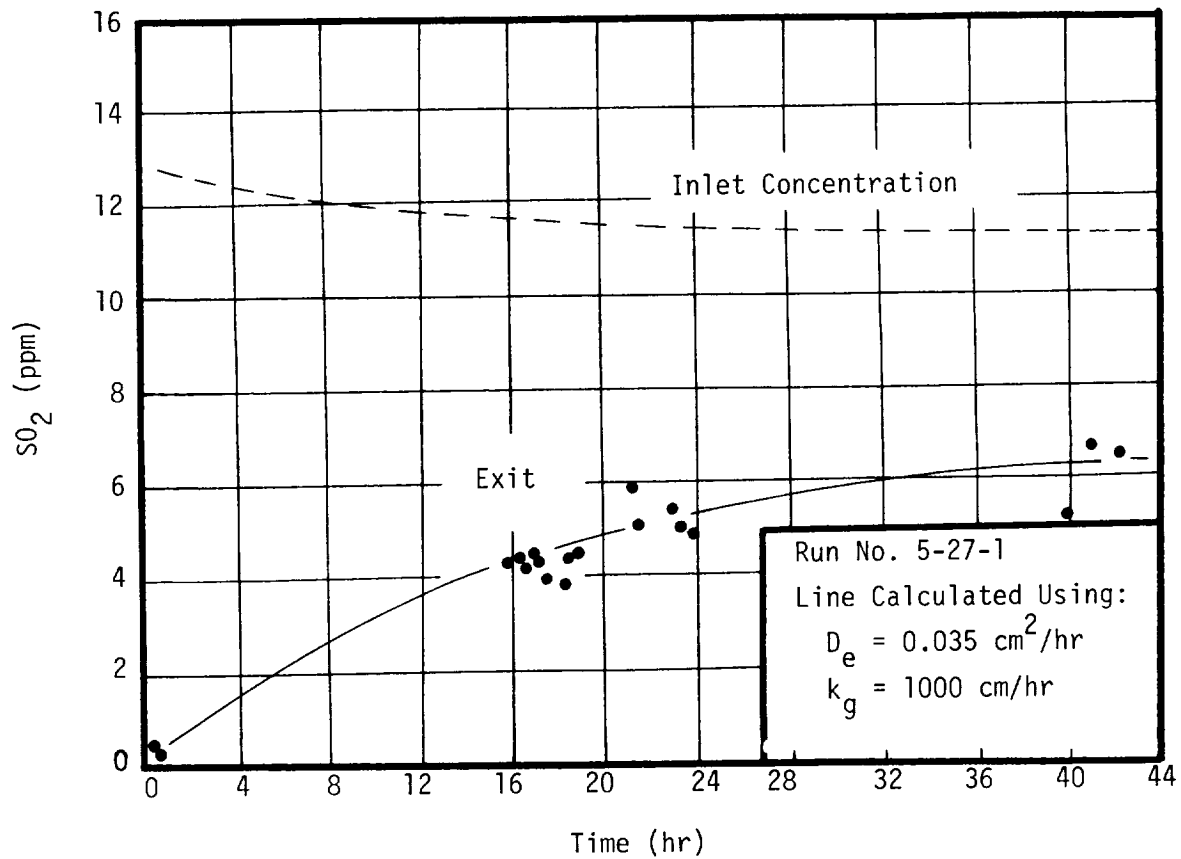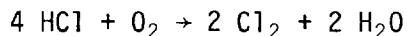### 7.4.1 Reaction of Chlorine and Manganese Dioxide. - Manganese dioxide was found to react to remove trace concentrations of chlorine from air. The exact reaction for this removal is not known; however, due to the several oxidation states which manganese exhibits the possible reaction products include $MnCl_2$, $MnCl_3$, and/or $MnCl_4$. Experimental evidence indicates that one mole of MnO_2 reacts with approximately two moles of chlorine. For estimation purposes the reaction equation was assumed to be

$$MnO_2 + 2 \ Cl_2 \rightarrow Products \tag{7.3}$$

Two experimental runs were made to measure the rate of the reaction between chlorine and MnO_2. The conditions for these two runs are shown in Table 7.6. Constants for the shrinking core model were determined from these data using
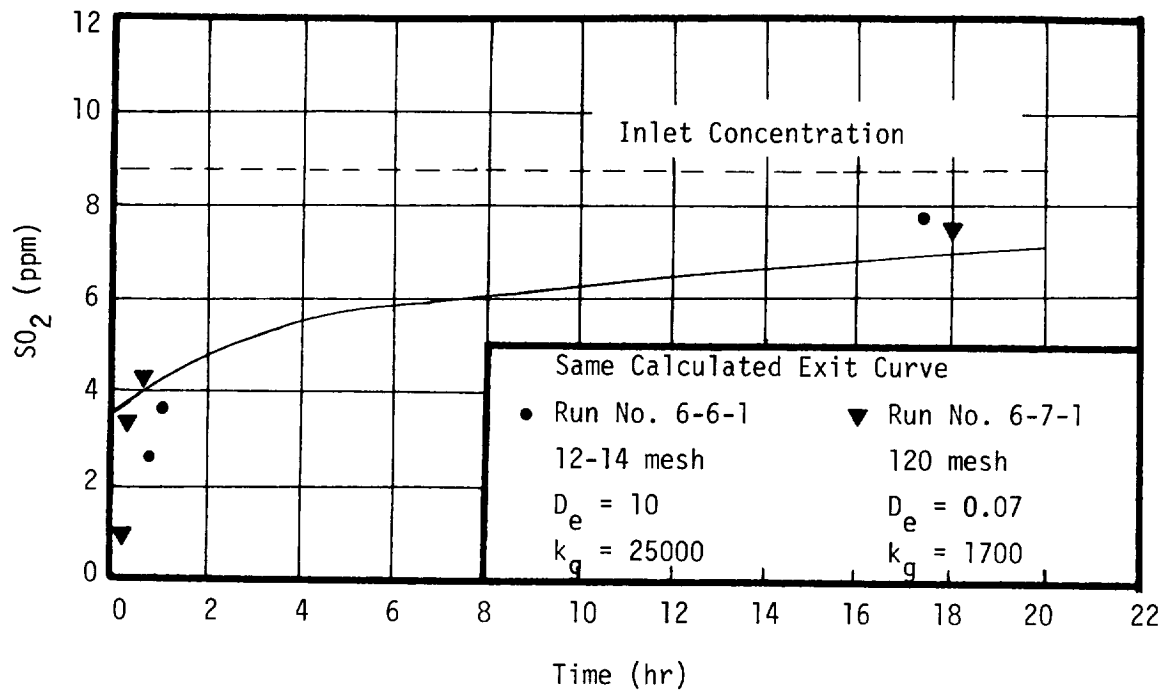
Figure 7.10 - Comparison Of Sulfur Dioxide Reaction
On Two Sizes Of Sintered Lithium
Carbonate Granules

TABLE 7.6

EXPERIMENTAL CONDITIONS FOR REACTION

OF CHLORINE AND MnO_2

Packing Material	Mallinckrodt MnO_2 12-14 Mesh	
Run Number	7-25-1	7-29-1
Amount of Packing, g	0.4023	0.4019
Bed Diameter, cm	0.94	0.94
Bed Temperature, °C	342	342
Air Flow Rate, mole/hr	4.21	14.66
Air Pressure, atm	0.9	0.9
Contaminant	Cl_2	Cl_2
Inlet Concentration, ppm	52	16.0
Humidity, mole/mole	0.013	0.013
Carbon Dioxide, mole %	0.5	0.5
Test Duration, hr	25	23

the assumed reaction of Equation (7.3). Values for the constants at a temperature of 342°C were

$$D_e = 700 \ cm^2/hr$$

$$k_g = 300000 \ cm/hr$$

Shown in Figure 7.11 is the exit concentration history for Run 7-29-1.

7.4.2 Reaction of Chlorine and Lithium Carbonate. - Lithium carbonate readily removes trace quantities of chlorine from air at a temperature of 342°C; probably, according to the equation

$$LiCO_3 + Cl_2 \rightarrow LiCl + LiOCl + CO_2$$

Lithium hypochlorite (LiOCl) is reported to be very stable (56 p. 526). Based on the above reaction, lithium carbonate has a theoretical capacity for chlorine of 0.964 g Cl_2/g Li_2CO_3. Conditions for the two experimental runs made to measure the rate of the reaction are shown in Table 7.7. The value of the constants in the shrinking core model for a temperature of 342°C were determined to be

$$D_e = 50 \ cm^2/hr$$

$$k_g = 20000 \ cm/hr$$

Shown in Figures 7.12 and 7.13 are the experimental and calculated outlet concentration histories for the two runs.

Comparison of these data with those for the reaction of chlorine with MnO_2 clearly indicates a faster rate of reaction of chlorine with manganese dioxide than with lithium carbonate at the same conditions of temperature and flow rate. This was also found to be true in sulfur dioxide reactions.

7.5 Removal of Hydrogen Chloride

Hydrogen chloride is a primary product produced when most chlorinated hydrocarbons are oxidized; a typical example is the combustion of methyl chloride

$$CH_3Cl + \frac{3}{2} O_2 \rightarrow CO_2 + H_2O + HCl$$
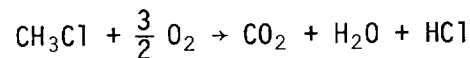
The hydrogen chloride produced in this manner can also be further oxidized to chlorine at a temperature of 400-600°C in the presence of certain catalytic materials such as manganese and copper.

67
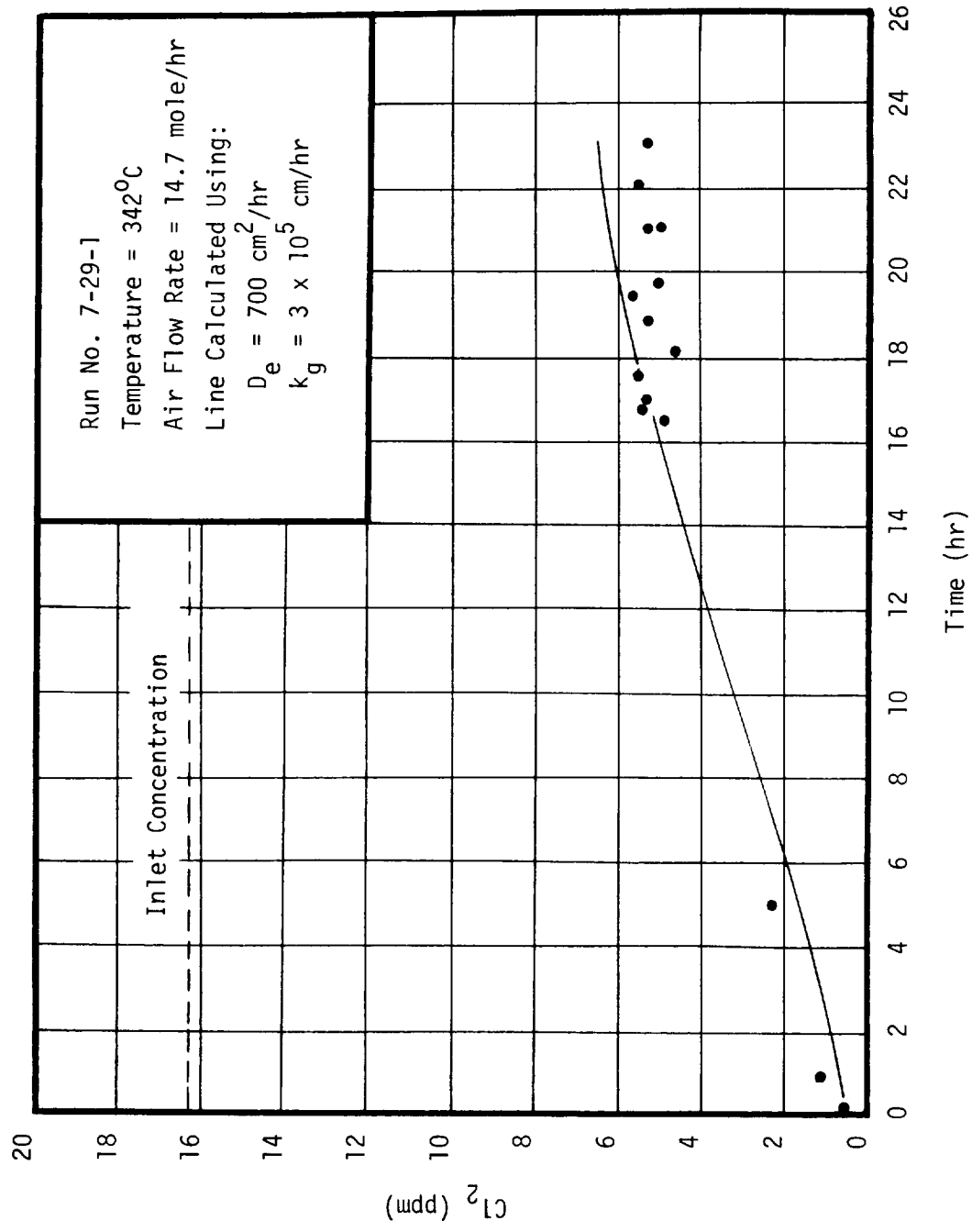
Figure 7.11 - Removal Of Chlorine Using MnO_2

68

TABLE 7.7

EXPERIMENTAL CONDITIONS FOR REACTION

OF CHLORINE AND Li_2CO_3

Packing Material	Fused Li_2CO_3 12-14 Mesh	
Run Number	7-22-1	8-21-1
Amount of Packing, g	0.401	1.0
Bed Diameter, cm	0.94	0.94
Bed Temperature, °C	342	342
Air Flow Rate, mole/hr	1.29	8.78
Air Pressure, atm	0.9	0.9
Contaminant	Cl_2	Cl_2
Inlet Concentration, ppm	See Fig. 7.12	30 ± 1
Humidity, mole H_2O/mole air	0.014	0.014
Carbon Dioxide, mole %	0.5	0.5
Test Duration, hr	50	50
Theoretical Bed Capacity, g Cl_2/g Li_2CO_3	0.96	0.96
Average Bed Loading, g Cl_2/g Li_2CO_3	0.20 after 48 hr	0.34 after 48 hr
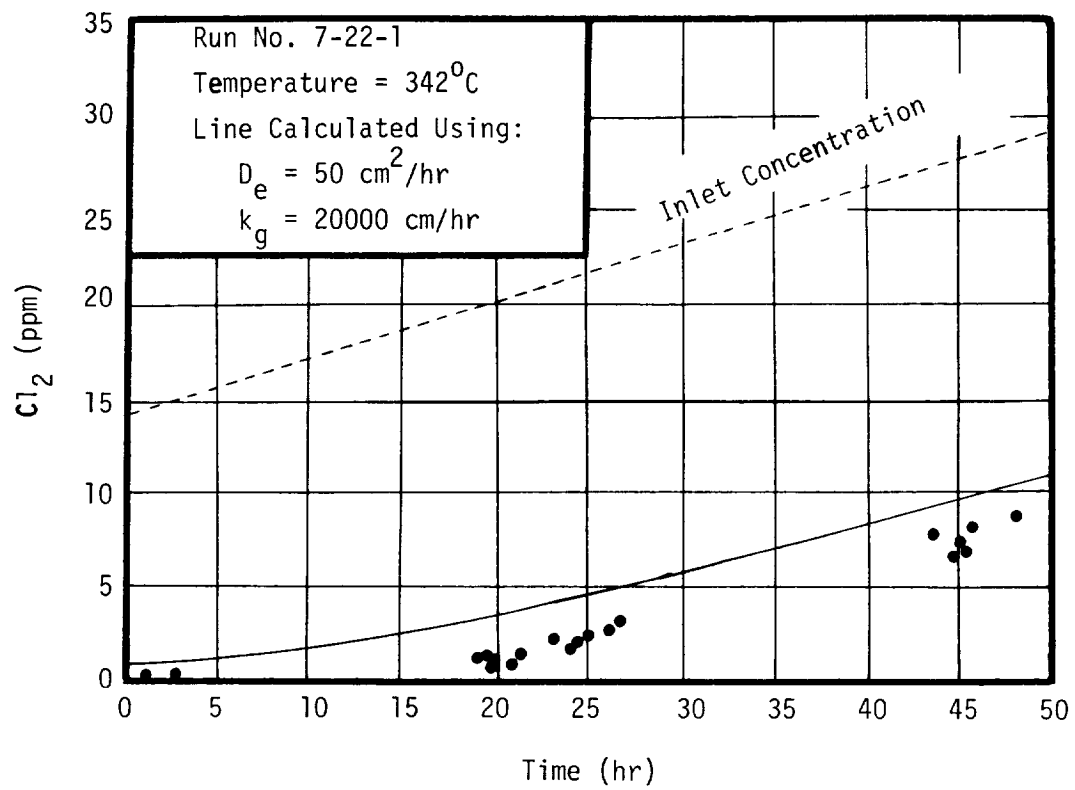
Figure 7.12 - Removal Of Cl_2 At An Air Flow Rate Of 4.2 Mole/Hr Using Sintered Li_2CO_3
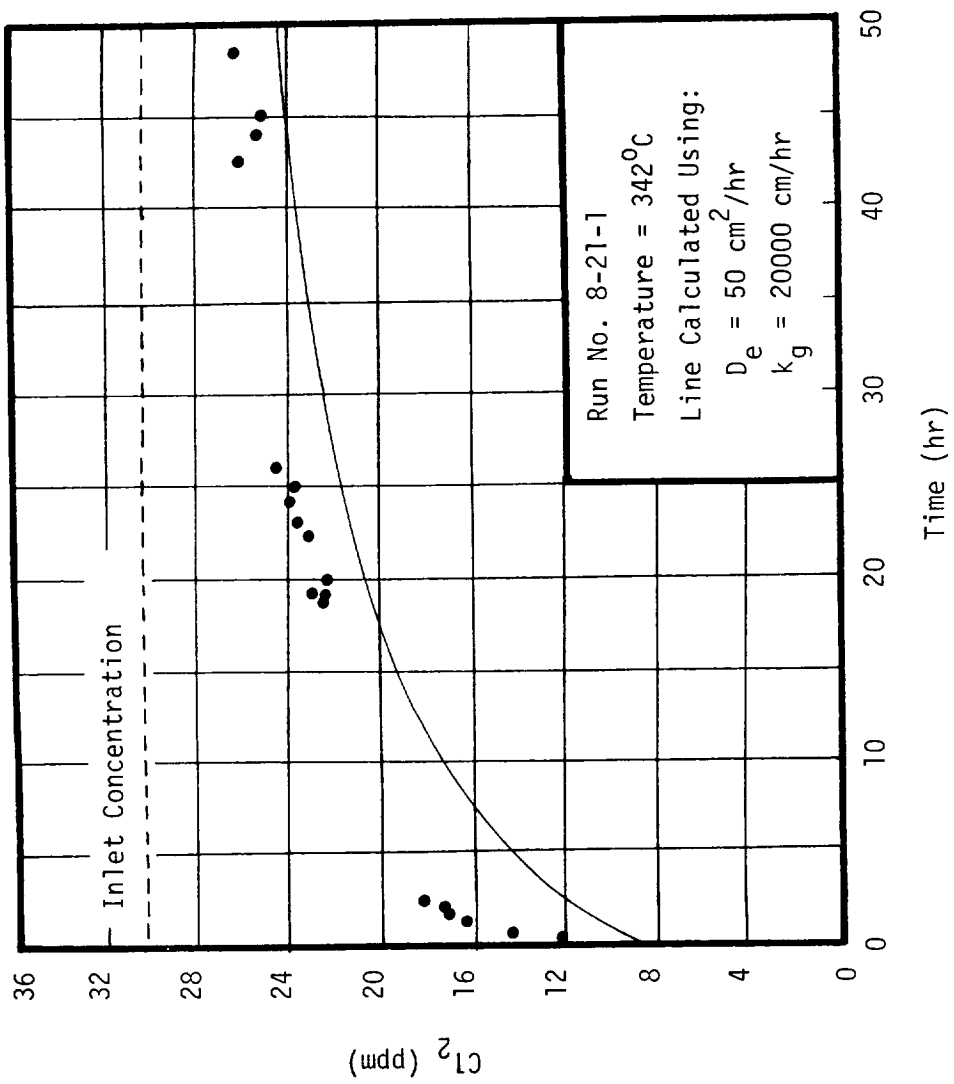
Figure 7.13 - Removal Of Cl_2 At An Air Flow Rate Of 14.7 Mole/Hr Using Sintered Li_2CO_3

71

$$4 \text{ HCl} + \text{O}_2 \rightarrow 2 \text{ H}_2\text{O} + 2 \text{ Cl}_2$$
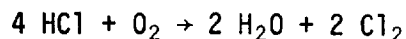
Hydrogen chloride is a very acidic gas and consequently reacts rapidly with basic materials such as lithium carbonate. The stoichiometric equation for this reaction is

$$\text{Li}_2\text{CO}_3 + 2 \text{ HCl} \rightarrow 2 \text{ LiCl}_2 + \text{H}_2\text{O} + \text{CO}_2$$
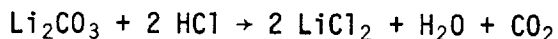
which results in a theoretical capacity for HCl of 0.99 g $\text{HCl/g Li}_2\text{CO}_3$.

Experimentally determined reaction rates for $\text{HCl-Li}_2\text{CO}_3$ indicate that the reaction is so rapid that a principal resistance is the rate of external mass transfer to the Li_2CO_3. Thus, provided the pellet size is kept small (0.1 to 0.3 cm diameter) removal of very acidic gases such as HCl, HF, SO_3, etc., should be easily accomplished. Experimental data indicated that Li_2CO_3 is far superior to MnO_2 for the removal of HCl. This is clearly shown in Figure 7.14 where the exit concentration curves for the two different materials are plotted. The conditions for these runs are listed in Table 7.8.

The quality of the HCl experimental data was relatively poor due to the insensitivity of the analytical method for this gas. For this reason the constants for the shrinking core model were set to values which resulted in a conservative fit of the Li_2CO_3 data. The values of the constants were thus determined to be

$$k_g = 100000 \text{ cm/hr}$$

$$D_e = 400 \text{ cm}^2/\text{hr}$$

7.6   Removal of Hydrogen Fluoride

In the presence of water or humid air, hydrogen fluoride (HF) is an extremely strong acid which readily attacks most metals and all bases. Since it has been determined that the reaction of HCl with lithium carbonate is very rapid at 342°C, then it would be expected that the reaction of HF would be as fast or faster. Attempts were made to experimentally check this assumption; however, it was found that at room temperature the reaction of HF with the stainless steel transfer lines was fast enough to remove over 80% of the HF in a 65 cm (25 in.) length. Because of the extreme reactivity in HF and in view of the rapid rate of reaction of HCl it is believed that any system capable of removing the relatively slow reacting compounds such as SO_2 will easily remove HF, therefore, no further experimental work was undertaken.
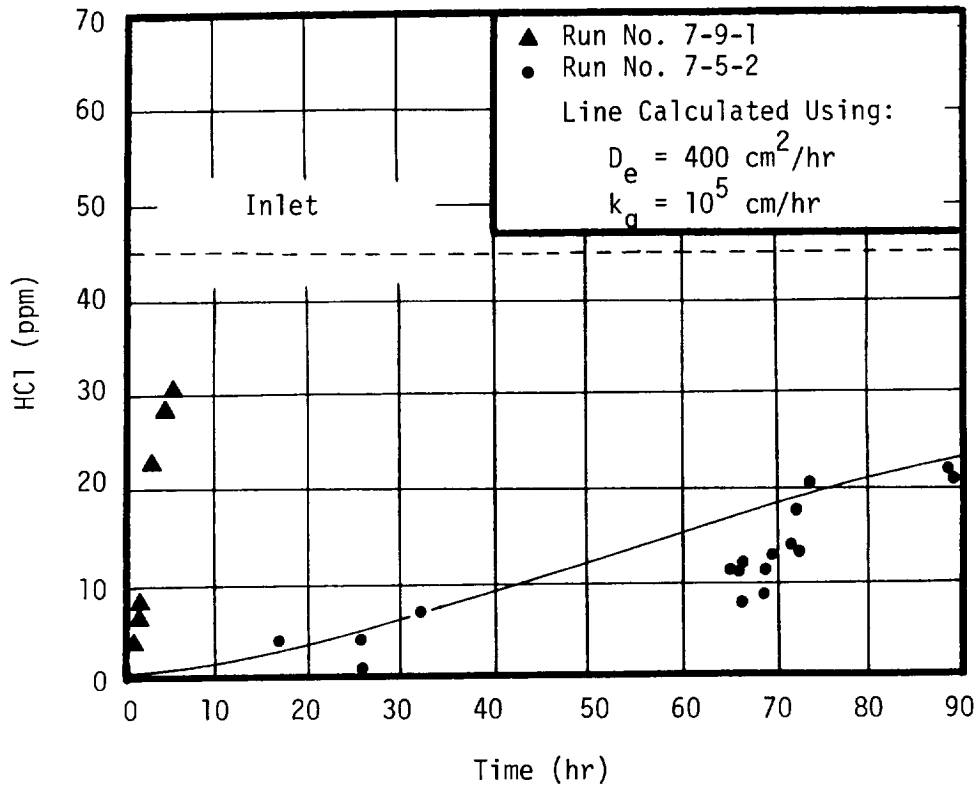
Figure 7.14 - Hydrogen Chloride Reaction With
Lithium Carbonate And With
Manganese Dioxide

TABLE 7.8

EXPERIMENTAL CONDITIONS FOR HYDROGEN CHLORIDE REMOVAL

Run Number	7-5-2	7-9-1
Packing Material	Fused Li_2CO_3 12-14 Mesh	Mallinckrodt MnO_2 12-14 Mesh
Amount of Packing, g	0.400	0.400
Bed Diameter, cm	0.94	0.94
Bed Temperature, °C	342	342
Air Flow Rate, mole/hr	2.9	3.0
Air Pressure, atm	0.9	0.9
Contaminant	HCl	HCl
Inlet Concentration, ppm	45 ± 2	45 ± 2
Humidity, mole H_2O/mole air	0.014	0.014
Carbon Dioxide, mole %	0.0	0.0
Test Duration, hr	89	4.7
Theoretical Capacity, g HCl/g packing	0.9	---
Average Bed Loading g HCl/g packing	0.675	Nil

8.0 ADSORPTION OF ACID GASES

In some designs of a contaminant removal system, the catalytic burner and post catalytic burner subsystems are in series with and preceded by a rather extensive activated carbon adsorption bed. Therefore, the amount of any contaminant originating within the cabin which reaches the post catalytic burner subsystem is dependent on the efficiency of the carbon bed for removal of that contaminant. Therefore, exploration of the behavior of the acid gases toward activated carbon was thought to be important. The work on adsorption which was undertaken for this purpose is presented in this chapter.

8.1 Characteristics of Adsorption Data

Experimental data was obtained on the adsorption of the gases nitrogen dioxide, chlorine, and sulfur dioxide. The data were in the form of breakthrough curves as shown in Figure 8.1
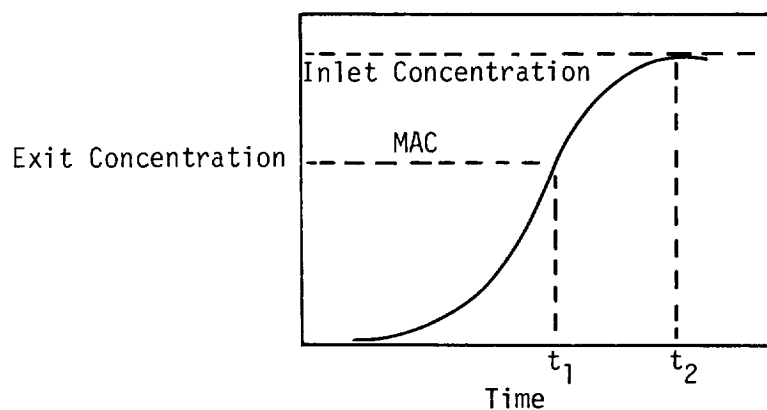
Figure 8.1 - A Breakthrough Curve

Of particular interest from this data is the following information:

(1) A method of estimating the time (t_1) when the exit concentration reaches the MAC level for a given bed geometry, inlet concentration, and gas flow rate.

(2) The slope of the exit concentration curve. The steeper the slope the faster is the rate of adsorption.

(3) The bed loading at dynamic equilibrium (t_2)

8.2 Adsorption of Nitrogen Dioxide on Activated Carbon

Several experimental runs were made in order to explore the physical adsorption of nitrogen dioxide on activated carbon. The principal carbon used was Witco grade 164 in 6-12 mesh size. Shown in Table 8.1 are the experimental conditions for six of the runs made to measure NO_2 adsorption rates and capacity.

The effect of humidity on the adsorption capacity may be seen in Figure 8.2. Run 11-18-6 which was made using zero humidity air is compared to Run 12-27-1 in which the air contained 50% RH. The presence of the water resulted in a three fold increase in the NO_2 adsorption capacity.

Run 3-11-3 was made at a slightly higher temperature. The effect of the increased temperature is not great; however, the capacity appears to be decreased about 5%. Shown in Figure 8.3 are the breakthrough curves for Runs 3-11-3, 2-7-1, and 2-21-1. Comparison of the slopes of the breakthrough curves indicates a slightly increased adsorption rate (steeper slope) for the higher temperature run. The addition of $NaHCO_3$ to the activated carbon caused a 15% reduction in adsorption capacity with little change in rate.

The run using a sample of coconut charcoal (2-21-1) showed very similar adsorption capacity and rate as that of the previously tested activated carbon. The major conclusion from this run is that the Witco activated carbon used previously is not unique in its behavior toward nitrogen dioxide.

Analyses were made to determine the concentration of nitric oxide (NO) in the exit gas from the activated carbon bed. Concentration levels of NO in the exit gas from 3-11-3 ranged from 9.2 ppm to below 1 ppm.

Since the feed gas to the bed contains 1 ppm or less NO, the most probable origin of this nitric oxide is the reaction

$$3\ NO_2 + H_2O \rightarrow 2\ HNO_3 + NO \qquad\qquad (8.1)$$
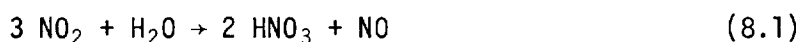
The presence of a reaction either on the surface of the carbon or within the gas phase greatly complicates the mathematics describing the behavior of the system. If all of the NO_2 removed from the gas stream reacted according to the above reaction then one mole of NO would be produced for each three moles of NO_2 removed. After the NO is produced several things could happen, two of the more probable are:

(1) The nitric oxide could react with oxygen to give NO_2. Morrison (57) has reported on the gas phase oxidation of NO.

(2) The nitric oxide can be adsorbed by the carbon.

Figure 8.4 shows the experimentally measured exit concentration of nitric oxide for Run 3-11-3. Also shown in Figure 8.4 is the exit concentration of NO assuming that all of the nitrogen dioxide removed by the bed reacts according to reaction (8.1) and none of the NO is adsorbed or oxidized. Calculations

TABLE 8.1

NITROGEN DIOXIDE ADSORPTION ON ACTIVATED CARBON

| Packing Material	Witco Activated Carbon Grade 164, 6-12 Mesh				Witco Treated With NaHCO$_3$	Coconut Charcoal 8-12 Mesh
Run Number	11-18-6	12-26-1	12-27-1	3-11-3	2-7-1	2-21-1
Amount of Packing, g	2.7439	2.8491	2.7986	2.9072	2.8796	2.0564
Bed Diameter, cm	0.94	0.94	0.94	0.94	0.94	0.94
Bed Temperature, °C	30	29	28	36	27	27
Air Flow Rate, mole/hr	4.65	4.66	4.77	4.66	4.66	4.71
Air Pressure, atm	0.9	1.09	1.09	1.09	1.09	0.9
Inlet Concentration, ppm	39	37	36	39	36	36
Humidity, mole/mole	0	0.013	0.013	0.012	0.014	0.012
Carbon Dioxide, mole %	0	0.5	0.5	0.5	0.5	0.5
Test Duration, hr	75	28	234	170	170	139
Bed Loading at Equilibrium g NO$_2$/g carbon	0.115	-----	0.352	0.335	0.307	0.356
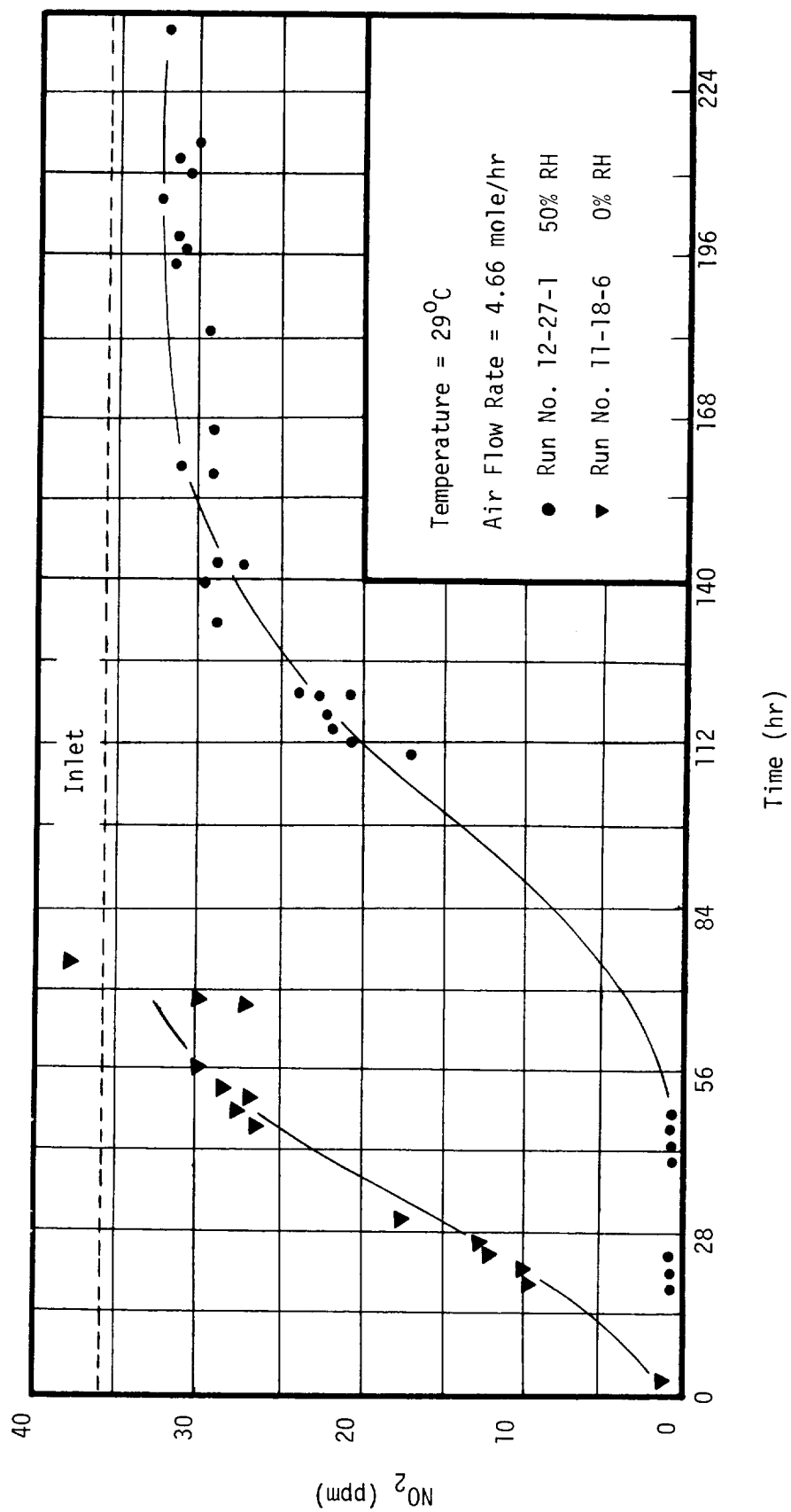
Figure 8.2 - Effect of Humidity On NO_2 Adsorption
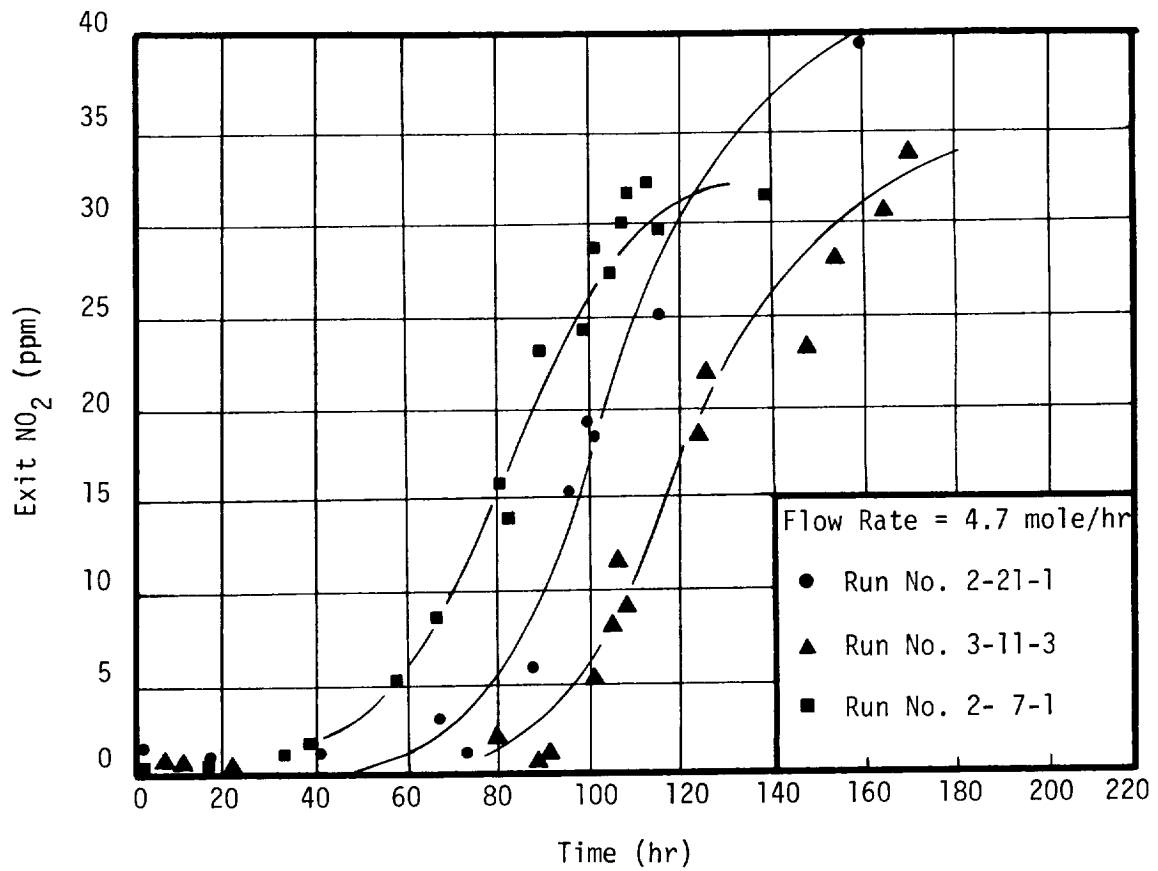
Figure 8.3 - Breakthrough Curves For NO_2 Adsorbed

On Activated Carbon
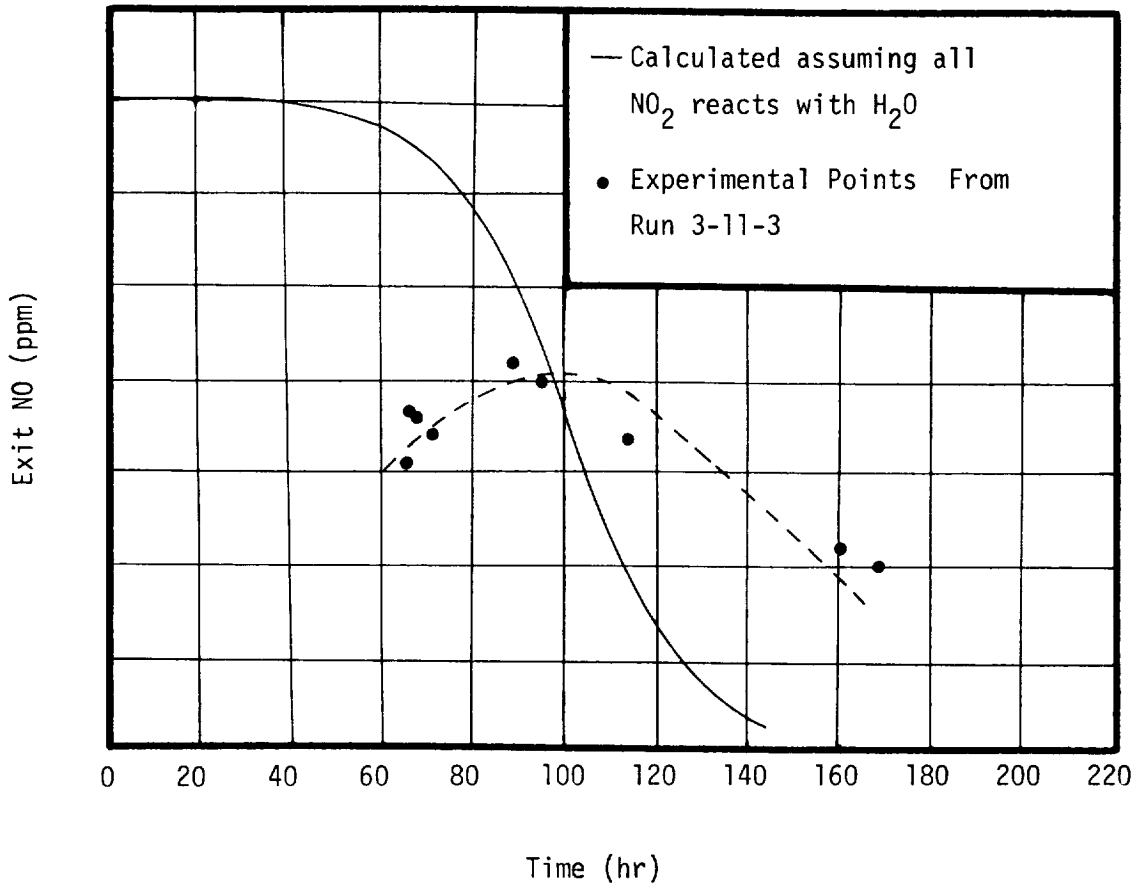
Figure 8.4 - Nitric Oxide in the Effluent From

An Activated Carbon Bed

based on the work of Morrison (57) indicate that in the short residence time in the system less than 1 ppm of NO would be oxidized. Therefore, apparently some of the NO is adsorbed by the carbon and then later in the cycle is replaced thus causing the experimentally measured NO concentration to pass through a maximum and then drop. It is also very probable that some of the NO_2 is adsorbed without undergoing reaction to form NO.

8.3 Regeneration of Activated Carbon Saturated With Nitrogen Dioxide

In order to develop limited qualitative information on the regeneration ability of activated carbon, regeneration of the NO_2 saturated carbon bed was attempted following Run 3-11-3. The first step in the regeneration was to heat the bed to 194°F (90°C) with a very small air flow. The outlet from the bed contained NO_2 in the gross percent concentration region. The bed was flushed with dry air for a total of 105 hours at temperatures ranging from 22 to 83°C. The bed was again saturated with an air stream containing 39 ppm of NO_2. At equilibrium the bed loading was calculated to be 0.252 g NO_2/g carbon, 70% of the original capacity.

The information developed indicates that activated carbon can be regenerated. Capacity of the regenerated material would be expected to be a strong function of regeneration conditions. The use of high vacuum and higher temperatures would almost certainly restore a higher percentage of the original adsorptive capacity.

8.4 Adsorption of Chlorine on Activated Carbon

Activated carbon effectively removed trace quantities of chlorine from both high and low humidity air. The conditions for the two runs made using activated carbon are shown in Table 8.2 and the outlet concentration histories are shown in Figure 8.5. In the run at high humidity (6-25-1) the carbon adsorbed 0.28 g of Cl_2 per g of carbon with a feed gas containing 30-32 ppm of Cl_2. The adsorption effectiveness of the carbon was much lower when zero humidity air was used. Even though the flow rate was lower for Run 6-21-1 the exit concentration increased faster than for Run 6-25-1, thus the humidity level is an important variable. When humidified air is used the carbon surface is probably covered with water which may react with chlorine according to the reactions

$$2 Cl_2 + C + 2 H_2O \rightarrow 4 HCl + CO_2 \qquad (8.2)$$

$$Cl_2 + H_2O \rightleftarrows HCl + HClO \qquad (8.3)$$
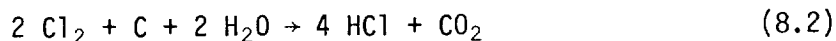
In either case the highly polar HCl is probably readily adsorbed by the remaining carbon.

TABLE 8.2

CHLORINE ADSORPTION ON ACTIVATED CARBON

Run Number	6-21-1	6-25-1
Packing Material	Activated Carbon	Activated Carbon
Amount of Packing, g	0.400	0.400
Bed Diameter, cm	1.27	1.27
Bed Temperature, °F	88	88
Air Flow Rate, mole/hr	1.43	2.22
Air Pressure, atm	0.9	0.9
Contaminant	Cl_2	Cl_2
Inlet Concentration, ppm	20 $\pm$ 1	31 $\pm$ 1
Humidity, mole H_2O/mole air	0.0	0.014
Carbon Dioxide, mole %	0.0	0.0
Test Duration, hr	25	90
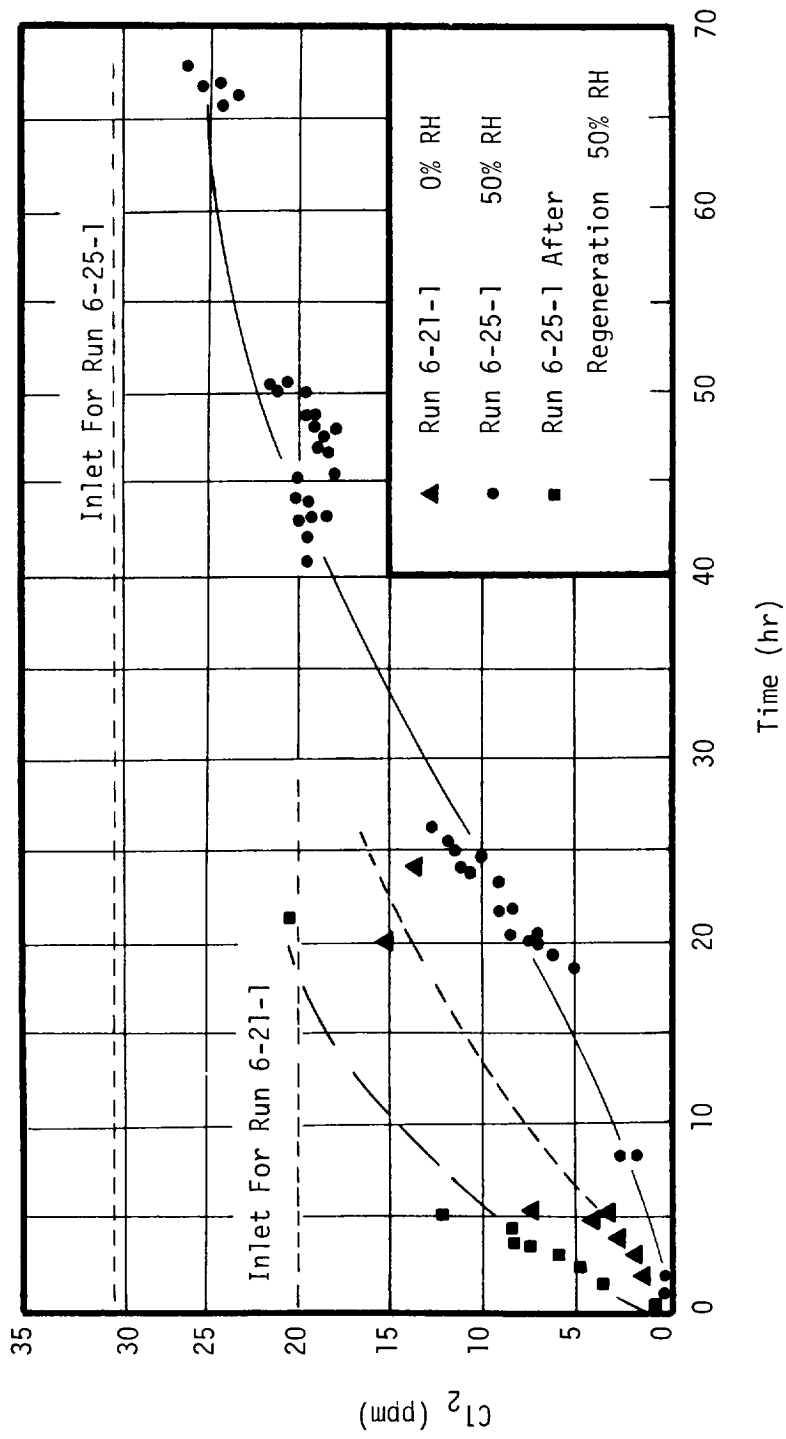
Figure 8.5 - Chlorine Adsorption On Activated Carbon

8.5 Adsorption of SO_2 in Activated Carbon

Activated carbon was tested using dry air contaminated with SO_2 and showed a very slow rate of adsorption at a space velocity of 1.7 (mole air)/(hr)(g carbon) and a temperature of 30°C. At these conditions the fresh bed removed only 14% of the incoming SO_2. At the extremely low space velocity of 0.12 the carbon initially removed 85% of the SO_2 and was still removing 38% of the 12 ppm inlet SO_2 after 12 days of continuous operation. This small amount of data indicates that activated carbon has a rather large capacity for SO_2, but that the slow rate of adsorption limits its usefulness for removal of this contaminant.

8.6 Summary of Acid Gas Adsorption on Activated Carbon

Activated carbon was found to readily adsorb NO_2 and Cl_2 when these compounds were present as trace contaminants in air. Sulfur dioxide adsorption rates were found to be much slower than the rates for the other two gases. The effect of humidity was very pronounced for both NO_2 and Cl_2. In the case of NO_2 the presence of a high humidity increased the carbon capacity by a factor of three. The treatment of a carbon with sodium bicarbonate did not cause the carbon to exhibit any appreciably different adsorption characteristics. Carbon beds saturated with either NO_2 or Cl_2 were found to be relatively easy to partially regenerate.

Coconut charcoal was found to be effective for NO_2 removal as was the Witco carbon. No difference between the two was apparent. When operated at a higher temperature (36°C compared to 26°C) the bed capacity was reduced and a higher adsorption rate was recorded. During the higher temperature run, NO was found in the exit stream. This appearance of NO has been confirmed with later work at 26°C. The presence of the NO is thought to be due to reaction with adsorbed water to form HNO_3 and NO.

Work performed in this laboratory shows that MnO_2 is also active as a room temperature adsorbing medium. In most cases (SO_2 being the exception) activated carbon is either as effective or more effective than MnO_2 for room temperature adsorption.

9.0 REMOVAL OF THE NITROGEN OXIDES THROUGH CATALYTIC REDUCTION

Three of the oxides of nitrogen are potentially hazardous contaminants which must be removed from a closed system such as a spacecabin. These oxides are nitrogen dioxide (NO_2), nitric oxide (NO), and nitrous oxide (N_2O). Of these three, nitrogen dioxide has the lowest threshold limit value.

A simple and very desirable method of removing these materials would be the catalytic reduction to elemental oxygen and nitrogen. If a suitable catalyst could be found then the oxides could be removed with no consumption of a reagent. There are several promising catalytic materials; these include nickel oxide, copper oxide, manganese dioxide, and platinum where these materials are supported on a high surface area material such as alumina.

Considerable work (58,59) has been undertaken on the catalytic removal of the nitrogen oxides from gas streams under conditions of a reducing atmosphere. A fuel such as hydrogen, methane, or carbon monoxide is utilized to effect the chemical reduction of the nitrogen oxides with the aid of a solid catalyst. These studies have been oriented toward removal of these oxides from nitric acid manufacturing plant tail gas and from internal combustion engine exhaust where the oxides concentration is in the range of 100 ppm to 5000 ppm. Investigations of the catalytic decomposition of pure N_2O have been made. Sterbis (3) reports that using finely ground pure nickel oxide 70% conversion of N_2O to elemental nitrogen and oxygen was achieved at temperatures as low as 300°C. One patent (4) claims to produce a breathing quality atmosphere from a feed of pure N_2O at a temperature of 490°C. Each of these reports indicate that N_2O can be decomposed to the elements under relatively mild conditions as compared to the reported conditions of NO_2 decomposition. The dissociation of NO_2 (to form N_2 and O_2) in a nitrogen background gas over a CuO-alumina and over a CeO_2-alumina catalyst was studied by Wikstrom and Nobe (60). They also did limited work on this reaction in the presence of air and obtained a 45% conversion of NO_2 to nitrogen and oxygen at 520°C using a CuO-alumina catalyst. At a temperature of 370°C the conversion was about 10%. In all instances reported, the presence of oxygen reduces considerably the activity of the catalyst for the decomposition reaction.

After a review of the literature it is evident that there has been very little work directed toward accomplishing the catalytic reduction of the oxides of nitrogen in the presence of excess oxygen. Since, no doubt, these decomposition reactions are complex and would thus require a large effort in order to study each one, the work on this project was of necessity confined to the decomposition of NO_2. It is believed that a catalyst which is active toward NO_2 should also be active toward the other oxides.

9.1 Thermodynamics of the Reduction of Nitrogen Oxides

The set of reactions by which the removal of the nitrogen oxides is visualized as follows:

$$NO_2 \rightleftharpoons NO + 1/2\ O_2$$

$$2\ NO \rightleftharpoons N_2O + 1/2\ O_2$$

$$N_2O \rightleftharpoons N_2 + 1/2\ O_2$$
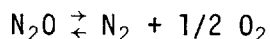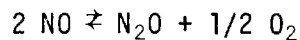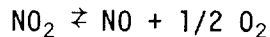
From a theoretical viewpoint, the oxides could be reduced to the thermodynamic equilibrium concentration which, since all of the reactions are endothermic, decreases with decreasing temperature. Shown in Figure 9.1 are the equilibrium constants for the nitrogen oxide decomposition reactions as a function of temperature. Using the calculated equilibrium constants and an atmosphere with an oxygen partial pressure of 0.2 atm and a nitrogen partial pressure of 0.48 atm, equilibrium concentrations of the oxides were calculated. In order to reduce the NO_2 concentration of the continuous exposure threshold limit value of 0.2 ppm the catalyst would have to be active at a temperature of 370°C (700°F) or less. The equilibrium concentration of NO is less than that of NO_2 for temperatures below 430°C (806°F). The equilibrium concentration of N_2O is extremely low being less than 10^{-5} ppm at 400°C.

From the thermodynamics calculations it becomes clear that the catalytic removal of nitrogen dioxide down to fractional ppm levels without a reducing reactant puts rather severe activity requirements on the catalyst since it must promote the reduction reaction at a relatively low temperature if the threshold limit value is to be reached by catalytic reduction alone. On the other hand, thermodynamic limitations are insignificant for nitrous oxide and are not as severe for nitric oxide.

9.2 Correlation of Integral Type Data from a Tubular Catalytic Reactor

In trying to obtain kinetic data for the catalytic reduction of nitrogen dioxide a major problem is accurate chemical analysis at the low concentrations of interest in this study. Because of this difficulty experimental data must be of the integral reactor type, that is, the reactor must be operated such that a large fraction of the inlet contaminant is reacted. Data of this type is somewhat more difficult to correlate than that from a differential reactor since the contaminant concentration and hence the reaction rate vary significantly down the length of the reactor. However, the primary goal of the work reported here was to explore the qualitative behavior of several catalytic materials rather than to study in detail any single material. Obviously much more work is needed in the area.

9.3 Experimental Data for Catalytic Reduction of Nitrogen Oxides

During the course of this study reaction rate data were taken using five different catalysts. These were as follows:

(1) Nickel oxide on Gridler T-126 alumina (laboratory preparation).
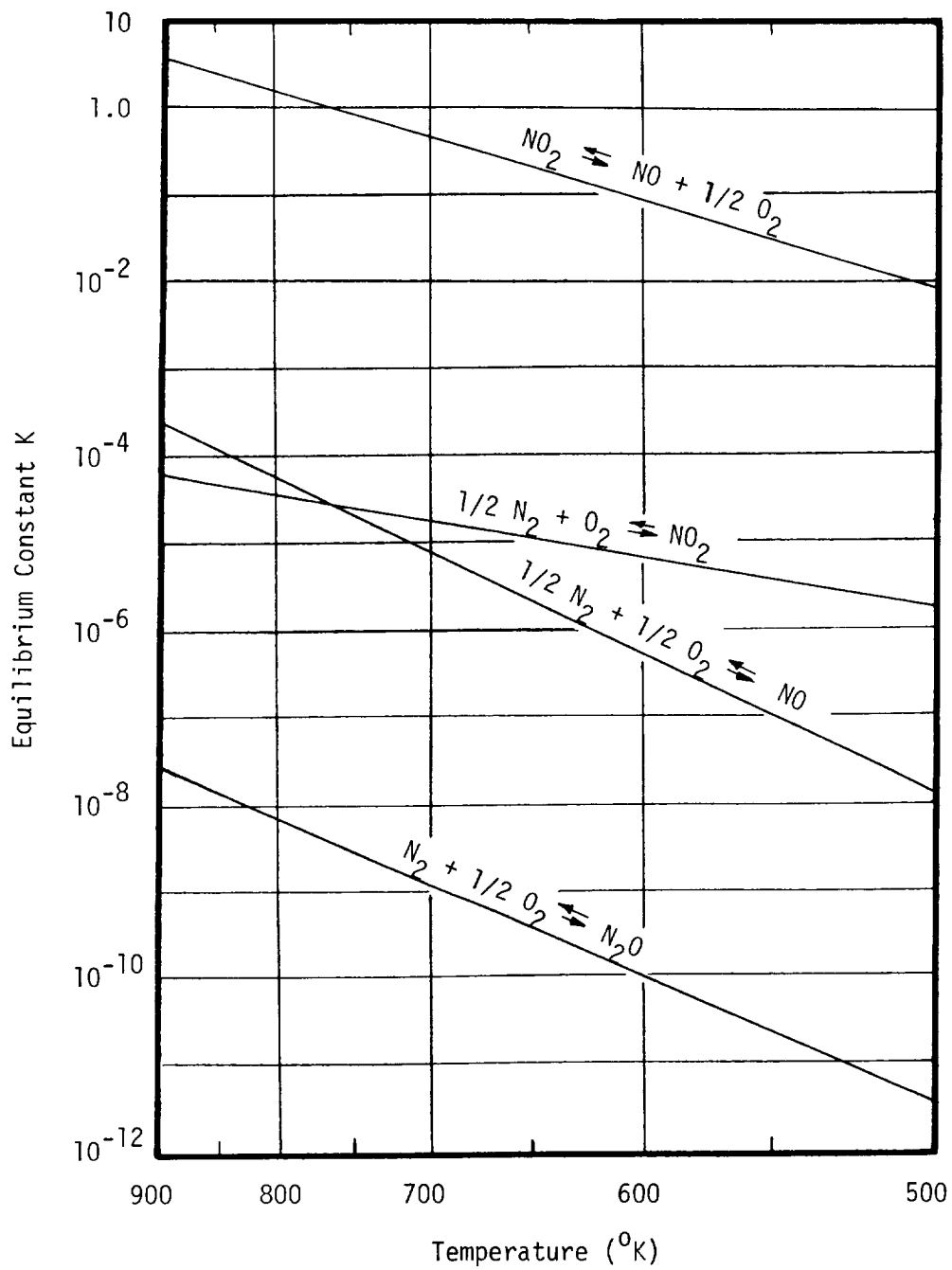
Figure 9.1 - Equilibrium Constants For Nitrogen
Oxides Formation

(2) Nickel oxide on Grace silica gel (laboratory preparation).

(3) Girdler alpha alumina.

(4) Harshaw supported copper oxide Cu-0803.

(5) Harshaw supported manganese dioxide Mn-0201.

Shown in Table 9.1 are the physical properties for each of these materials. Experimental data showed that each of these catalysts except the manganese dioxide (No. 5) was active in promoting the reduction of NO_2 with the copper oxide being the most active and the alumina alone the least active.

Since the activity of many catalysts is sensitive to the oxidation state of the metal and to the method of activation, a flowing air stream containing NO_2 was passed over each catalyst while the temperature was maintained at approximately 350°C as a pretreatment. The charge was pretreated in this manner for at least 24 hours prior to the collection of rate data.

The principal reaction observed at the lower temperatures with each of the catalyst was the reduction to nitric oxide (NO). Further reduction to either N_2O or N_2 determined by difference, was observed; however, the reaction rate was much slower than was desired especially at the lower temperatures (370°C). Shown in Table 9.2 are typical experimental results for the supported copper oxide. As may be seen from the data given in Table 9.2 the reaction rate increases rather rapidly as the temperature is increased. The conversion to NO is in the range of 30-35% at a temperature of 432°C and space velocity of one to two mole air/hr g cat. Further reduction to N_2O and N_2 was also observed. In the one to two space velocity range 6 to 12% of the inlet NO_2 was reduced to either N_2O or N_2 at a temperature of 342°C.

At higher temperatures and lower values of space velocity the nickel oxide catalysts also removed large percentages of the inlet NO_2. Shown in Table 9.3 are typical experimental results from the two nickel oxide catalysts tried. The data indicate that the nickel catalyst may promote the reduction to N_2 and N_2O slightly better than does the copper, while the copper is more active at reduction to NO.

Shown in Figure 9.2 is the natural log of the NO_2 inlet to NO_2 outlet ratio versus 1/T for the nickel oxide silica gel catalyst at a F/W of 1.21.

The exit concentration ratio of NO_2 to NO approached the thermodynamic equilibrium values for these oxides as may be seen in Figure 9.3. The fact that considerable NO is present in the reactor outlet indicates that the rate of reduction of this compound is relatively slow.

The major conclusions to be drawn from this exploratory work on nitrogen oxides reduction in the presence of excess oxygen are:

(a) There are materials which will catalytically reduce NO_2 to yield the lower oxides and nitrogen.

TABLE 9.1

PHYSICAL PROPERTIES OF CATALYSTS

	Catalyst				
	1	2	3	4	5
Supported Oxide	Nickel	Nickel	None	Copper	Manganese
Percent Metal Oxide	5%	5%	----	10%	19%
Pellet Shape	Cylinder	Granules	Cylinder	Cylinder	Granules
Pellet Diameter, in.	3/16	0.03	3/16	1/8	1/8
Surface Area, m^2/g	175	Unknown	6.4	137	69
Pore Volume, cm^3/g	0.29	Unknown	0.02	0.42	0.23

*(1) Nickel Oxide on Gridler gamma alumina (laboratory preparation)

*(2) Nickel Oxide on Grace Grade 28 silica gel (laboratory preparation)

(3) Girdler alpha alumina

(4) Harshaw Cu-0803

(5) Harshaw Mn-0201

*These catalyst were made by saturating the support material with nickel nitrate solution followed by calcining in air at 550°C for 24 hours.

TABLE 9.2

CATALYTIC REDUCTION OF NO_2 USING SUPPORTED COPPER OXIDE

Temp., °C	$\frac{F^*}{W}$	C_{NO_2} (inlet) ppm	% Conversion to		
			$NO+N_2O+N_2$	NO	N_2O+N_2
356	0.9	44.6	6.7	NM**	NM
356	1.12	34.7	7.5	NM	NM
356	1.56	23.7	2.9	NM	NM
390	1.05	31.6	22.7	NM	NM
400	1.05	31.6	19.0	NM	NM
400	1.72	19.5	17.0	NM	NM
400	2.39	12.2	22.1	NM	NM
432	0.91	40.0	41.5	NM	NM
432	1.52	23.6	37.3	NM	NM
432	2.13	16.5	39.4	NM	NM
432	2.0	18.2	45.0	33.0	12.0
432	1.36	25.3	39.5	30.5	9.0
432	1.05	33.0	42.5	36.4	6.1
432	0.81	44.2	41.1	34.6	6.5
432	1.71	21.5	39.2	31.6	7.6

*mole air/hr/g cat

**not measured

90

TABLE 9.3

CATALYTIC REDUCTION OF NO_2 USING SUPPORTED NICKEL OXIDE

Temp. °C	$\frac{F^*}{W}$	C_{NO_2} (inlet) ppm	% Conversion to		
			$NO+N_2O+N_2$	NO	N_2O+N_2
For Nickel Oxide - Alumina					
404	0.24	40	20	8	12
435	1.03	40	22	NM**	NM
460	0.24	40	50	NM	NM
465	0.24	40	58	NM	NM
465	0.24	40	45	17.5	27.5
516	0.24	40	50	28.3	22.5
For Nickel Oxide - Silica Gel					
430	0.31	40	27.5	11.6	15.9
437	1.21	40	21.2	5.0	16.2
482	0.31	40	53	33.2	19.8
482	1.21	40	32.3	21.6	10.7
500	1.21	40	50	15.2	35.8

*mole air/hr/g cat

**not measured
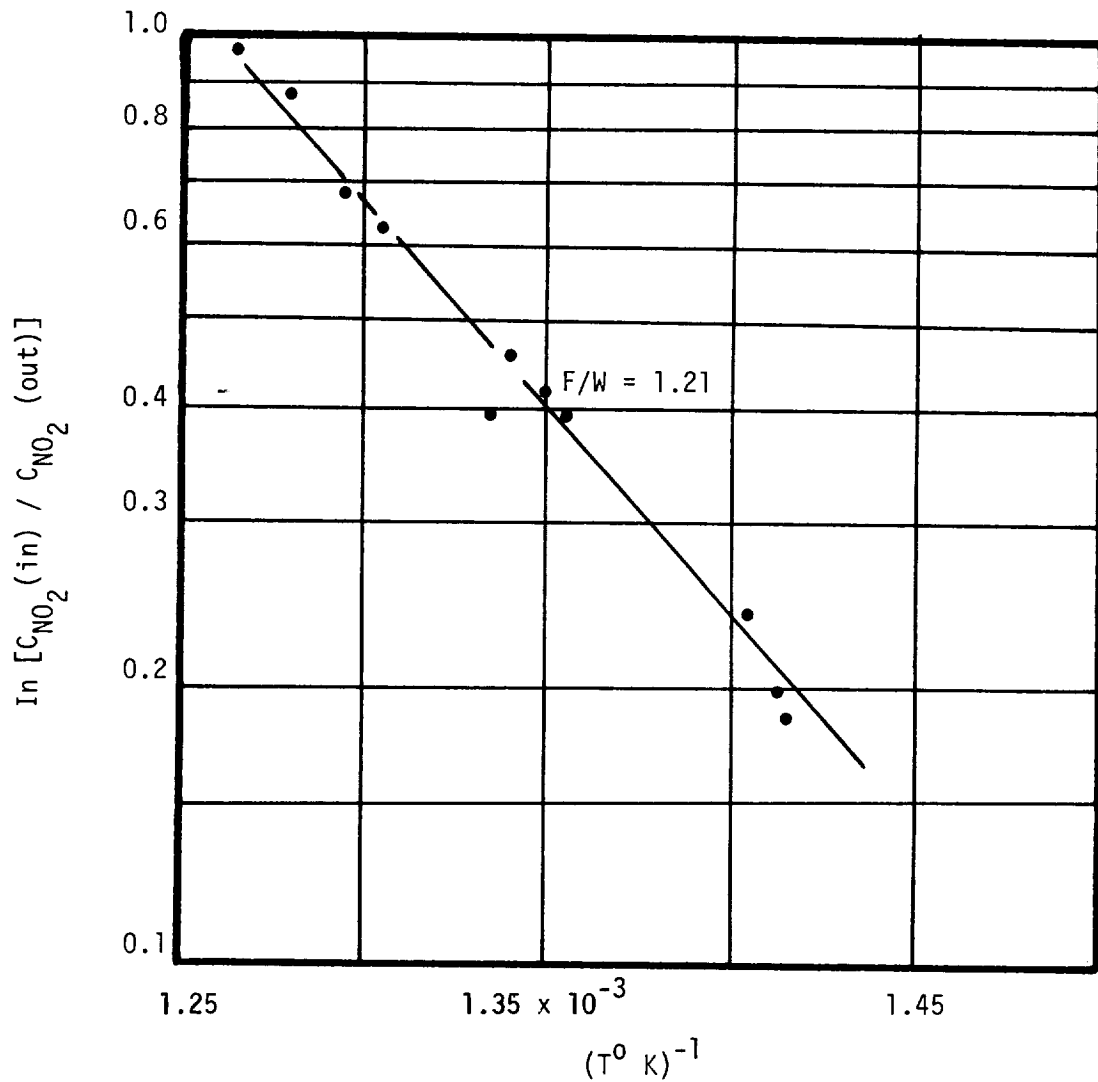
Figure 9.2 - Effect of Temperature On The Reduction of NO_2
Using A Nickel Oxide On Silica Gel Catalyst
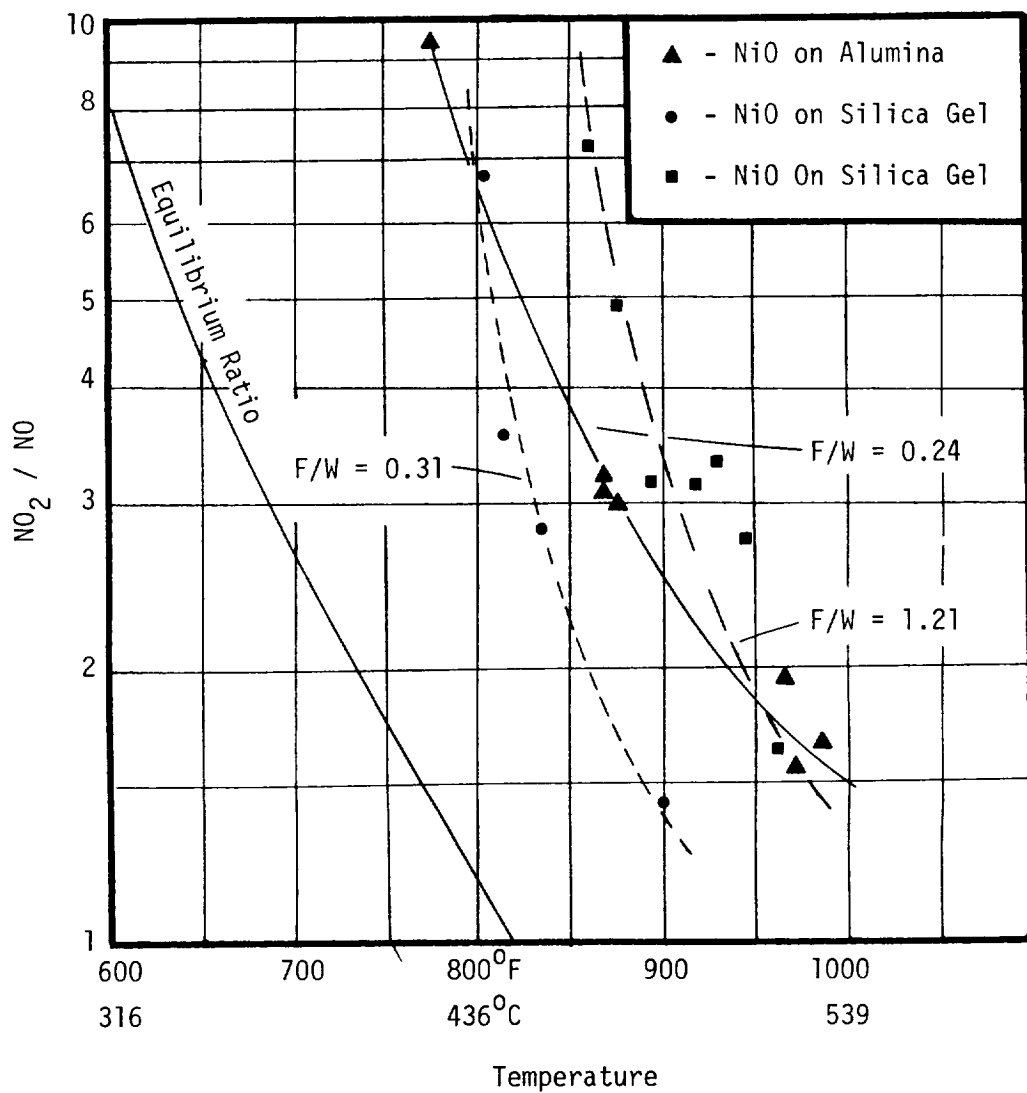
Figure 9.3 - The Ratio Of NO_2 Concentration to NO
Concentration In The Reactor Effluent

(b) For the catalyst evaluated, the equilibrium concentration of NO_2 and NO may be approached relatively easily.

(c) Analytical techniques for the convenient precise quantitative analysis of NO and N_2O are needed.

(d) Much more work is needed in order to evaluate more materials for their catalytic activity.

10.0 ENGINEERING ESTIMATES OF POST CATALYTIC SUBSYSTEM PERFORMANCE

The object of this research project was to provide information from which an improved post-catalytic contaminant removal system could be designed and information which would predict its performance. In the previous sections the experimental work for each contaminant considered has been presented. Because of severe analytical problems, work on mixtures of these contaminants has been brief; however, based on single contaminant information reasonably accurate predictions can be made for the operation of the system.

Several mathematical simulations have been made to illustrate the predicted performance of the proposed contaminant removal system. In order to make these calculations, the various possible chemical interactions between the contaminants, both in the gas phase and on the solid particle surface, were neglected. From a practical standpoint the assumption of no interaction probably does not greatly reduce the reliability of the simulation provided some reserve of basic material is maintained. The salts formed by the acid gas reactions are very stable so that solid phase displacement interactions probably are minor. The apparent porosity of the manganese dioxide is very high since the solid is reactive until it is almost depleted. Therefore, sealing off of the internal area by any one gas appears unlikely in the case of the MnO_2. The fused lithium carbonate is much less porous and consequently more susceptible to sealing of the pore structure.

Gas phase interaction reactions would be very slow under practical conditions due to the extremely low concentrations plus the fact that the products of most of the interactions which can be invisioned would be as easily removed as the original contaminants. Possible interactions include:

$$SO_2 + Cl_2 + 2\ H_2O \rightarrow HCl + H_2SO_4$$

$$NO_2 + SO_2 \rightarrow NO + SO_3$$

$$2\ NO + Cl_2 \rightarrow 2\ NOCl$$
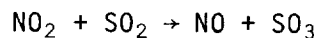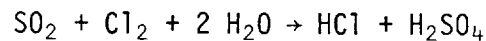
10.1 Recommended Reactor Construction

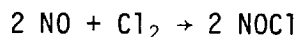The experimental data generated during this project has demonstrated that feasible, spaceworthy materials are available which will remove the contaminants under consideration. However, as would be expected there is no one material which is universally superior for all the contaminants. Thus an optimal bed composition depends on the relative amounts of the contaminants and their generation rates. A preferred system would consist of a layer of manganese dioxide granules for removal of sulfur dioxide and chlorine, a layer of lithium carbonate granules for removal of strongly acidic gases such as HCl, HF, and SO_3 and incorporated within the catalytic burner a supported copper oxide catalyst

for the decomposition of nitrogen oxides. A single layer of lithium carbonate would remove the contaminants chlorine, sulfur dioxide, hydrogen chloride, and hydrogen fluoride although the single component bed would be less efficient since the reaction rate for SO_2 is roughly twice or three times as fast with MnO_2 as with Li_2CO_3 when compared on a mass basis.

10.2 Calculated Performance for a Multi-Contaminant System

Optimal size and composition of a post-catalytic acid gas removal bed depends on the relative amounts of the contaminants initially present and on their net rates of generation within the entire system. Given these basic design data, the data and mathematical relationships developed in this study make possible the prediction of the performance of any specific gas scrubber using MnO_2 and/or Li_2CO_3.

Since reliable data on contaminant generation rates were unavailable, simulations of scrubber performance were made for three specific designs, and operating conditions using an assumed inlet air composition. Contaminant concentrations in the air entering the scrubber were assumed constant at the MAC levels reported by Robell (61). At 10 psia and 72°F the MAC levels expressed in ppm are:

NO_2	0.7 ppm
SO_2	0.445 ppm
Cl_2	0.75 ppm
HCl	0.144 ppm
HF	0.142 ppm

While it is very unlikely that contaminant concentrations would continuously run as high as MAC levels, the assumption results in conservative predictions and makes possible reliable performance comparisons. The three cases chosen for simulation were selected to illuminate the performance characteristics of designs believed to be reasonable.

CASE I

A mathematical simulation of the contaminant removal subsystem was made using the assumed inlet air composition and the following reactor specifications:

Air Flow Rate	= 77.2 mole/hr	(4.95 lb/hr)
Temperature	= 342°C	(650°F)
Reactor Diameter	= 2.54 cm	(1 in.)
Overall Reactor Length	= 11 cm	(4.33 in.)
MnO_2 Packed Section	= 5 cm	(1.97 in.)
Li_2CO_3 Packed Section	= 6 cm	(2.36 in.)
MnO_2 Particle Diameter	= 0.16 cm	(0.063 in.)

96

```
Li₂CO₃ Particle Diameter     = 0.16 cm          (0.063 in.)
Pressure                     = 0.68 atm         (10 psia)
```

Using the program discussed in Section 4.6 and the specifications above the calculated contaminant removal efficiencies (percent of inlet contaminant removed by reactor) for each compound are given in Table 10.1.

TABLE 10.1

CONTAMINANT REMOVAL EFFICIENCY FOR CASE I

Contaminant Removal, %

Time	NO_2	SO_2	Cl_2	HCl	HF
Initial	61.0	99.8	99.9	99.9	99.9
After 100 hr	46.0	99.5	99.9	99.9	99.9
After 200 hr	36.0	98.5	99.9	99.9	99.9
After 300 hr	30.0	97.5	99.9	99.9	99.9
After 400 hr	24.5	95.7	99.9	99.9	99.9
After 500 hr	21.0	93.7	99.9	99.9	99.9
After 600 hr	18.0	91.2	99.9	99.9	99.9
After 700 hr	16.5	88.7	99.9	99.9	99.9
After 750 hr	15.6	87.6	99.8	99.9	99.9

The concentration profiles for the two typical contaminants SO_2 and HCl are shown in Figure 10.1. These profiles take the form of decaying exponentials. The performance of a shorter bed may be roughly estimated from Figure 10.1. As may be seen from this figure, the optimum bed construction for Case I would have a longer section of MnO_2 and shorter section of Li_2CO_3 than was assumed for the simulation.

The progressive utilization of the solid reagents for Case I is shown in Figure 10.2. For this case the MnO_2 is used much faster than the Li_2CO_3 because of the high content of SO_2 and Cl_2 which react very fast with MnO_2. Since the inlet HCl and HF concentrations are relatively low then the Li_2CO_3 is not appreciably depleted. Also contributing is the considerable difference in density of the two packed sections. The MnO_2 packed density is only 0.45 g/cm³ compared to 0.78 g/cm³ for the sintered Li_2CO_3.

CASE II

The simulation for Case II was the same as for Case I except that the reactor was assumed to contain no MnO_2. Instead a packed section of Li_2CO_3 11 cm in length was assumed. The removal efficiency of this bed is shown in Table 10.2.

97
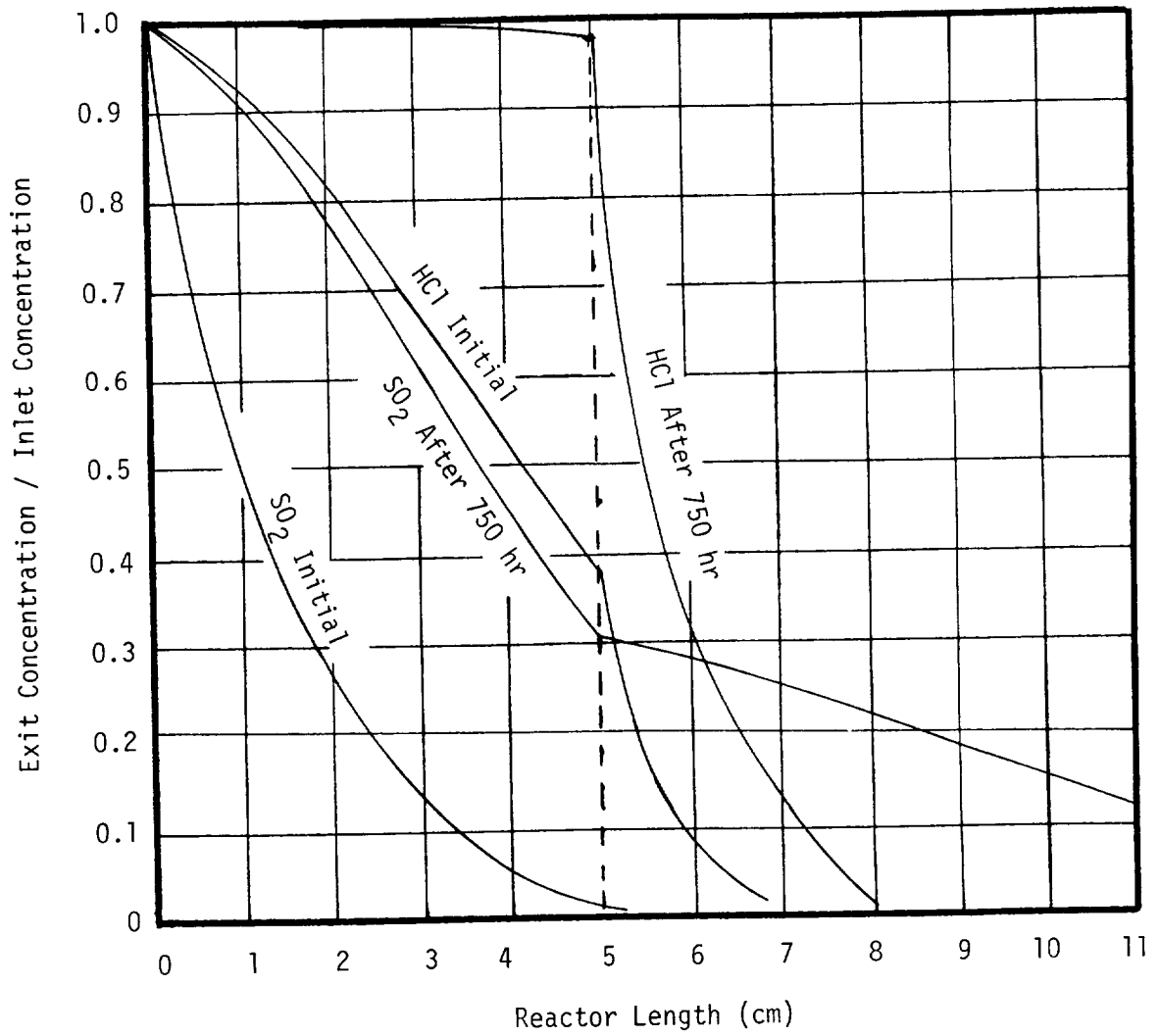
Figure 10.1 - Contaminant Concentration Profiles For Case I
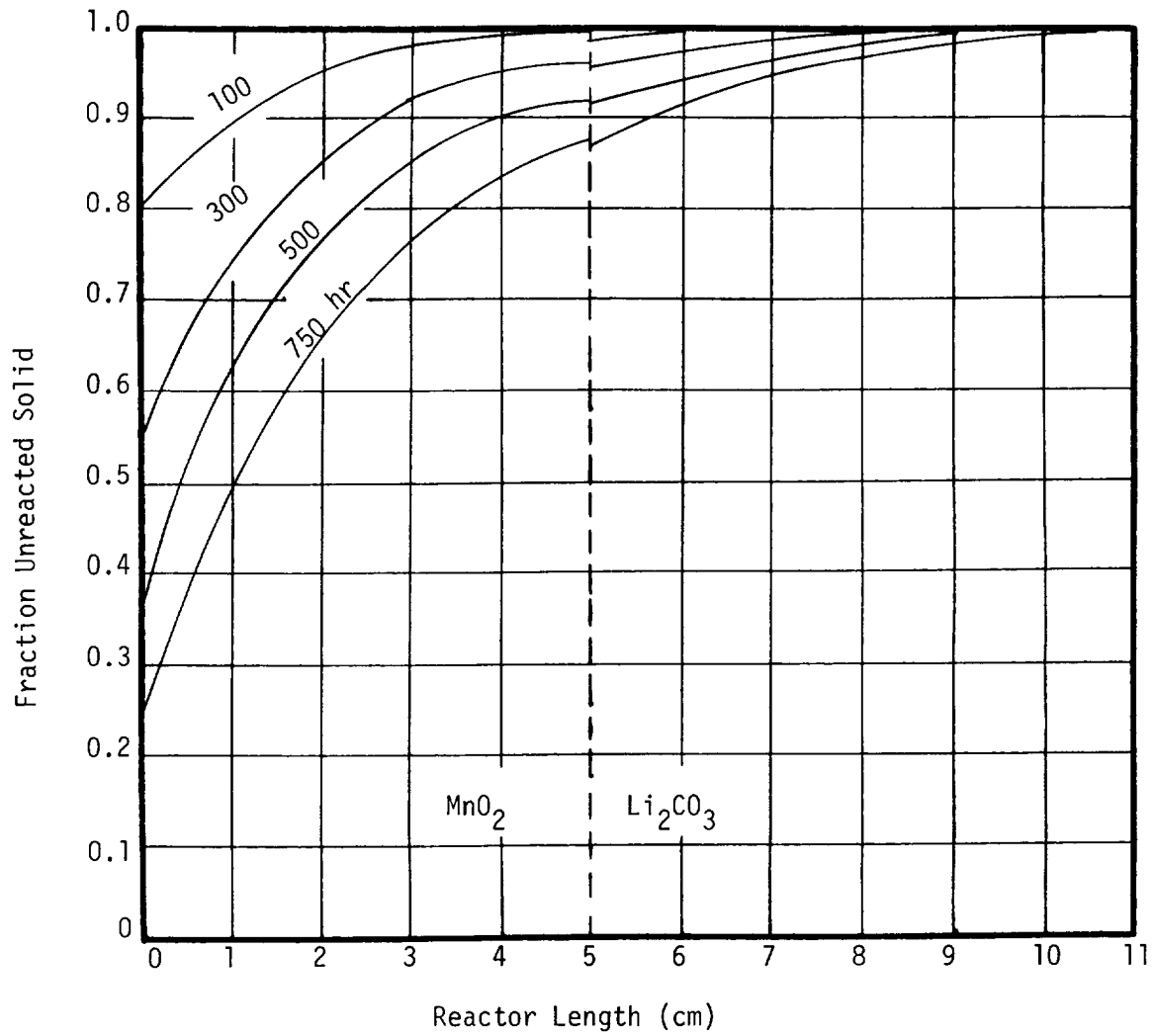
Figure 10.2 - Solid Reactant Utilization For Case I

TABLE 10.2

CONTAMINANT REMOVAL EFFICIENCY FOR CASE II

Contaminant Removal, %

Time	NO_2	SO_2	Cl_2	HCL	HF
Initial	61.0	99.6	99.1	99.9	99.9
After 100 hr	42.9	95.7	98.4	99.9	99.9
After 200 hr	30.0	88.5	97.1	99.9	99.9
After 300 hr	23.0	80.5	95.9	99.9	99.9
After 400 hr	18.5	73.0	94.4	99.9	99.9
After 500 hr	15.4	65.6	92.9	99.9	99.9
After 600 hr	13.0	60.2	90.9	99.9	99.9
After 700 hr	11.4	55.3	89.9	99.9	99.9
After 750 hr	10.8	53.5	88.3	99.9	99.9

This reactor is not nearly as effective for SO_2 and Cl_2 control as was Case I. Since the weight of packing is greater and since the removal efficiency is lower than for Case I the bed utilization after 750 hours of operation would be lower as is shown in Figure 10.3.

CASE III

For Case III the reactor specifications are the same as for Case I except that the air flow rate is increased to 154.4 mole/hr. Therefore, for this case since the inlet concentration is the same as for Case I but the flow rate is twice that of Case I, the amount of contaminant entering the reactor is twice that of Case I. The removal efficiency under this condition is shown in Table 10.3.

TABLE 10.3

CONTAMINANT REMOVAL EFFICIENCY FOR CASE III

Contaminant Removal, %

Time	NO_2	SO_2	Cl_2	HCl	HF
Initial	41.3	96.4	99.9	99.9	99.9
After 100 hr	28.5	89.3	99.7	99.5	99.5
After 200 hr	13.2	80.5	99.6	99.4	99.4
After 300 hr	9.7	72.1	99.0	99.4	99.4
After 400 hr	7.6	64.6	98.0	98.6	98.6
After 500 hr	6.2	58.0	96.4	98.6	98.6
After 600 hr	5.1	51.6	94.5	98.0	98.0
After 750 hr	4.1	44.7	91.1	96.6	96.6
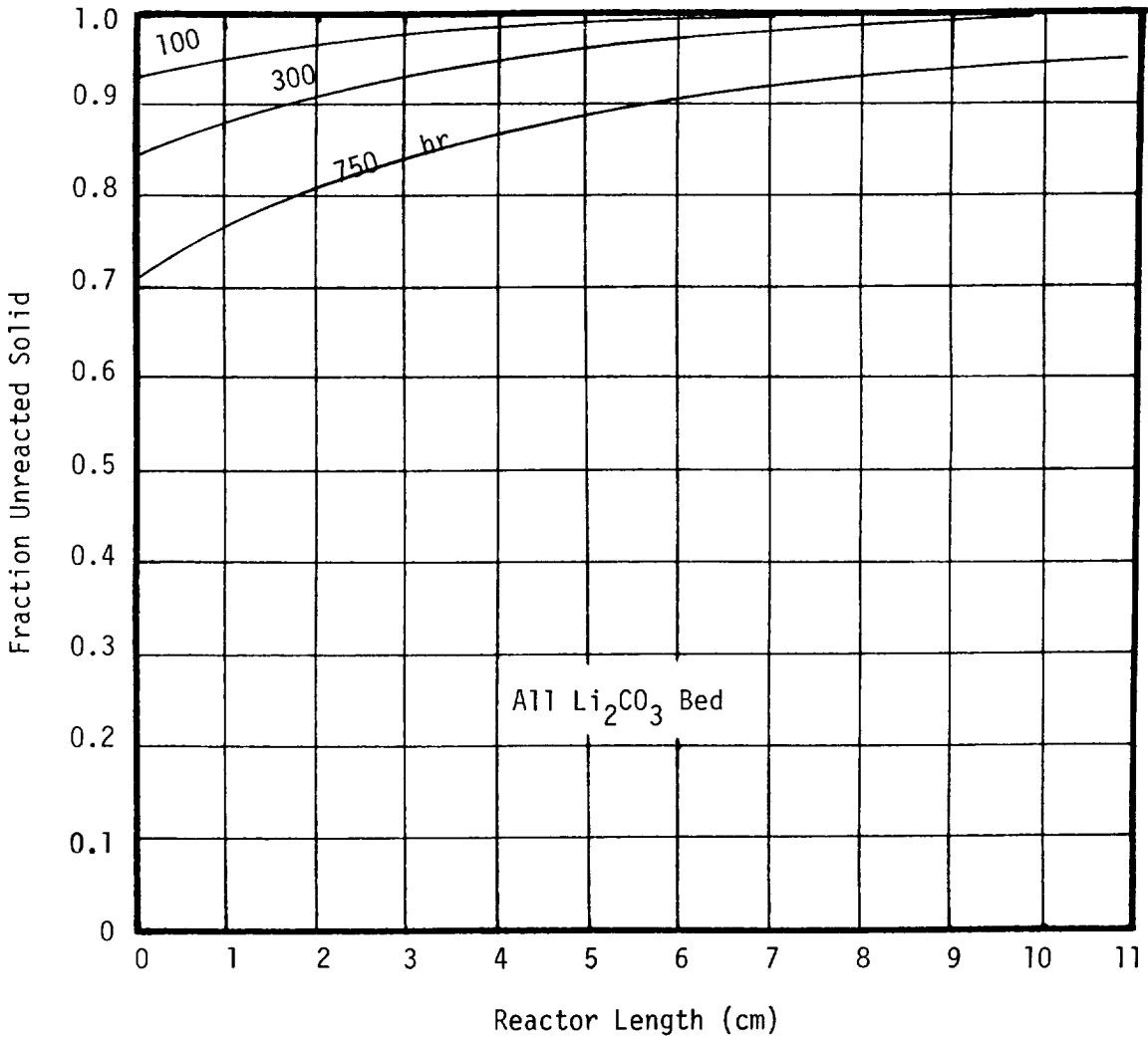
Figure 10.3 - Solid Reactant Utilization For Case II

The solid reactant concentrations for Case III are shown in Figure 10.4.

The three typical cases presented are intended to illustrate the performance of two possible bed constructions. The composite construction consisting of approximately 5 cm of MnO_2 and 6 cm of Li_2CO_3 is believed to be much preferred over the bed containing only Li_2CO_3. Our data indicated that even the Li_2CO_3 bed would greatly out perform a $CaCO_3$ bed for SO_2 removal at the temperatures of interest to this project.

The performance data generated through simulation show that reasonably sized scrubbers can be designed which will be effective for a long period of time in acid gas removal. Case I results shows that even after 750 hours operation at MAC levels in the inlet gas, the single pass removal of the contaminants SO_2, Cl_2, HCl, and HF is good with the last three being almost completely removed.
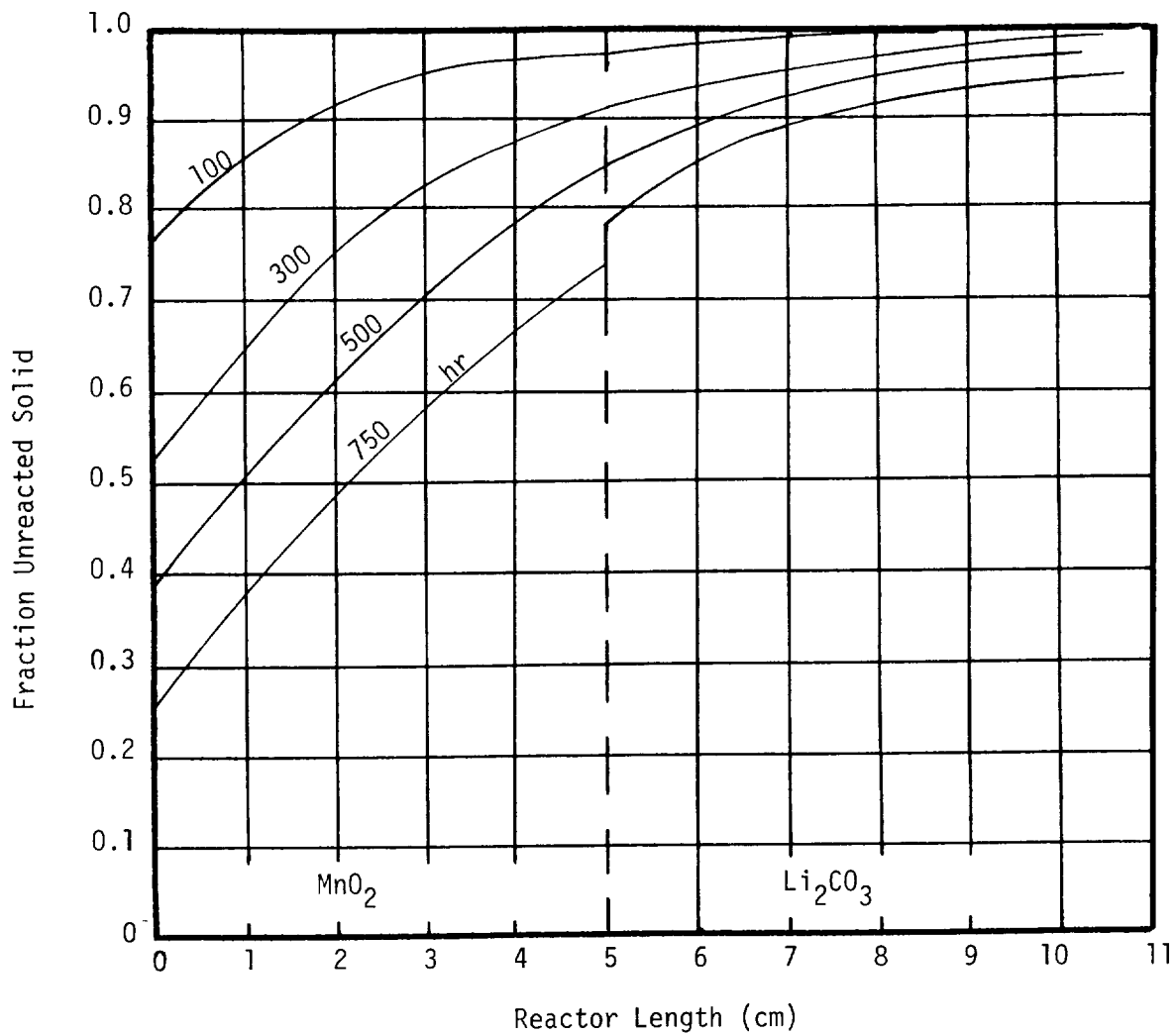
Figure 10.4 - Solid Reactant Utilization For Case III

11.0 CONCLUSIONS

1. The reaction between the gases NO_2, SO_2, Cl_2, HCl, and several solid basic materials including Li_2CO_3, $CaCO_3$, and MnO_2 have been studied and equations developed to estimate the rate of the reactions.

2. At the temperatures of interest (340-380°C) the most effective solid material tested for removal of SO_2 and Cl_2 in trace quantities from air was a porous form of MnO_2.

3. At the temperatures of interest the most effective solid tested for removal of HCl was Li_2CO_3. Since HF is similar to HCl in many ways it may safely be assumed that Li_2CO_3 would also be very effective for removal of HF.

4. Nitrogen dioxide is removed at best to only a limited extent by reaction with basic materials at temperatures of 150° to 480°C.

5. A suitable physical form of Li_2CO_3 for use in acid gas removal subsystems may be made by sintering a mixture of Li_2CO_3, and $CaCO_3$ reagent grade powders, followed by crushing and screening to the desired particle size.

6. By using a composite bed having first a 5 cm layer of MnO_2 and second a 6 cm layer of Li_2CO_3, over 88% of the SO_2 and over 99% of the Cl_2, HCl, and HF can be removed up to 750 hours of operation when the MAC levels of these compounds are used as the inlet concentration to the reactor. This assumes operation at a temperature of 340°C or higher, and an air flow rate of 15.6 g mole/hr cm^2.

7. A convenient and relatively simple method for the correlation of experimental data from solid-gas reactions as well as the design of solid-gas reactors is based on the concept of a shrinking core of unreacted solid.

8. At the MAC level of 0.7 ppm and assuming a linear isotherm, activated carbon at saturation will adsorb approximately 4.3% by weight of NO_2 at a temperature of 25°C with 50% RH and 10 psia air. With dry air this adsorption is reduced to approximately 1.3%. Chlorine and to a lesser extent SO_2 are adsorbed by activated carbon.

9. Supported copper oxide and supported nickel oxide are both fairly active catalyst for the reduction of NO_2 at temperatures of 350°C or higher. Several more materials should be screened for their catalytic activity in the reduction of nitrogen oxides.

10. A limiting factor in work on the removal of trace contaminants is the availability of reliable and sensitive methods of quantitative analysis, particularly analysis of mixtures of contaminants.

```
C       PROGRAM TO CALCULATE THE OUTLET CONCENTRATION FOR A
C       SOLID-GAS REACTOR.  THE PROGRAM USES A SHRINKING CORE
C       MODEL AND IS FOR A DOUBLE LAYER OF SOLID AND FOR FIVE
C       CONTAMINANTS.

C       THE CODE NUMBERS FOR THE VARIOUS CONTAMINANTS ARE
C               NITROGEN DIOXIDE ************* 1
C               SULFUR DIOXIDE ************** 2
C               CHLORINE ******************** 3
C               HYDROGEN CHLORIDE *********** 4
C               HYDROGEN FLUORIDE *********** 5

C       BED NUMBER ONE IS MANGANESE DIOXIDE
C       BED NUMBER TWO IS LITHIUM CARBONATE

        DIMENSION C(5,12,20),X(12,20),PPM(5,20),DE(5,3),FKG(5,
       13),ROBED(3),
       1DIAP(3), CIN(5),PARNUM(3), GMW(5,3)
        DIMENSION OMEG(5),GASC(5),SNUM(5),FKF(5,2),GASMW(5),DI
       1FF(5)
        DIMENSION FJD(2),RENUM(2)
      1 FORMAT (8F10.0)
      2 FORMAT (6I4)
      3 FORMAT (/26H BED TEMPERATURE (DEGK) = , F6.1,2X,24H AI
       1R DENSITY (M
       1OLE/CC) = ,E12.4   )
      4 FORMAT (/35H REACTOR CROSS-SECTION AREA (CM2) = ,F10.5
       1,24H GAS VEL
       1OCITY (CM/SEC) =,E10.3)
      5 FORMAT (/22H TIME INCREMENT (HR) = ,F9.6, 24H LENGTH I
       1NCREMENT (CM
       1) =,F9.6)
      6 FORMAT (8E15.6)
```

```
   28 FORMAT (/4H GAS ,I4,12H CON PROFILE , 12F8.3)
   29 FORMAT(12H TIME (HR) = , F6.2)
   31 FORMAT (/18H SOLID CON PROFILE , 12F8.4)
   41 FORMAT (/32H NUMBER OF PARTICLES/CC BED 1 = ,F10.1,25H
      1 PARTICLES/C
      1C FOR BED 2 = ,F10.1)
   43 FORMAT (14H DE (CM2/HR) = ,F10.4,14H FKG(CM/HR) = , F1
      10.2,16H COMP
      1OUND NUMBER , I4,3X,6H GMW = ,F10.2)
   44 FORMAT (/30H PACKING DIAMETER BED 1 (CM) = ,F10.4,30H
      1PACKING DIAM
      1ETER BED 2 (CM) = ,F10.4)
   45 FORMAT (/,36H NUMBER OF INCREMENTS IN FIRST BED = ,I4,
      13X,37H NUMBE
      1R OF INCREMENTS IN SECOND BED = , I4)
   46 FORMAT (/11H COMPOUND = , I4,2X,21H GAS DIFF (CM2/SEC)
      1 = ,F10.4,
      13X,16H SCHMIDT NUMBER= , F10.4)
   47 FORMAT (/12H RENUM (1) = ,F10.4,5X,12H RENUM (2) = ,F1
      10.4,5X,24H A
      1IR VISCOSITY (POISE) = ,E12.4)
   48 FORMAT(/18H COMPOUND NUMBER = ,I4,5X,36H MASS TRANSFER
      1 COEFF (CM/H
      1R) DED 1 = ,F10.1,3X,24H MASS TRAN COEFF BED 2 = ,F10.
      11)
      NGAS = 5
C     OMEG(1) IS THE COLLISION INTERGAL FOR GAS 1
      READ 1, (OMEG(J), J=1,NGAS)
      READ 1, (GASC(J) , J=1,NGAS)

C     GASMW(1) IS THE MOLECULAR WEIGHT OF CONTAMINANT 1
      READ 1,(GASMW(J) ,J=1,NGAS)
C     ROBED IS THE DENSITY OF THE BED  G/CC
C     DIAB IS THE DIAMETER OF THE REACTOR   CM
      READ 1,ROBED(1),ROBED(2),DIAB,DIAP(1),DIAP(2)

C     DE(5,1) IS THE DIFFUSIVITY OF GAS 5 THROUGH SOLID 1
C     THE UNITS ON DE ARE CM2/HOUR
C     FKG(5,1) IS THE FORWARD RATE CONSTANT  FOR GAS 5 IN
C     BED 1 .  THE UNITS ARE CM/HOUR
      READ 1, (DE(I,1),FKG(I,1), I=1,NGAS)
      READ 1, (DE(I,2),FKG(I,2), I=1,NGAS)

C     GMW(5,1) IS THE EQ WEIGHT OF THE SOLID (G SOLID/MOLE
C     GAS) FOR GAS 5 IN BED 1
      READ 1, (GMW(I,1) , I=1,NGAS)
      READ 1, (GMW(I,2), I=1,NGAS)
   50 CONTINUE
C     TIMET IS THE TOTAL NUMBER OF HOURS FOR WHUCH THE SIMU-
C     LATION IS DESIRED. TEMP IS IN DEG K.  PATM IS IN ATM.
C     DELT IS THE TIME INCREMENT IN HOUR.  DELZ IS LENGTH
```

```
C        INCREMENT IN CM. NZ1 IS MUMBER OF INCREMENTS IN BED 1
         READ 1, TIMET,FLOW,TEMP,PATM,DELT,DELZ
         READ 2, NZ1,NZ2
C        CIN(1) IS THE INLET CONCENTRATION OF GAS 1 IN PPM.
         READ 1,(CIN(I),I=1,NGAS)
         TIME =0.0
         PRINT 5, DELT,DELZ
         PRINT 44, DIAP(1),DIAP(2)
         PRINT 45, NZ1,NZ2
         ROGAS = PATM/82.06/TEMP
         PRINT 3, TEMP,ROGAS
C        THE NUMBER OF PARTICLES PER CC IS BASED ON A FCC PACK
         PARNUM(1) = 1.41/(DIAP(1)**3.)
         PARNUM(2) = 1.41/(DIAP(2)**3.)
         PRINT 41, PARNUM(1),PARNUM(2)
         NZT = NZ1 + NZ2
         XAREA = 3.1416 * DIAB * DIAB/4.
         VEL = FLOW / ROGAS / XAREA/ 3600.
         PRINT 4, XAREA,VEL
         DO 10 J=1,NZT
   10 X(1,J)=1.0
C        CALCULATION OF THE VISCOSITY OF AIR   POISE
         AMU = 2.6693*10.**(-5.)*((29.*TEMP)**.5)/3.617/3.617/.
      1865
         GMOLE = FLOW/XAREA/3600.
         RENUM(1) = DIAP(1)*GMOLE*29./AMU
         RENUM(2)= DIAP(2)*GMOLE*29./AMU
         PRINT 47, RENUM(1) , RENUM(2), AMU
         FJD(1) = .725/((RENUM(1)**.41)-1.5)
         FJD(2) = .725/((RENUM(2)**.41)-1.5)
         TEMP3 = TEMP*TEMP*TEMP
         DO 17 J=1,NGAS
         AVEMW = (1./29. + 1./GASMW(J))
         DUM = (TEMP3*.5*AVEMW)**.5
         DIFF(J) = .002628*DUM/PATM/GASC(J)/GASC(J)/OMEG(J)
         SNUM(J) = AMU/ROGAS/29./DIFF(J)
C        CALCULATION OF THE EXTERNAL MASS TRANSFER COEFFICIENT
         FKF(J,1)=(FJD(1)*GMOLE/(SNUM(J)**.6666)/PATM)*82.*TEMP
      1*3600.
         FKF(J,2)=(FJD(2)*GMOLE/(SNUM(J)**.6666)/PATM)*82.*TEMP
      1*3600.
         PRINT 48, J,FKF(J,1),FKF(J,2)
         PRINT 46, J,DIFF(J),SNUM(J)
   17 CONTINUE
         DO 15 L=2,NZT
         DO 15 J=1,NGAS
   15 C(J,1,L) = 0.0
         DO 12 J=1,NGAS
         PRINT 43, DE(J,1),FKG(J,1) ,J,GMW(J,1)
         PRINT 43, DE(J,2),FKG(J,2) ,J, GMW(J,2)
   12 C(J,1,1) = CIN(J)*ROGAS * 10.**(-6.)
```

```
   20 CONTINUE
      PRINT 29, TIME
      PRINT 31, (X(1,J) ,J=1,NZT)
      DO 26 M=1,NGAS
      DO 25 L=1,NZT
      PPM(M,L) = C(M,1,L)/ROGAS*10.**6.
   25 CONTINUE
      PRINT 28, M,(PPM(M,L) ,L=1,NZT)
   26 CONTINUE
      DO 200 I=1,11
      DO 100 L=1,NZT
      IF (L.LT.NZ1) K=1
      IF (L.GE.NZ1) K=2
      FRAC = X(I,L)
      DO 102 M=1,NGAS
      C(M,I+1,1) = C(M,I,1)
      DEN1 =   (X(I,L)**.3333)*DIAP(K)/2./DE(M,K)
      DEN2 =   (X(I,L)**.6666)*DIAP(K)/2./DE(M,K)
      DEN3 = (X(I,L)**.6666)/FKF(M,K)
      DEN4 = 1./FKG(M,K)
      DEN = DEN1-DEN2+DEN3+DEN4
      TOP = (12.566*DIAP(K)*DIAP(K)*PARNUM(K) *DELZ* X(I,L)*
     1*.6666)/VEL
     1/14400.
      C(M,I,L+1) = C(M,I,L)*EXP(-TOP/DEN)
      FRAC = FRAC          -(C(M,I,L)-C(M,I,L+1))*VEL*DELT*GMW(M
     1,K)*3600./
     1ROBED(K)/DELZ
  102 CONTINUE
      X(I+1,L) = FRAC
      IF (X(I+1,L).LT. 0.0)  X(I+1,L) = 0.0
  100 CONTINUE
      TIME = TIME + DELT
  200 CONTINUE
      DO 203 L=1,NZT
      DO 202 M=1,NGAS
      C(M,1,L) = C(M,11,L)
  202 CONTINUE
      X(1,L) = X(11,L)
  203 CONTINUE
      IF (TIME.LT.TIMET) GO TO 20
  499 GO TO 50
  500 CONTINUE
      CALL EXIT
      END
/*
```

APPENDIX B

ANALYTICAL METHODS - LITERATURE REVIEW

B.1 Colorimetric Analysis of Nitrogen Dioxide

A great deal of work has been done on the analysis of nitrogen dioxide at very low concentrations because of its importance in air pollution. Most of the work was based on adapting the Griess-Illosvay reagent (a mixture of sulfanilic acid and alpha-naphthylamine long used for detection of nitrites) for the quantitative determination of NO_2 in air. The major problem was the difficulty in absorbing the gas from a sufficiently large sample. Patty and Petty (24) reported an absorption efficiency of only 5% with a midget impinger.

In 1953, Saltzman (16) reported the development of what has become known as Saltzman's reagent. The reagent was specific for NO_2 and produced a stable, direct color which could be measured visually or spectrophotometrically. The effect of various interfering gases was found to be slight. The fading caused by SO_2 in concentrations up to ten times that of NO_2 could be greatly retarded by the addition of 1% acetone to the reagent before use. With air sampled at a rate of 0.4 liter per minute, a sensitivity of a few parts per billion was attained with 10 minute samples. Color development required 15 minutes. The reagent consisted of 0.5% sulfanilic acid, 0.002% N-(1-naphthyl)-ethylene diamine dihydrochloride. This method has been widely accepted and frequently improved.

Jacobs and Hochheiser (62) developed a method for NO_2 using reagents similar to those of Saltzman. Their method was developed for use with a Wilson semi-automatic 24-hour air sampler (63). The NO_2 was absorbed in a 0.1 N NaOH solution containing 2 ml 1-butanol per liter to promote foaming. Color development was conducted manually in a second step which was external to the sampler. The change from Saltzman's techniques was made because of interference encountered from SO_2, instrument damage caused by the high acidity of the mixed reagent and lack of stability. In the manual color development procedure, the interfering SO_2 was absorbed along with other atmospheric acidic gases and was oxidized to sulfate with hydrogen peroxide. Color development was achieved by using a 0.002% solution of N-(1-naphthyl)-ethylene diamine dihydrochloride for coupling and a diazotizing reagent consisting of sulfanilamide and ortho-phosphoric acid in water. Sensitivity for NO_2 was in the order of several parts per hundred million in air.

Hochheiser and Ludmann (64) compared the Saltzman and Jacobs-Hochheiser methods in a very thorough study presented in 1965. Nitrogen dioxide concentrations were 0.01-0.18 ppm; SO_2 concentrations were 0.01-0.25 ppm; and NO concentrations were 0.01-0.26 ppm.

Saltzman (20,65) has suggested minor modifications to his original reagent in order to decrease the cost and color development time for use in continuous analyzers. The amount of acetic acid was reduced and the amount of N-(1-naphthyl)-ethylene diamine dihydrochloride was increased. The resulting reagent yielded

slightly less color than the original reagent, but color development time was decreased to just over one minute.

Lyshkow (18) improved the rate of color development and sensitivity by adding 0.05% 2-naphthol-3,6 disulfonic acid disodium salt (R-salt) to Saltzman's NO_2 coupling reagent. He also optimized the concentrations of the diazotizing and coupling reagents. Lyshkow also found that if tartaric acid was substituted for acetic acid as the solvent for the absorbing reagents, the absorbing efficiency was increased and color development was 96% complete in one minute.

B.2 Colorimetric Analysis of Sulfur Dioxide

In 1942, Steigman (66) modified the Schiff reaction to produce a sensitive, highly specific test for the bisulfite ion. Acid-bleached fuchsin (a mixture of para-rosaniline and rosaniline) was reacted with formaldehyde and bisulfite ion to form an intense violet color. This reaction was applied to the analysis of air for sulfur dioxide by Urone et al. (67). Early erratic results with this method were attributed to varying impurities in different lots of the commercial dye.

West and Gaeke (30) suggested a two step procedure for the determination of trace quantities of sulfur dioxide in air. The SO_2 was absorbed in 0.1 N sodium tetrachloromercurate (II) which prevented the oxidation of SO_2 to SO_3 by the formation of dichlorosulfitomercurate (II). The stability of this compound to air oxidation was reported by Ephraims (68). West and Gaeke also substituted para-rosaniline for the fuchsin. This increased the sensitivity of the method but did not completely eliminate the irregularities in the results. Although the West and Gaeke method has been widely used for the determination of atmospheric SO_2, the method has been criticized for its lack of reproducibility and for its relative unreliability. Interferences associated with the method were reviewed by Thomas (69) and Mueller et al. (70). However, at that time, no better method was available.

Various improvements have been made in the West and Gaeke method to eliminate interferences from other atmospheric contaminants. NO_2 interferes if present in the air sample at concentrations greater than that of SO_2. West and Ordoveza (32) proposed the use of sulfamic acid in the absorbing reagent to destroy the NO_2. This might result in SO_2 losses during sampling and during storage of the sample for more than 48 hours after collection. Pate et al. (71) recommended adding the sulfamic acid after the collection was complete. They observed a suppression of color formation with the procedure. Scaringelli et al. (31) attributed this to the effect of sulfamic acid on pH. Careful control of the pH between 1.5 and 1.9 eliminated this problem.

Scaringelli et al. (31) recommended a 20 minute delay period after absorbing SO_2 in the tetrachloromercurate (II) solution to allow any ozone to decompose in the water of the reagent solution. Ozone did not affect the dichlorosulfitomercurate (II) complex but would interfere with the reaction if color developing reagents were added.

110

Zurlo and Griffini (72) reported that the ions of heavy metals (especially iron) interfered with the SO_2 determinations. They recommended the use of ethylene diamine tetracetic acid to complex these heavy metals. Scaringelli et al. (31) verified these findings.

West and Gaeke (30) reported the color produced to be independent of temperature in the range of 11 to 30°C. Scaringelli et al. (31) noticed slight fading above 35°C.

A great deal of difficulty in using this method has been caused by the use of impure para-rosaniline hydrochloride according to Pate et al. (73). These authors recommend a spectral assay of the dye before use. All lots of dye that did not exhibit maximum absorbance at 540 mμ were to be rejected. Several researchers recommended a commercial brand specially selected for the analysis of SO_2 (Fisher Scientific Company, catalog No. P-389). Scaringelli et al. (31) purified the dye by a four step extraction process from an HCl solution with 1-butanol. Lyshkow (23) used the commercial dye dissolved in a 1:1 solution of HCl and water without further purification. He found that any pre-solution of the dye with water, organics or lower concentration acid solutions altered the sensitivity of the mixed reagent and greatly increased the absorbance of the blank.

Scaringelli et al. (31) published an exhaustive study of the West and Gaeke method for SO_2. The pH value and other parameters for reagent color stability for the method were optimized and the para-rosaniline dye was purified. Interfering effects of the oxides of nitrogen were minimized. Greater sensitivity and reproducibility and adherence to Beer's law throughout a greater concentration range than with the original West and Gaeke method were achieved. This method is the most accurate and reproducible method for SO_2 now available. However, the use of the poisonous tetrachloromercurate (II) is still required.

Lyshkow (23) showed that water could be used as an absorbing reagent for SO_2 thereby eliminating the sodium tetrachloromercurate (II) of the West and Gaeke method. Sulfur dioxide is rapidly oxidized in the presence of oxygen and high humidity. It must be absorbed rapidly to avoid this. Lyshkow used a rotary disk absorber for this purpose. The SO_2 was first absorbed in water. The para-rosaniline was then added. The mixed solution was passed through a time delay coil to allow sufficient color development before reading in a colorimeter.

Stephens and Lindstrom (74) have also developed a technique which does not involve the use of any mercury salts. In their procedure, the gas samples are passed through a solution of ferric alum and 1,10-phenanthroline. The SO_2 present reduces the Fe^{+++} to Fe^{++} causing the formation of the orange colored tris (1,10-phenanthroline) iron (II) complex which is read at 510 mμ. In this method, it is necessary to mask the green-orange color of the excess hydrolized Fe^{+++} with ammonium bifluoride in order to obtain a colorless blank. The absorbance of the blank is 0.027 which corresponds to an SO_2 concentration of 7 μl SO_2 per 100 ml or 70 ppm when sampling at the rate of 2 liter/min air at 50°C. As the lower detection limit for SO_2 by this procedure is greater than the upper operating concentration for this project, the technique was not selected for use.

111

B.3 Colorimetric Analysis of Free Chlorine

Because of the wide use of free chlorine as a disinfectant, many methods have been developed for its analysis. The ortho-tolidine method was among the first to be developed. This method received wide acceptance because of its simplicity and accuracy.

A very thorough study of the ortho-tolidine method for the analysis of free Cl_2 in water was conducted by Chamberlin and Glass (35) in 1943. They investigated the effect of ortho-tolidine concentration, final reagent acidity, the method of adding the ortho-tolidine, and the preparation of the ortho-tolidine reagent itself. Their improvements in the existing ortho-tolidine method provided more rapid color formation, increased color stability, and less interference due to iron and nitrites. In their method, the developed color obeys Beer's law up to 1.5 ppm in water and deviates from it at a uniform rate from 1.5 to 10.0 ppm.

Many other methods were developed for the analysis of free chlorine in water. All of the important methods available in 1964 were evaluated and compared by Nicolson (33). A preliminary study was made of all the methods reported in the literature. Any method that obviously had serious disadvantages was excluded from further study. The more promising ones were examined in greater detail. The criteria for comparison were: stability of the colored products, reproducibility, specificity for free chlorine, sensitivity, lower limit of detection, conformance to Beer's law, accuracy, effect of temperature, reagent stability, simplicity, and convenience. Twelve methods were evaluated. Nine of these were colorimetric, including ortho-tolidine; three were titrimetric.

The advantages of the ortho-tolidine method listed by Nicolson were: a 5 minute color development time with a low decomposition rate; highly reproducible results; good sensitivity for free chlorine; acceptable reagent stability; simplicity and convenience. Some disadvantages of the method were that the results were temperature dependent and that Beer's law was not followed throughout the useful range. The main disadvantage of the ortho-tolidine method is that it is not specific for free chlorine. The method cannot distinguish between hypochlorite ion, hypochlorous acid, ammonia-chlorine complexes, and molecular chlorine. Fortunately, in the present research program, neither ammonia nor any of those various forms of dissolved chlorine were involved. The method is not affected by the presence of chloride ions.

Andrew and Nichols (34) proposed using ortho-tolidine for the continuous analysis of free chlorine in air. They modified a commercial SO_2 meter designed by Cummins and Redfearn (75) for this purpose. The ortho-tolidine flowed through the meter at 3 ml/min. Air flowed through the meter at 10 liters/min. The lower detection limit was reported to be 0.01 ppm by volume.

B.4 Colorimetric Analysis of Hydrogen Chloride

For many years, the Mohr and Volhard titrimetric methods were the primary methods for analysis of chloride ion in water. They are difficult to use and

are relatively insensitive. Although other methods have been developed over the years, none has proven entirely satisfactory for low chloride ion concentrations in water. In 1952, Iwasaki, Utsumi, and Ozawa (36) proposed the analysis of Cl^- using slightly dissociating mercuric thiocyanate and ferric ion based mainly on the following reactions:

$$2\ Cl^- + Hg(SCN)_2 \rightleftarrows HgCl_2 + 2\ SCN^-$$

$$4\ Cl^- + Hg(SCN)_2 \rightleftarrows HgCl_4^{--} + 2\ SCN^-$$

$$SCN^- + Fe^{+++} \rightleftarrows Fe(SCN)^{++}$$
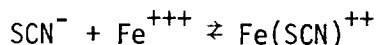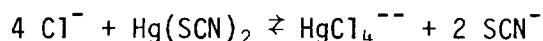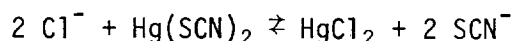
The orange color of the ferric thiocyanate formed was determined colorimetrically. As the mercuric thiocyanate has very limited solubility in water, substitution of 95% ethyl alcohol gave a slight increase in sensitivity. Ferric ammonium sulfate dodecahydrate (ferric alum) was dissolved in 6 N nitric acid. The lower detectable concentration was 0.05 ppm Cl^- in water but best results were obtained in the range of 0.1 to 20 ppm. Interfering substances in the method were bromide, iodide, cyanide, thiosulfate, and nitrite ions. The calibration curve did not follow Beer's law.

Swain (76) reviewed the various methods for analysis of chloride ion in water available in 1956. He found the method of Iwasaki et al. to be the most promising. After a careful investigation he found that Beer's law was obeyed for Cl^- concentrations less than 10 ppm. He found the absorption maximum to be at 470 mμ versus 460 mμ reported by Iwasaki et al.

Iwasaki et al. (37) improved the previous method by dissolving the mercuric (II) thiocyanate in a mixed solvent consisting of 1,4-dioxane and ethyl alcohol. The calibration curves were found to conform to Beer's law at concentrations up to 50 ppm chloride with the improved method.

West and Coll (77) recommended the analysis of chloride by complexing with ferric perchlorate. The yellow color of the complex was then read spectrophotometrically. The lower detection limit was a few ppm Cl^-. Interference by nitrate, iodide, phosphate, and fluoride ions was negligible. Sulfate ion, if present in an amount greater in weight than six times that of the chloride ion was found to exert a noticeable influence. The interference caused by mercury (II) is excessive so it must be completely eliminated from the sample and reagents.

Bergmann and Sanik (78) analyzed for chlorine in naphthas after conversion to the chlorine to chlorides. The chloride ion was then analyzed in aqueous solution. They tried nephelometry, amperometry, differential potentiometry, mercuric nitrate titration, and a microdiffusion colorimetric method. Each method was investigated for the determination of less than 100 ppm of chloride ion in liquid solution. Accuracy of these methods was poor, particularly below 50 ppm, because the total amount of chloride ion present approached the sensitivity limits of the procedures. The authors also evaluated the first

method of Iwasaki et al. (36). They found the lower detection limit to be 0.5 ppm of chloride ion in water. The standard deviation of the method was 0.5 ppm in the range of 1 to 100 ppm.

Bertolacini and Barney (39) proposed colorimetric determination of chloride in water by reaction with mercuric (II) chloranilate to liberate the reddish-purple acid chloranilate ion. The color was then read spectrophotometrically. The lower detection limit was 0.05 ppm chloride ion in water. The precision and accuracy were both within about 1% absolute. The analysis time was 30 min. The chloranilate and ferric thiocyanate colorimetric methods were found to be essentially equivalent in accuracy, precision, ease of operation, and freedom from interferences.

Hoffman (79) used mercurimetry to determine microgram quantities of bromide, iodide, and chloride. The method utilized the fact that a mercuric nitrate solution which contained these ions gave a weaker coloration with diphenyl-carbazone than a solution which was free of them. The method required precise control of pH. The method allowed analysis of Cl^- in the presence of Br^- and I^-. The lower detection limit was 2 µg $\pm$ 0.5 µg.

Andrew and Nichols (34) used a reagent consisting of 100 ml 1.4% ferric perchlorate and 50 ml 0.07% mercuric thiocyanate in water diluted to 500 ml for analysis of chloride ion in air in the form of HCl. The chloride was absorbed directly into the reagent in an automatic analyzer. The liquid reagent flow was 3 ml/min and the air rate was 10 liters/min. A direct color was formed which was read spectrophotometrically. The lower limit of detectability was estimated to be 0.15 ppm.

B.5 Colorimetric Analysis of Hydrogen Fluoride

Spectrophotometric methods are widely used for the analysis of fluorides both in air and water. The colorimetric method generally depends upon the reaction of fluoride ions with a metal-dye complex. The metal of the complex is from the group Th, Zr, La, Ce, Y, Bi, Fe, and Al. All are capable of forming insoluble or only slightly ionized fluorides. A few of the commonly used dyes are alizarin red S, eriochrome cyanine R, PAN, SPADNS, arsenazo, ferron, and xylenol orange. Some of these dyes also function as acid-base indicators and require close control of pH for accurate fluoride determination.

Colorimetric methods for fluoride analysis are divided into two types: color bleaching and color developing. The bleaching methods were the first to be developed. These include the bleaching action of fluoride on zirconium alizarin lake; ferric sulfosalicylate; sodium 2-(p-sulfophenylazo)-1,8-dihydroxynaphthalene-3,6-disulfonate-zirconium lake (SPADNS); zirconium-eriochrome cyanine-R; and 8-hydroxy-7-ido-5- quinoline-sulfonic acid complex (ferron). The reagents which develop a color on exposure to fluoride ions include lanthanum, thorium and strontium chloranilates; the zirconium salt of p-dimethylazobenzene arsonic acid; and lanthanum, praseodymium, and cerium chelates of alizarin complexone.

One of the first important bleaching methods for the analysis of fluoride ions involved the formation of zirconium-alizarin lake. Work on the reaction was begun in the twenties by DeBoer (80). Subsequent modifications to improve the method for analysis of fluorides (81,82) in water included those of Thompson and Taylor (83), Sanchis (84), Scott (81,82), and Megregian and Maier (85). The resulting method has been widely accepted for the analysis of fluoride ion in water.

Lacroix and Labalade (38) proposed the bleaching action of fluoride ions on ferric sulfosalicylate for colorimetric analysis. Andrew and Nichols (34) used this reagent for the continuous analysis of fluorides, specifically HF, in air. Their lower limit of detection was estimated to be 0.05 ppm.

Megregian (86) proposed a colorimetric analysis involving the bleaching action of fluoride ions on zirconium-eriochrome cyanine R. Adams and Koppe (87) used this procedure for the continuous analysis of HF in air. The method was applicable in the range of 0.4 to 35 ppm. Adams, Koppe, and Matzek (88) modified this method to remove the interferences of aluminum and sulfate ions.

Bellack and Schouboe (89) proposed the use of sodium 2-(p-sulfophenylazo)-1,8-dihydroxynaphthalene-3,6-disulfonate-zirconium lake as a substitute for the alizarin-zirconium lake for the analysis of fluoride ions in water. The method was recommended for its speed and relative insensitivity to interferences.

Adams (90) described a continuous atmospheric HF analyzer which used the bleaching action of fluoride ions on the iron-ferron (8-hydroxy-7-iodo-5-quinoline-sulfonic acid) complex. The range of analysis was 0.112 ppm to 224 ppm.

Color developing methods for the analysis of fluoride ions were developed later. Semiquantitative results were achieved by Harrold and Hurlbut (91) using a paper treated with the zirconium salt of p-dimethylazobenzene arsonic acid to yield a pink color. Various metal chloranilates have been proposed as color developing reagents for halogen ions. Bertolacini and Barney (39) used strontium chloranilate for the analysis of fluoride ions in water. The absorption was measured in the ultraviolet region at 332 mμ. Although color development methods are preferable to bleaching reactions, the method was not selected for further evaluation because the lower detection limit was 5 ppm in water.

Belcher and West (92) compared the cerium (III), lanthanum, and praseodymium chelates of alizarin complexone as reagents for the spectrophotometric determination of fluoride ions in water. The lanthanum reagent was the most sensitive. The absorption maximum occurred at 281 mμ. The lower detection limit was approximately 1 ppm. A semiautomatic method for the determination of fluorine after conversion to fluoride using lanthanum alizarin complexone was reported by Weinstein et al. (92). The lower detection limit was 0.04 ppm fluoride ion in water.

B.6 Previous Gas Chromatographic Research

Outlined briefly below are the results of previous investigations for specific reactive gases.

B.6.1 Methods for Oxides of Nitrogen.

- Morrison, Rinker, and Corcoran (40) used 10 wt% SF-96 methyl silicone oil on 20-80 mesh Fluoropak 80 in columns 3/32 in. I.D. × 15 ft long for the separation of NO_2 in air. Nitrogen carrier gas was used at 10 ml/min. Scavenger gas for the electron capture detector was also N_2 and was used at 85 ml/min. The column was operated at 22°C. Sharp peaks with only slight tailing were obtained for samples containing 18.3 ppm NO_2 in a 1/2 ml air sample. The estimated lower detection limit for NO_2 is 1 ppm.

Smith and Clark (94) investigated five different columns for the separation of N_2O, NO, NO_2, NH_3, O_2, N_2, and CO_2. Activated coconut charcoal, 60-120 mesh, washed with 0.1 N sulfuric acid was the only column which provided satisfactory separations of CO_2 and N_2O. This separation was accomplished in a 9 in. column with a helium flow rate of 104 ml/min. Type 5A molecular sieve, 32-80 mesh, was used for the separation of NO and NO_2 in a 4 ft column with a helium flow rate of 100 ml/min. NH_3 was satisfactorily analyzed by a C22 firebrick column, 60-80 mesh, (washed with 1 N NaOH) containing 33% polyethylene glycol 600. This separation was done in a 40 in. column with a He flow rate of 112 ml/min. These authors were able to obtain complete separations of this complex mixture of gases by using these three columns in a multiple column system with suitable valving arrangement.

Bethea and Adams (95) used a 20 ft. column filled with 65-80 mesh activated charcoal impregnated with 2 g of squalane per 100 g of the activated charcoal at 22°C and 66 ml He/min for the separation of NO and NO_2 in concentrations of 2 to 12 mole percent. Nitrogen was not separated from NO_2. This column was also suitable for the analysis of CO and formaldehyde.

Dietz (96) used a 6 ft. column filled with Type 5A molecular sieve for the programmed temperature separation of N, NO, and N_2O. The initial column temperature of 60°C was maintained for 4 min, after which the temperature was increased to 250°C at a rate of 30°C/min. The upper temperature limit was maintained for 8 min to insure the elution of CO_2 in the sample. Helium flow was 25 ml/min at 40 psig. This column had a reported lower detection limit using 5 cc samples of 12 ppm NO, 6 ppm CO, 25 ppm N_2O, and 4 ppm CO_2.

Trowell (97) developed a three column system for the separation of H_2, O_2, N_2, NO, CO, N_2O, CO_2, H_2O, and NO_2. Column 1 was a 1 ft length of 1/8 in. O.D. tubing packed with 0.5% Carbowax 1500 on 60-80 mesh silanized glass beads. It was operated at 70°C and 30 ml He/min for the separation of CO and CO_2. Column 2 was 20 ft long packed with 40% dimethyl sulfoxide on 60-80 mesh Gas Chrom RZ. This column was operated at 25°C for the separation of N_2O only. H_2, O_2, N_2, NO, and CO were separated on Column 3 consisting of 8 ft of 30-60 mesh type 13X molecular sieve. This column was activated at 250°C for 5 min with a helium purge. After all these compounds had been eluted from the system, the initial sample trap was raised from -78°C to +70°C for the release of H_2O and NO_2 which were then analyzed on Column 1. The carrier gas flow rate

through this system was 75 ml He/min for Column 1 and 30 ml He/min for Columns 2 and 3. This method was considered too complicated for use in this research. It could probably be improved by the use of cryogenic temperature programming rather than step function programming.

Sakaida et al. (98) used a 8 ft column packed with the 48-60 mesh fraction of Davison No. 912 silica gel at 28 to 31°C with helium carrier rates of 40-50 ml/min for the separation of NO and N_2. Even though this column was pretreated with NO and NO_2, NO_2 was not analyzed. The peak shapes for both N_2 and NO were such that this column was believed unsatisfactory for use in this research project.

Phillips and Coyne (99) separated NO and NO_2 in a variety of nitrogen compounds containing organic on a 6 ft column packed with 25% dinonyl phthalate on Chromosorb B at 110°C and a hydrogen flow rate of 60 ml/min. Their analyses were confirmed by mass spectroscopy. The NO was quantitatively scrubbed out of the sample gas by acidified ferrous sulfate. It was determined by difference from samples taken before and after the scrubber.

Borland and Schall (100) developed an involved procedure for the analysis of N_2, O_2, NO, N_2O, and NO_2 using a column packed with grade F-20 alumina which had been activated by heating in an inert atmosphere at 750°F for 4 hours. Their procedure involved the separation of O_2 and N_2 at -78°C, NO and NO_2 at room temperature, and N_2O at 100°C. Other workers have not been able to duplicate these results.

Greene and Pust (101) used a 10 ft type 5A molecular sieve column (20-40 mesh) for the determination of NO and NO_2. This column was not activated prior to use. The He carrier gas flow rate was 60 ml/min; the column temperature was 23°C. While NO is directly eluted from this column it was necessary to convert all NO_2 to NO by reaction with H_2O on the column packing.

Morrison and Corcoran (102) used a 20 ft 1/8 in. O.D. column packed with 10% methyl silicone oil SF-96 on 40-80 mesh Fluoropak 80 at 22°C for the separation of NO_2 from NO, N_2, and O_2 appearing as a single peak. The lower detection limit appeared to be approximately 3 ppm NO_2 when using 0.5 ml samples. Argon was used at 10 ml/min as the carrier and also as the scavenger gas for the electron capture detector.

Kipping and Jeffery (103) used a 5 ft type 5A molecular sieve column at 100°C for the determination of NO in air. An argon ionization detector was used. Sample sizes ranged from 0.01 to 0.1 µl. They noted that the retention time of NO was dependent on the absolute amount of NO present.

Beskova et al. (104) separated N_2O, NO, NO_2, and CO_2 in mixtures of light hydrocarbons at various temperatures on a 0.5 m long by 4 cm diameter column packed with different active solids. The lower detection limit for H_2O was reported to be 10 ppm.

Marvillet and Tranchant (105) used a 5 m long by 4 mm I.D. precolumn at 20°C filled with silica gel impregnated with 10% triethanol amine followed by a

4 m long by 4 mm I.D. column filled with activated type 5A molecular sieve at 10°C for the separation of O_2, N_2, NO, CO, N_2O, and CO_2. Both packings were 0.125 to 0.160 mm diameter. Helium was used as the carrier gas at 30 ml/min.

Smith, Swinehart, and Lesnini (106) used a 10 ft column half filled with Davison grade 12 silica gel (28-200 mesh) followed by 8 in. of iodine pentoxide powder then 1/2 in. of metallic silver powder and then filled with additional silica gel for the separation of CO from CO_2 and N_2O appearing as a single peak. NO_2 does not pass through this column at 115°C and 30 ml He/min.

B.6.2 Methods for SO_2. - Hodges, Pickren, and Matson (107) developed a system for the analysis of SO_2 (and other acidic gases not related to this research) which had a lower detection limit of 200 ppm when using a thermal conductivity detector. This column was a 1/4 in. O.D. by 8 in. long aluminum tube packed with 80-100 mesh Davison grade 08 silica gel. The helium carrier was supplied at a flow rate of 40 ml/min and was at an inlet pressure of 80 psig. As the electron capture detector is three to five orders of magnitude more sensitive than thermal conductivity (depending, of course, on the specific sample involved), this method is definitely worth further investigation.

Robbins, Bethea, and Wheelock (48) separated CO_2, H_2S, and SO_2 in 15 min at 60°C and a He flow rate of 40 ml/min using a 20 ft column packed with 10% dibutyl sebacate on 20-80 mesh Fluoropak. Further work on this system showed that NH_3 could also be separated from these compounds and from air. This column was used daily for over 15 months for the routine analytical separation of the gases produced in the reductive decomposition of gypsum. The lower detection limits for all of these gases was approximately 0.2% in air when using a thermal conductivity detector.

B.6.3 Combined Methods for SO_2, NO, and NO_2. - Beuerman and Meloan (108) used a 1/4 in. by 20 ft long column packed with 30 wt% dinonylphthalate on the 40-60 mesh fraction of Chromosorb P. Column temperature was 90-95°C. Helium carrier was used at a flow rate of 45 ml/min. The analysis requires only 9 min. A relative error of less than 1% can be expected. This procedure will be tested for the separation of the other acid gases of interest.

Hollis and Hayes (49) have found that NO, N_2O, CO_2, H_2S, HCN, and SO_2 can be easily separated (in that elution order) on 0.10 in. I.D. by 6 ft, long stainless steel columns filled with the 100-200 micron range of any untreated Porapak available at that time operated at 26 or 65°C. Helium carrier is used at 30 ml/min. Of all the Porapak materials tested, Porapak Q gave superior results. It was necessary to condition the Porapak columns in an inert atmosphere at 20-30°C higher than the intended operating temperature for 24 hours prior to use. This ensured that any volatile and/or unpolymerized material in the Porapak would be driven off prior to use for analytical work.

Wilhite and Hollis (52) investigated several Porapak columns for the analysis of NO, CO_2, N_2O, H_2S, CO_2, NH_3, HCHO, NO_2, and SO_2. The best separations were obtained using a 8 ft Porapak Q column in series with an 8 ft Porapak R column. Both columns were 0.1 in. I.D. Both Porapaks were 50-80 mesh. The flow rate

was held constant at 40 ml He/min. These columns were programmed from 25 to 150°C at 12°C/min. Sample size was 0.1 ml.

West (109) used a four column system for the separation of O_2, N_2, NO, N_2O, SO_2, and H_2S in steam. Two of the columns were 5% Carbowax 1500 on 110-120 mesh Teflon 6, both 2 ft long, but operating at different temperatures. A 3 in. column containing 4% 2,5-hexandione was used to separate H_2S and N_2O. The solid support for this column was activated charcoal. O_2, N_2, and NO were separated on a 4 ft column packed with 30-60 type 5A molecular sieves. The last three of these columns operated at 25°C, the first one at 160°C. The carrier gas flow rate was constant throughout at 50 ml He/min. The lower detection limits for this system ranged from 0.6% SO_2 to 3% H_2S.

B.6.4 Methods for Cl_2, HCl, and HF. - Ellis and Iveson (110) used a 1/4 in. I.D. by 4.5 ft monel column packed with 10 g Kel-F No. 10 oil per 100 g of 30-60 mesh Fluoropak at 48°C and an argon carrier rate of 16.5 ml/min for the separation of HF and Cl_2. These separations were improved by Ellis, Forrest, and Allen (111) by increasing the column length to 11.5 ft. They reported satisfactory analyses of 30 µl (at S.T.P.) of Cl_2 and HF. The detector used was a Martin gas density balance.

Cieplinski (45) found that 3×10^{-12} g/Cl_2 would be detected in a 50 µl air sample when using a 1 m column packed with 20 wt% silicone fluid DC-200 on 60-80 mesh Chromosorb W at 50°C. The carrier gas was 1% CH_4 in argon. An electron capture detector was used.

Isbell (41) achieved the separation of Cl_2 and NO in less than 1 min on a 1/4 in. O.D. by 8 ft long column packed with 25 wt% triacetin on 30-60 Chromosorb P at 75°C with a helium carrier rate of 108 ml/min. A thermal conductivity detector was used.

Priestley et al. (42) used a 4.7 mm I.D. by 2 m long aluminum column packed with 30 wt% didecyl phthalate on 100-200 mesh GC-22 Super Support at 50°C with a nitrogen carrier rate of 50 ml/min. The potential supplied to the electron capture detector was 90 for the analysis of phosgene in the 1 ppb to ppm region. This column should be satisfactory for Cl_2, HF, and HCl.

Ellis and Forrest (112) used an 11 ft 6 in. column packed with 50 wt% Kel-F grade 10 oil on 30-60 mesh polytetrafluoroethylene powder for the quantitative separation of ClF, HF, ClO_3F, Cl_2, ClO_2F, and ClF_3. The argon carrier gas flow rate was 27.5 ml/min. The separation was accomplished at 48°C. A Martin gas density balance was used as a detector.

Million, Weber, and Kuehn (113) used a 5 ft by 1/2 in. O.D. column with 20% Kel-F No. 10 oil on 40-50 mesh Kel-F powder at 60°C for the quantitative separation of F_2, HF, Cl_2, ClF_3, and Freon-114. Air was used as the carrier gas at a rate of 24 ml/min. The lower detection limits were 0.2 to 0.5 micromole of each individual gas when using a sampling chamber with a volume of 31.1 ml. A gas density balance was used as a detector.

Obermiller and Charlier (114) achieved quantitative separation of a mixture of H_2S, HCl, and H_2O at 90°C using a 5% Carbowax 20M on a Fluoropak 80 column. The lower detection limit for HCl was 0.1% when using 1 ml samples. The helium carrier gas rate was 33 ml/min. It was necessary to precondition this column with 5 ml HCl prior to the analysis of any samples. If this was not done, the HCl results were invariably low.

Rochefort (115) developed a precolumn system for use with the columns described by Ellis et al. (104,107,108) for the indirect analysis of HF and F_2. The precolumn retains or destroys those compounds and the chromatograph column separated their remaining derivatives. The lower detection limit for these compounds was reported to be 100 ppm F_2 in air.

Hamlin et al. (116) used a 14 ft column packed with 16.7% Kel-F 40 oil supported on Kel-F 300 low density molding powder (178-211 microns) at 90°C for the separation of Cl_2 and HF in the presence of other reactive inorganic fluorides. The nitrogen carrier gas was supplied at a rate of 10 ml/min for this on-line process analyzer.

Horton (117) used a 1/4 in. O.D. by 0.6 m column filled with 20-35 mesh silica gel operated at 90°C at a helium flow of 500 ml/min for the analysis of Cl_2 down to 5000 ppm in less than 1 min.

B.6.5 Combined Methods for NO_2 and Cl_2. - Huillet and Urone (44) made a comprehensive survey of amount and type of liquid phases, type solid support, and operating conditions of the analysis of Cl_2, NOCl, NO_2Cl, and NO_2. Their results showed that Halocarbon 11-14 columns, 1/4 in. O.D. by 12 ft long were best suited for the separation of these gases. The column packings (equally effective) were 30 wt% Halocarbon 11-14 on 40-60 mesh acid washed, DMCS treated Chromosorb P or 10 wt% Halocarbon 11-14 on 60-80 mesh acid washed, DMCS treated Chromosorb W. Both columns were operated at -10°C. Helium carrier was used at 50 ml/min with high nickel alloy thermal conductivity filaments. All columns were prepared in nickel, inconel, or stainless steel tubing. Using these columns, Cl_2 and NO_2 are easily separated by 3-4 min out of an 8 min analysis time. Cl_2 shows neither leading nor tailing. NO_2 exhibits severe leading but no tailing. These systems will be examined for use with HCl, HF, NO, and SO_2.

Evrard et al. (118) separated CO_2, CO, NO_2, N_2, O_2, H_2, and Cl_2 on a silica gel column using argon as a carrier gas and a polarized diode detector. The analyses were free from memory effects. The calibration curves were approximately linear. Flow rates varied from 50 to 200 ml/min.

B.6.6 Combined Methods for Cl_2, HCl, NOCl, HCN, SO_2, and H_2S. - Talbot and Thomas (119) separated NOCl and HCl using a 12 ft Celite 545 column packed with 50 wt% dimethyl phthalate. The carrier gas used in these kinetic studies was hydrogen. The column temperature and carrier gas flow rate were not given.

Engelbrecht et al. (120) used a 4 m activated silica gel column treated with 30% Halocarbon oil for the separation of NO, HCl, CO_2, H_2S, Cl_2, and SO_2. The hydrogen carrier gas flow rate was 150 ml/min. The column was operated at 30°C.

120

Runge (43) used a column 7 mm I.D. by 9 m long packed with one part Arochlor 1232 per 20 parts by weight of 20-60 mesh Haloport F at 22°C, and 200 ml H_2/min for the separation of CO_2, HCl, Cl_2, and SO_2 (among other acidic gases) in less than 5 min. The results of his work are definitely worthy of investigating further.

Araki et al. (121) obtained well separated symmetric peaks for Cl_2, Br_2, NOCl, HCN, SO_2, and H_2S. They also achieved separations of HCl and HBr for which tailing increased in the presence of significant amounts of H_2O or NH_3. The column used was 7 m long packed with 50% No. 3 Daifuloil on 30-60 mesh Polifulon powder.

Jones (122) used two Porapak Q columns for the separation of H_2, O_2, N_2, CO, CO_2, H_2S, NH_3, and H_2O. One of these columns was 4 ft long, the other 6 ft. The 6 ft column was used at -78°C for the separation of N_2, O_2, and CO. The 4 ft column was used for the separation of all other components in the sample at room temperature. The flow rate through both columns was 100 ml/min. The carrier gas used was a mixture of 8.5% hydrogen and 91.5% helium. When using 10 ml gas samples, the lower detection limit for all compounds of the sample was 0.1%.

APPENDIX C

ANALYTICAL PROCEDURES

C.1 Determination of Nitrogen Dioxide and Nitric Oxide in the Atmosphere by the Lyshkow-Modified Saltzman Method

This method is intended for the manual determination of nitrogen dioxide in the atmosphere in the range of 1 to about 50 ppm. Sampling is conducted in 50 ml syringes. The method is also applicable to the determination of nitric oxide after it is converted to an equivalent amount of nitrogen dioxide. The nitrogen dioxide is absorbed in modified Griess-Saltzman reagent. A stable pink color is produced within 1-2 min which may be read visually or in an appropriate instrument. Only slight interfering effects occur from other gases.

Reagents

All reagents are made from analytical grade chemicals in nitrite-free water prepared, if necessary, by redistilling distilled water in an all-glass still after adding a crystal each of potassium permanganate and of barium hydroxide. They are stable for several months if kept well-stoppered in amber bottles in the refrigerator. The absorbing reagent should be allowed to warm to room temperature before use.

Absorbing Reagent. - 0.050 g N(1-napthyl) ethylene-diamine dihydrochloride
0.050 g 2-naphthol 3,6-disulfonic acid disodium salt
1.500 g sulfanilamide
15.0   g tartaric acid
0.25 ml Kodak Photoflow (as a wetting agent)
         deionized water to make one liter

Standard Sodium Nitrite Solution (0.004406 g/liter). - One ml of this solution diluted to 25 ml produces a color equivalent to 5 ppm as measured by a syringe using 45 ml of gas. Prepare fresh just before use by dilution from a stronger solution containing 0.4406 g/liter reagent grade granular solid. The stock solution should be stable for 90 days if kept under refrigeration.

Apparatus

Syringes. - 50 ml disposable polypropylene with Luer-lok tip (Becton, Dickinson, and Company, No. 850L/S) fitted with 22 gage 1 1/2 in. stainless steel Luer-lok needles with polypropylene hubs (Becton, Dickinson and Company, No. 1000).

Spectrophotometer or Colorimeter. - A laboratory instrument with a wavelength adjustment and 1 cm diameter stoppered tubes or cuvettes.

122

Analytical Procedure for Nitrogen Dioxide

Sampling Procedure. - Draw exactly 5 ml of absorbing reagent into the syringe. Draw a 45 ml air sample through it at the rate of 2 ml per sec (or less) and then shake gently for 1 min for full color development. If the sample air temperature and pressure deviate greatly from 25°C and 760 mm Hg, measure and record the values.

Determination. - After collection or absorption of the sample, a direct red-violet color appears. Color development is complete within 1-2 min at room temperature. Transfer the sample to stoppered cuvettes and read in a spectrophotometer at 550 mμ using unexposed reagent as the 100 %T reference. Colors may be preserved, if well stoppered, with only 3 to 4% loss in absorbance per day. If strong oxidizing or reducing gases are present in the sample in concentrations considerably exceeding that of the nitrogen dioxide, the colors should be determined as soon as possible to minimize any loss.

Analytical Procedure for Nitric Oxide

A stack of 25 sheets of 7 cm diameter paper is impregnated with 24 ml of 2.5% $Na_2Cr_2O_7$, 2.5% H_2SO_4, and dried in a vacuum oven at 160°F, or on a hot plate at 200°F. Discard top and bottom sheets and store the remainder in a closed bottle. Cut one sheet of the impregnated glass fiber paper into 1/4 in. wide strips and pack loosely into a 17 mm O.D. glass U tube. Conversion efficiency is 95-100%. The useful life of the paper is limited, and it deteriorates rapidly when exposed to reagent vapors downstream from a bubbler. Hence, a different sampling train, comprised of a rotameter, paper, fritted absorber, and pump is used. The sample is passed through the paper which oxidizes the NO to NO_2. A separate analysis of the latter gas must be made and deducted to give the concentration of nitric oxide.

Calibration Using Permeation Tubes. - Prepare a permeation tube as described in Section 5.2.2. The tube requires 24 hours to achieve a constant permeation rate. Place the tube in an appropriate holder such as a Podbielniak double pass drying tube in a constant temperature bath. Determine the permeation rate by periodically removing and weighing the tube over at least a 24 hour period. Set the flow rate of the diluent gas to achieve the desired concentration with the known permeation rate. For example, if the desired concentration was 10 ppm, and the permeation rate was 2.5×10^{-5} moles/hr, the needed molal flow rate would be:

$$F = \frac{(2.5 \times 10^{-5} \text{ moles contaminant/hr}) \ (10^6)}{10 \text{ ppm}} = 2.5 \text{ moles diluent/hr}$$

Various concentrations covering the range of interest should be obtained.

Make three analyses at each concentration using the syringe technique. Expel the liquid into a 1 cm cuvette and read the transmittance in a colorimeter.

<u>Chemical Standardization</u>. - Add graduated amounts (1 ml, 2 ml, 3 ml, etc.) of the standard sodium nitrite solution up to 10 ml (measured accurately in a graduated pipet or small buret) to a series of 25 ml volumetric flasks, and dilute to marks with absorbing reatent. Mix, allow 1-2 min for complete color development, and read the colors. The 1 ml standard is equivalent to 5 ppm as measured with a syringe using 5 ml reagent and 45 ml gas sample.

Calculations

For convenience, standard conditions are taken as 760 mm of mercury and 25°C, thus only slight correction by means of the perfect gas equation are necessary.

If the concentration of NO_2 in air was 5 ppm and 45 ml air were drawn into a syringe, then (5 moles $NO_2/10^6$ moles air)(45 ml air)(1 mole air/24,470 ml/ mole air) = 9.195×10^{-9} moles NO_2 were drawn into the syringe. This entire amount will be absorbed into the 5 ml of liquid in the syringe to produce a NO_2 equivalent concentration of

$$\frac{9.195 \times 10^{-9} \text{ moles } NO_2}{0.005 \text{ liter}} = 1.839 \times 10^{-6} \text{ moles/liter}$$

Saltzman found empirically that 0.72 mole of sodium nitrite produces the same color as 1 mole of nitrogen dioxide. To produce an equivalent concentration in a 2 ml volumetric flask using 1 ml of standard $NaNO_2$ solution, the required concentration of the standard $NaNO_2$ solution would be:

$$\frac{(0.025 \text{ liter})(1.839 \times 10^{-6} \text{ mole/liter})}{(0.001 \text{ liter})(0.72)} = 6.3854 \times 10^{-6} \text{ moles } NaNO_2/\text{liter}$$

or

$(6.3854 \times 10^{-6} \text{ moles } NaNO_2/\text{liter})(69.00 \text{ g } NaNO_2/\text{mole } NaNO_2) = 0.00406 \text{ g/liter}$

124

C.2 Determination of Sulfur Dioxide by the Lyshkow Modified West and Gaeke Method

This method is intended for the manual determination of sulfur dioxide in the atmosphere in the range of 0.17 to about 50 ppm. Sulfur dioxide in the air sample is absorbed into the para-rosaniline solution. A direct red-purple color is produced by the formation of para-rosaniline methyl sulfonic acid and is determined spectrophotometrically.

Reagents

All chemicals used must be ACS analytical-reagent grade prepared in nitrite and sulfite free water.

Para-rosaniline Hydrochloride. - (A) Concentrated reagent: 640 ml of 1:1 HCl/H_2O. 0.800 g para-rosaniline dihydrochloride (Fisher P-389). Allow to stand with periodic mixing for 1 hour and filter through Eaton-Dikeman filter paper grade 512 or equivalent. (B) Dilute reagent: 32 ml concentrated reagent. Dilute to 900 ml. Add 1.1 ml formaldehyde (37% ACS). Dilute to 1 liter. Mix thoroughly and allow to stand for 12 hours prior to use.

The concentrated reagent should be stable for at least 6 months. The dilute reagent should be prepared fresh weekly.

Standard Sulfite Solution, 0.02323 g/liter. - One ml of this solution diluted to 25 ml produces a color equivalent to 5 ppm as measured by a syringe using 47 ml of gas. Prepare fresh just before use by dilution from a stronger solution (which should be kept in the refrigerator) containing 2.323 g sodium metabisulfite (assay 65.5% as SO_2) in 1.0 liter of water. The dilute solution should be standardized by titration with standard 0.01 N iodine using starch as the indicator.

Apparatus

The apparatus is identical to that used for the analysis of NO_2.

Analytical Procedure

Draw exactly 3 ml of absorbing reagent into the syringe. Draw in a 47 ml air sample at the rate of 2 ml per sec (or less) and then shake gently for 3 minutes for full color development. Transfer the sample to a stoppered 1 cm cuvette and read the percent transmittance at 560 mμ with respect to unexposed reagent as 100 %T. The exposed reagent should be read within an hour.

Preparation of Calibration Curve

Calibration Using Permeation Tubes. - Prepare a SO_2 permeation tube as described in Section 5.2.2. The calibration is conducted in the same way as that for NO_2.

Chemical Standardization. - Carefully pipette graduated amounts (1 ml, 2 ml, 3 ml, etc.) of the standard sodium metabisulfite solution up to 10 ml into a series of 25 ml volumetric flasks, and dilute to marks with the dilute para-rosaniline solution. Mix, allow 3 min for complete color development and read the colors. The 1 ml standard is equivalent to 5 ppm in a 47 ml air syringe sample when using 3 ml dilute reagent for SO_2 absorption.

C.3 Determination of Chlorine in Air by the Ortho-Tolidine Method

Reagents

All reagents are prepared from analytical reagent grade chemicals in demineralized deionized water. Reagents should be refrigerated in amber, UV absorbing glass bottles. The reagents should be allowed to warm to room temperature prior to use.

Concentrated O-Tolidine Reagent. - Weigh out 1.0 g ortho-tolidine, transfer to a 6 in. mortar or evaporating dish. Add 5 ml dilute hydrochloric acid (previously prepared by adding 150 ml of concentrated HCl to 400 ml of distilled water). Grind sufficiently to achieve a very smooth, thin paste. Add 150 to 200 ml of distilled water. The ortho-tolidine goes into solution immediately if ground sufficiently. Transfer to a 1 liter volumetric flask. Add 200 ml distilled water. Add the balance of dilute acid prepared above. Dilute to mark with distilled water.

This solution should be stored in amber bottles, should not be kept longer than 6 months, should not be subjected to high temperatures and should not be allowed to stand in direct sunlight.

Apparatus

The apparatus is identical to that used for the analysis of NO_2.

Analytical Procedure

Draw exactly 3 ml of the ortho-tolidine testing reagent into the syringe. Draw in exactly 47 ml of gas at a rate of 2 ml/sec (or less). Shake gently for 1 min for full color development. Be sure to hold the syringe perpendicular to the sampling point so that the gas will bubble through the reagent. In this way, the majority of the Cl_2 will be immediately absorbed and losses due to absorption of Cl_2 on the syringe walls will be minimized.

After collection of the sample, a yellow green color appears. Color development is complete within 1-2 min. Transfer the sample to a 1 cm cuvette and read in a spectrophotometer at 450 mμ, using unexposed reagent as the 100 %T reference. The color of the exposed reagent is stable for 2 hours.

Calibration

Calibration Using Permeation Tubes. - Prepare a chlorine permeation tube as described in Section 5.2.2. The calibration is then conducted as described for NO_2 in Section C.1.

Note: There is no good chemical method of standardization for free chlorine.

C.4 Determination of HCl in Air by the Modified Iwasaki, Utsumi, Hagino and Ozawa Method

Reagents

All reagents are made from analytical grade chemicals in distilled water which is free from all interfering ions. Specifically, fluoride and chloride ions must be excluded. Reagents should be stored in UV-light absorbing amber glass bottles in a refrigerator. Reagents should be warmed to room temperature prior to use.

Reagent A. - Dissolve 144.981 g of $FeNH_4(SO_4)_2 \cdot 12H_2O$ in 1 liter of 6N HNO_3.

Reagent B. - Dissolve 0.100 g of $Hg(SCN)_2$ in 100 ml solvent.

Solvent. - Mix 200 ml spectrograde 1,4-dioxane and 100 ml absolute (100%) ethanol.

Chloride Test Reagent. - Mix 20 ml Reagent A and 30 ml Reagent B just prior to use. Use 2 ml of this mixed reagent plus 1 ml distilled water for each Cl^- determination. This reagent has a shelf life at room temperature of 2 months.

Standard Cl^- Solution, 2.401×10^{-4} M. - Dissolve 0.1403 g of NaCl in 100 ml of Cl^- and F^- free water. Dilute 10 ml of this solution to 1 liter to achieve the final concentration.

Analytical Procedure

Sampling Procedure. - Draw exactly 3 ml of absorbing reagent into the syringe. Draw a 47 ml air sample through it at the rate of 2 ml per sec (or less) then shake gently for 2 min for full color development. If the sample air temperature and pressure deviate greatly from 25°C and 760 mm Hg, measure and record the values.

The reagent changes from straw yellow to reddish brown on exposure to HCl. Color development is complete within 1-2 min. Transfer the sample to a 1 cm cuvette and read spectrometrically at 460 mμ after zeroing the unit at 100 %T using unexposed reagent as a blank. The developed color is stable for 30-40 min.

Calibration

To ten 25 ml volumetric flasks add graduated amounts (1 ml, 2 ml, ..., 10 ml) of the 2.401×10^{-4} M NaCl solution. Dilute each to the mark with Cl^- and F^- free distilled water. Add 1 ml of each calibration solution to 2 ml of the mixed chloride test reagent for each calibration point. Points should be determined in triplicate. The first point will be equivalent to 5 ppm HCl in air as measured with a 47 ml syringe air sample. The last point will be equivalent to 50 ppm.

128

C.5 Determination of HF in Air by the Lacroix and Labalade Method

Reagents

All reagents are made from analytical grade chemicals in distilled water which is free from all interfering ions. Specifically, fluoride and chloride ions must be excluded. Reagents should be stored in UV-light absorbing amber glass bottles in a refrigerator. Reagents should be warmed to room temperature prior to use. As this method involves a bleaching reaction, the water must be free from any dissolved chlorine, chlorides, sulfites, and nitrites.

Ferric Sulfosalicylate. - Add 40 ml of 0.954 wt percent sulfosalicylic and 6.85 ml of 1 N sodium hydroxide to 100 ml of 7.5 $\times$ 10^{-3} M ferric nitrate. Dilute to 250 ml with sodium monochloroacetate buffer (pH = 2.9). Then 50 ml of the ferric sulfosalicylate solution are mixed with 50 ml of the buffer solution and diluted to 1 liter with distilled water. This reagent is specific for HF and other ionic fluorides.

Buffer Solution. - Mix 18.9 g of monochloroacetic acid and 100 ml of 1 N sodium hydroxide. Dilute to 1 liter with distilled water. Adjust pH to 2.9.

Standard F-Solution, 2.401 $\times$ 10^{-4} M. - Dissolve 0.1008 g of NaF in 100 ml distilled water. Dilute 10 ml of this solution to 1 liter to achieve the final concentration.

Apparatus

The apparatus is identical to that used for the analysis of NO_2.

Analytical Procedure

Sampling Procedure. - Draw exactly 3 ml of absorbing reagent into the syringe. Draw a 47 ml air sample through it at the rate of 2 ml per sec (or less) and then shake gently for 2 min for full color development. If the sample air temperature and pressure deviate greatly from 25°C and 760 mm Hg, measure and record the values.

When exposed to HF in air, the reagent bleaches from a bright pink to almost colorless at the F⁻ concentration increases. Bleaching is complete within 1 min. Transfer the sample to a 1 cm cuvette and read spectrophotometrically at 520 mμ. The instrument is zeroed with unexposed reagent at 80 %T representing 0 ppm HF. As this is a bleaching reaction, the percent transmittance rises as the ppm increases, i.e., 47 ppm HF in air gives 94.1 %T. The reagent should be read within 30 min after exposure.

Calibration

Prepare a HF permeation tube as described in Section 5.2.2. The calibration is then conducted in the same manner as for NO_2.

Calibration With Standard NaF. - To ten 25 ml volumetric flasks add graduated amounts (1 ml, 2 ml, ..., 10 ml) of the 2.401 × 10⁻⁴ M NaF solution. Dilute each to the mark with Cl⁻ and F⁻ free distilled water. Add 1 ml of each calibration solution to 2 ml of the mixed fluoride test reagent for each calibration point. Points should be determined in triplicate. The first point will be equivalent to 5 ppm HF in air as measured with a 47 ml syringe air sample. The last point will be equivalent to 50 ppm.

REFERENCES

1. Christian, J. G.: The Present Status of Chemical Research in Atmospheric Purification and Control on Nuclear Powered Submarines, Chapter 9, N.R.L. Report 6053, H. W. Carhart and V. R. Piatt, editors (1963).

2. Carhart, H. W. and Piatt, V. R.: The Present Status of Chemical Research in Atmospheric Purification and Control on Nuclear Powered Submarines, U. S. Naval Research Laboratory, N.R.L. Report 6053, Washington, D. C.

3. Sterbis, E. E.: Decomposition of Nitrous Oxide Catalyzed by Nickel Oxide, M.S. Thesis, University of Colorado, Boulder (1966).

4. Isomet Corp., U. S. Patent 3,351,562, November 7, 1962.

5. Yagi, S. and Kunii, D.: "Studies on Combustion of Carbon Particles in Flames and Fluidized Beds," Fifth Symposium (International) on Combustion, p. 231, Reinhold, New York (1955).

6. Lacey, D. T., Bowen, J. H., and Basdin, K. S.: "Theory of Noncatalytic Gas-Solid Reactions," I&EC Fundamentals, 4, 275 (1965).

7. Ausman, J. M. and Watson, C. C.: "Mass Transfer in a Catalyst Pellet During Regeneration," Chem. Eng. Sci., 17, 323 (1962).

8. Bischoff, K. B.: "Accuracy of the Pseudo Steady State Approximation for Moving Boundary Diffusion Problems," Chem. Eng. Sci., 18, 711 (1963).

9. Ishida, M. and Wen, C. Y.: "Comparison of Kinetic and Diffusional Models for Solid-Gas Reactions," AIChE Journal, 14, 311 (1968).

10. Shen, J. and Smith, J. M.: "Diffusional Effects in Gas-Solid Reactions," I&EC Fundamentals, 4, 293 (1965).

11. Chilton, T. H. and Colburn, A. P.: "Mass Transfer Coefficients," Ind. & Eng. Chem., 26, 1183 (1934).

12. Smith, J. M.: Chemical Engineering Kinetics, McGraw-Hill, New York (1956).

13. O'Keeffe, A. E. and Ortman, G. C.: "Primary Standards for Trace Gas Analysis," Anal. Chem., 38, 761 (1966).

14. Scaringelli, F. P., Frey, S. A., and Saltzman, B. E.: "Spectrophotometric Determination of Atmospheric Sulfur Dioxide," Amer. Ind. Hyg. Assoc. J., 28, 260 (1967).

15. Thomas, M. D. and Amtower, R. E.: "Gas Dilution Apparatus for Preparing Reproducible Dynamic Gas Mixtures in Any Desired Concentration and Complexity," J. Air Poll. Control Assoc., 16, 618 (1966).

16. Saltzman, B. E.: "Colorimetric Microdetermination of Nitrogen Dioxide in the Atmosphere," Anal. Chem., 26, 1949 (1954).

17. Meadows, F. L. and Stalker, W. W.: "The Evaluation of Collection Efficiency and Variability of Sampling for Atmospheric Nitrogen Dioxide." Paper presented at the 26th Annual Meeting of the American Industrial Hygiene Association, Houston, Texas (1966).

18. Lyshkow, N. A.: "A Rapid and Sensitive Colorimetric Reagent for Nitrogen Dioxide in Air," J. Air Poll. Control Assoc., 15, 481 (1965).

19. Thomas, M. D., MacLeod, J. A., Robbins, R. C., Goetellman, R. C., and Eldridge, R. W.: "Automatic Apparatus for Determination of Nitric Oxide and Nitrogen Dioxide in the Atmosphere," Anal. Chem., 28, 1810 (1956).

20. Saltzman, B. E. and Mendenhall, A. L., Jr.: "Design Parameters and Performances of a Miniaturized Colorimetric Recording Air Analyzer," Anal. Chem., 36, 1300 (1964).

21. Bassett, R. M. and Davies, J.: "A Portable Sulfur Dioxide Recorder," Air & Water Poll. Int. J., 10, 633 (1966).

22. Schulze, F.: "Versatile Combination Ozone and Sulfur Dioxide Analyzer," Anal. Chem., 38, 748 (1966).

23. Lyshkow, N. A.: "The Continuous Analysis of Sulfur Dioxide in Gaseous Samples," J. Air Poll. Control Assoc., 17, 687 (1967).

24. Patty, F. A. and Petty, G. M.: "Nitrite Field Method for the Determination of Oxides of Nitrogen," J. Ind. Hyg. Toxic, 25, 361 (1943).

25. Averell, R. P., Hart, W. F., Woodbury, N. T., and Bradley, W. R.: "Determination of Nitrogen Oxides in Air," Anal. Chem., 19, 1040 (1947).

26. Jacobs, M. B.: The Analytical Chemistry of Industrial Poisons, Hazards, and Solvents, 2nd ed., p. 358, New York, Interscience (1941).

27. Griess, P.: "Bemerkungen ueder abhandlung der H. H. Werselsky und Benedict, 'Ueder Einige Azozerbindungen'," BER, 12, 426 (1879).

28. Hollings, H., Inst. Gas Engrs., "Removal of Sulfur Compounds from Gas," Commun., No. 154, pp. 4, 51 (1937).

29. Saltzman, B. E. and Wartburg, A. F.: "Absorption Tube for Removal of Interfering Sulfur Dioxide in Analysis of Atmospheric Oxidant," Anal. Chem., 37 779 (1965).

30. West, P. W. and Gaeke, G. C.: "Fixation of Sulfur Dioxide as Disulfitomercurate (II) and Subsequent Colorimetric Estimation," Anal. Chem., 28 1916 (1956).

31. Scaringelli, F. P., Saltzman, B. E., and Frey, S. A.. "Spectrophotometric Determination of Atmospheric Sulfur Dioxide," Anal. Chem., 39, 1709 (1967).

32. West, P. W. and Ordoveza, F.: "Elimination of Nitrogen Dioxide Interference in the Determination of Sulfur Dioxide," Anal. Chem., 34, 1324 (1962).

33. Nicolson, F. P.: "An Evaluation of the Methods for Determining Residual Chlorine in Water Part I Free Chlorine," Analyst, 90, 187 (1965).

34. Andrew, T. R. and Nichols, P. N. R.: The Application of the E.E.L. Sulphur Dioxide Meter to Other Atmospheric Contaminants, Material Research Laboratory Report No. MR 907, The Mullard Radio Valve Co., Ltd., Mitcham, Surrey, England (1961, Appended 1962).

35. Chamberlin, N. S. and Glass, J. R.: "Colorimetric Determination of Chloride Residuals up to 10 ppm with Ortho-Tolidine," J. Am. Water Works Assn., 35, 1065 (1943).

36. Iwasaki, I., Utsumi, S., and Ozawa, T.: "New Colorimetric Determination of Chloride Using Mercuric Thiocyanate and Ferric Ion," Bull. Chem. Soc. Japan, 25, 226 (1952).

37. Iwasaki, I., Utsumi, S., Hagino, K., and Ozawa, T.: "A New Spectrophotometric Method for Determination of Small Amounts of Chloride Using the Mercuric Thiocyanate Method," Bull. Chem. Soc. Japan, 29, 860 (1956).

38. Lacroix, S. and Labalade, M. M.: "Dosage Colorimetrique Precis Des Ions Fluorhydriques," Anal. Chemica. Acta., 4, 68 (1950).

39. Bertolacini, R. J. and Barney, J. E., II,: "Ultraviolet Spectrophotometric Determination of Sulfate, Chloride, and Fluoride with Chloranilic Acid," Anal. Chem., 30, 202 (1958).

40. Morrison, M. E., Rinker, R. G., and Corcoran, W. H.: "Quantitative Determination of Parts-per-Million Quantities of Nitrogen Dioxide in Nitrogen and Oxygen by Electron Capture Detection in Gas Chromatography," Anal. Chem., 36, 2256 (1964).

41. Isbell, R. E." "Determination of Hydrogen Cyanide and Cyanogen by Gas Chromatography," Anal. Chem., 35, 255 (1963).

42. Priestey, L. J., Crutchfield, F. E, Ketcham, N. H., and Cavendar, J. D.: "Determination of Subtoxic Concentrations of Phosgene in Air by Electron Capture Gas Chromatography," Anal. Chem., 37, 70 (1965).

43. Runge, H.: "Gas Chromatographiscke Analyse Anorganischer Gase," Fresenius Z. Anal. Chem., 189, 111 (1962).

44. Huillet, F. D. and Urone, P." "Gas Chromatographic Analysis of Reactive Gases: The Cl_2, NOCl, NO_2Cl, NO_2 System," J. Gas Chrom., 249 (1966).

45. Cieplinski, E. W.: Analysis of Trace Chlorine in Air, Application No. GC-DS-003. The Perkin Elmer Corp. (1964).

46. Lee, W. K.: Gas Chromatographic Analysis of Oxygenated Organic Compounds in the Presence of Water, M.S. Thesis, p. 40, Library, Texas Technological College (1968).

47. Spencer, S. F.: "Porous Polymer Separations," Facts and Methods, Vol. 8, No. 2, Hewlett Packard Company, Avondale, Pa. (1967).

48. Robbins, L. A., Bethea, R. M., and Wheelock, T. D.: "Single Detector and Forecolumn Trap for Series Gas-Chromatography Analysis," J. Chrom., 13, 361 (1964).

49. Hollis, O. L. and Hayes, W. V.: "Gas Separation on Microporous Polymers." Paper presented at Sixth International Symposium on Gas Chromatography and Associated Techniques, Rome, 1966; in Littlewood, A. B. (ed.) Gas Chromatography 1966, pp. 57-74, The Institute of Petroleum, London (1967).

50. Bombaugh, K. J.: Personal communication to R. M. Bethea concerning uncoated supports for acid gas analysis (1968).

51. Hollis, O. L.: Personal communication to R. M. Bethea concerning liquid-modified Porapak columns (1968).

52. Wilhite, W. F. and Hollis, O. L.: "The Use of Porous-Polymer Beads for Analysis of the Martian Atmosphere," J. Gas Chrom., 6, 84 (1968).

53. Miller, R. R. and Piatt, V. R.: Chemical Constituents of Submarine Atmospheres, N.R.L. Report No. 5465, p. 15 (1960).

54. McKee, H. C., Rhoades, J. W., Wheeler, R. J., and Burchfield, H. P.: in Gas Chromatographic Measurement of Trace Contaminants in a Simulated Space Cabin, NASA Tech. Note D-1825, p. 7 (1962).

55. Saunders, R. A.: Analysis of the Spacecraft Atmosphere, N.R.L. Report No. 5816 (1962).

56. Sconce, J. S., ed.: Chlorine, Its Manufacture, Properties, and Uses, Reinhold Publishing Corp., New York (1962).

57. Morrison, M. E. and Corcoran, W. H.: "Rate and Mechanism of Gas-Phase Oxidation of Parts-per-Million Concentrations of Nitric Oxide," Ind. & Eng. Chem., 17, 175 (1966).

58. Ryason, P. R. and Harkins, J.: "Studies on a New Method of Simultaneously Removing Sulfur Dioxide and Oxides of Nitrogen from Combustion Gases," J. Air Poll. Control Assoc., 17, 796 (1967).

59. Ayen, R. J. and Ng, Y. S.: "Catalytic Reduction of Nitric Oxide by Carbon Monoxide," Air & Water Poll. Int. J., 10, 1 (1966).

134

60. Wikstrom, L. L. and Kobe, K.: "Catalytic Dissociation of Nitrogen Dioxide," I&EC Process Design & Development, 4, 191 (1965).

61. Robell, A. J., Merrill, R. P., and Arnold, C. R.: Activated Charcoal Air Filter System for the NASA 1973 Basic Subsystem Module, Report No. 6-78-68-21 (1968).

62. Jacobs, M. B. and Hochheiser, S.: "Continuous Sampling and Ultramicro-determination of Nitrogen Dioxide in Air," Anal. Chem., 30, 426 (1958).

63. Wilson, W. L.: "An Automatic Impinger for Air Sampling." Paper presented at the Air Pollution Control Association Meeting, Chattanooga, Tenn. (1954).

64. Hochheiser, S. and Ludmann, W.: "Field Comparison of Methods of Determining Atmospheric NO and NO_2." Paper presented at the 150th Natl. ACS Meeting, Atlantic City, N. J. (1965).

65. Saltzman, B. E.: "Modified Nitrogen Dioxide Reagent for Recording Air Analyzers," Anal. Chem., 32, 135 (1960).

66. Steigman, A.: "Acid-Bleached Fuchsin Solution as Analytical Reagent," J. Soc. Chem. Ind., 61, 18 (1942).

67. Urone, P. and Boggs, W. E.: "Acid-Bleached Fuchsin in Determination of Sulfur Dioxide in the Atmosphere," Anal. Chem., 23, 1517 (1951).

68. Ephraims, F.: Inorganic Chemistry, 5th edition, Thorne, P. C. L. and Roberts, E. R., eds., New York, p. 562 (1948).

69. Thomas, M. D.: "Automatic Apparatus for Determination of Small Concentrations of Sulfur Dioxide in Air--III," J. Air Poll. Control Assoc., 14, 517 (1964).

70. Mueller, P. K., Terraglio, F. P., and Tokiwa, Y.: "Chemical Interferences in Continuous Air Analyses," 7th Conference on Methods of Air Pollution Studies, Union Oil Center, Los Angeles, Calif. (1965).

71. Pate, J. B., Ammons, B. E., Swanson, G. A., and Lodge, J. P., Jr.: "Nitrite Interference in Spectrophotometric Determination of Atmospheric Sulfur Dioxide," Anal. Chem., 37, 942 (1965).

72. Zurlo, N. and Griffini, A. M.: "Measurement of Sulfur Dioxide Content of the Air in the Presence of Nitrogen and Heavy Metals," Med. d. Lavoro, 53, 330 (1962).

73. Pate, J. B., Lodge, J. P., and Wartburg, A. F.: "Effect of Para-rosaniline in the Trace Determination of Sulfur Dioxide," Anal. Chem., 34, 1660 (1962).

74. Stephens, B. S. and Lindstrom, F.: "Spectrophotometric Determination of Sulfur Dioxide Suitable for Atmospheric Analysis," Anal. Chem., 36, 1308 (1964).

75. Cummins, W. G. and Redfearn, M. W.: "Instrument for Measuring Small Quantities of Sulfur Dioxide in the Atmosphere," J. Inst. Fuel, 30, 628 (1957).

76. Swain, J. S.: "Absorptiometric Determination of Low Concentrations of Chlorides," Chem. & Ind., 418 (1956).

77. West, P. W. and Coll, H.: "Direct Spectrophometric Determination of Chloride Ion in Water," J. Am. Water Works Assn., 49, 1485 (1957).

78. Bergmann, J. G. and Sanik, J., Jr.: "Determination of Trace Amounts of Chlorine in Naphtha," Anal. Chem., 29, 241 (1957).

79. Hoffman, E.: "The Microgram Determination of Iodides, Bromides, and Chlorides by Mercurimetry," Fresenius Z. Anal. Chem., 195, 89 (1963).

80. DeBoer, J. H.: "Sensitive Color Reactions of Zr, HF, and F With Hydroxy-Anthroquinones," Rec. Trav. Chim., 44, 1071 (1925).

81. Scott, R. D.: "Modification of the Fluoride Determination," J. Am. Water Works Assn., 33, 2018 (1941).

82. Scott, R. D.: "Modification of the Fluoride Determination--Addendum," J. Am. Water Works Assn., 34, 522 (1942).

83. Thompson, T. G. and Taylor, H. J.: "Determination and Occurrences of Fluorides in Sea Water," Ind. Eng. Chem., 5, 87 (1933).

84. Sanchis, J. M.: "Determination of Fluorides in Natural Waters," Ind. Eng. Chem., Analytical Edition, 6, 134 (1934).

85. Megregian, S. and Maier, F. J.: "Modified Zirconium-Alizarin Reagent for Determination of Fluoride in Water," J. Am. Water Works Assn., 44, 239 (1962).

86. Megregian, S.: "Rapid Spectrophotometric Determination of Fluoride with Zirconium-Eriochrome Cyanine R Lake," Anal. Chem., 26, 1161 (1954).

87. Adams, D. F. and Koppe, R. K.: "Automatic Atmospheric Fluoride Pollutant Analyzer," Anal. Chem., 31, 1249 (1959).

88. Adams, D. F., Koppe, R. K., and Matzek, N. E.: "Colorimetric Method for Continuous Recording Analysis of Atmospheric Fluoride," Anal. Chem., 33, 117 (1961).

89. Bellack, E. and Schouboe, P. J.: "Rapid Photometric Determination of Fluoride in Water," Anal. Chem., 30, 2032 (1958).

90. Adams, D. F.: "An Automatic Hydrogen Fluoride Recorder Proposed for Industrial Hygiene and Stack Monitoring," Anal. Chem., 32, 1313 (1960).

91. Harrold, G. C. and Hurlbut, R. V.: "Device and Technique for Rapid Determination of Efluent Fluorides," Anal. Chem., <u>21</u>, 1504 (1949).

92. Belcher, R. and West, T. S.: "A Comparative Study of Some Lanthanon Chelates of Alizarin Complexan as Reagents for Fluorides," Talanta, <u>8</u>, 863 (1961).

93. Weinstein, L. H., Mandl, R. H., McCune, D. C., Jacobson, J. S., and Hitchcock, A. E.: "A Semi-Automated Method for the Determination of Fluoride in Air and Plant Tissues," Contrib. Boyce Thompson Inst., <u>22</u>, 207 (1963).

94. Smith, D. H. and Clark, F. E.: "Some Useful Techniques and Accessories for Adaptation of the Gas Chromatograph to Soil Nitrogen Studies," Soil Sci. Am. Proc., <u>24</u>, 111 (1960).

95. Bethea, R. M. and Adams, F. S., Jr.: "Vapor-Phase Butane Nitration Product Analysis by Parallel Column Gas Chromatography," J. Chromatog., <u>10</u>, 1 (1963).

96. Dietz, R. N.: "Gas Chromatographic Determinaton of Nitric Oxide on Treated Molecular Sieve," Anal. Chem., <u>40</u>, 1576 (1968).

97. Trowell, J. M.: "Gas Chromatographic Separation of Oxides of Nitrogen." Paper presented at 16th Annual Pittsburgh Conference on Analytical Chemistry and Applied Spectroscopy, Pittsburgh, Pa. (1965).

98. Sakaida, R. P., Rinker, R. G., Cuffel, R. F., and Corcoran, W. H.: "Determinaton of Nitric Oxide in a Nitric Oxide-Nitrogen System by Gas Chromatography," Anal. Chem., <u>33</u>, 32 (1961).

99. Phillips, L. V. and Coyne, D. M.: "A Study of Isobutylene-Nitric Oxide Reaction Products," J. Org. Chem., <u>29</u>, 1937 (1964).

100. Borland, C. C. and Schall, E. D.: "Factors Contributing to the Loss of Nitrogen in 1:1:1 Ratio Fertilizers," J. Assoc. Offic. Agri. Chem., <u>42</u>, 579 (1959).

101. Greene, S. A. and Pust, H.: "Determination of Nitrogen Dioxide by Gas-Solid Chromatography," Anal. Chem., <u>30</u>, 1039 (1958).

102. Morrison, M. E. and Corcoran, W. H.: "Optimum Conditions and Variability in Use of Pulsed Voltage in Gas-Chromatographic Determination of Parts-per-Million Qualitities of Nitrogen Dioxide," Anal. Chem., <u>39</u>, 255 (1967).

103. Kipping, P. J. and Jeffery, P. G.: "Detection of Nitric Oxide by Gas Chromatography," Nature, <u>200</u>, 1314 (1963).

104. Beskova, G. S., Kontorovich, L. M., Russo, L. P., Bobrova, V. P., and Timokhina, Z. P.: "Determination of Nitrous Oxide in Gases," Gaz. Khromatogr., Moscow, Sb., <u>1964</u>, 65 (1964).

105. Marvillet, L. and Tranchant, M.: "Analysis of Permanent Gases Using a Gas-Liquid Precolumn Having an Adsorbant Support," Chem. Abstr., <u>64</u>, 18377c (1965).

106. Smith, N., Swinehart, J., and Lesnini, D. G.: "Chromatographic Analysis of Gas Mixtures Containing Nitrogen, Nitrous Oxide, Nitric Oxide, Carbon Monoxide, and Carbon Dioxide," Anal. Chem., 30, 1217 (1958).

107. Hodges, C. T., Pickren, R. A., and Matson, R. F.: "Chromatography Abroad a Liquid Sulfur Ship," Chem. Eng. Prog., 62, 95 (1966).

108. Beuerman, D. R. and Meloan, C. E.: "Determination of Sulfur in Organic Compounds by Gas Chromatography," Anal. Chem., 34, 319 (1962).

109. West, D. L.: "A Gas Chromatograph for Determining O_2, N_2, NO, N_2O, SO_2, and H_2S in Steam," Report DP-880, Explosives Department, Atomic Energy Division, Savannah River Laboratory, E. I. duPont de Nemours and Co., Inc. (1964).

110. Ellis, J. F. and Iveson, G.: "The Application of Gas-Liquid Chromatography to the Analysis of Volatile Halogen and Interhalogen Compounds," Gas Chromatography-Amsterdam 1958, Desty, D. H., ed., Butterworths, Inc., London, pp. 300-309 (1958).

111. Ellis, J. F., Forrest, C. W., and Allen, P. L.: "The Quantitative Analysis of Mixtures of Corrosive Halogen Gases by Gas-Liquid Chromatography," Anal. Chem. Acta., 22, 27 (1960).

112. Ellis, J. F. and Forrest, C. W.: "Some Studies in the Inorganic Chemistry of the Reaction Between Uranyl Fluoride and Chlorine Trifluoride," J. Inorg. & Nucl. Chem., 16, 150 (1960).

113. Million, J. G., Weber, C. W., and Kuehn, P. R.: "Gas Chromatography of Some Corrosive Halogen-Containing Gases," Report K-1639, Oak Ridge Gaseous Diffusion Plant, Union Carbide Corp., Nuclear Division (1966).

114. Obermiller, E. and Charlier, G.: "Gas Chromatographic Separation of Hydrogen Chloride, Hydrogen Sulfide, and Water," Anal. Chem., 39, 396 (1967).

115. Rochefort, O.: "Analyse Des Composes Fluores Corrosifs Par Chromatographic Gazeuse (Controle Du Fluor Libre)," Anal. Chim. Acta., 29, 350 (1903).

116. Hamlin, A. G., Iveson, G., and Phillips, T. R.: "Analysis of Volatile Inorganic Fluorides by Gas Liquid Chromatography," Anal. Chem., 35, 2037 (1963).

117. Horton, A. D.: "Gas Chromatographs as Applied to Nuclear Technology," Nuclear Sci. & Eng., 13, 103 (1962).

118. Evrard, E., Thevelin, M., and Joossens, J. V.: "Self-Sustained Discharge Detector for Chromatographic Analysis of Permanent Gases," Nature, 193, 59 (1962).

138

119. Talbot, P. J. and Thomas, J. H.: "The Reaction Between Hydrogen Chloride and Nitrogen Peroxide," Trans. Faraday Soc., 55, 1884 (1959).

120. Engelbrecht, A., Nachbauer, E., and Mayer, E.: "Gas Chromatographic Analysis of Inorganic Fluoride Mixtures," J. Chromatog., 15, 228 (1964).

121. Araki, S., Kato, T., and Atobe, T.: "Gas Chromatography of Reactive Inorganic Gases and Vapors," Bunseki Kagaku, 12, 450 (1963).

122. Jones, C. N.: "Gas Chromatographic Determination of Hydrogen, Oxygen, Nitrogen, Carbon Monoxide, Carbon Dioxide, Hydrogen Sulfide, Ammonia, Water, and C_1 through C_5 Saturated Hydrocarbons in Refinery Gases," Anal. Chem., 39, 1858 (1967).